The Permian and Triassic of the central Cantabrian Mountains (Eastern Asturias-Western Cantabria, N Spain)

Nemesio Heredia; José F. Barrenechea; Raúl de la Horra; José López-Gómez; Fidel Martín-González; Brais Gonzalo-Guerra; Bienvenido Diez; Carlos Galé; Teresa Ubide; Violeta Borruel-Abadía; Joaquín García-Sansegundo; Luis Buatois; Pedro Farias; Javier Martín-Chivelet; José Carlos García-Ramos; Laura Piñuela

AGPT

Association of Permian and Triassic Geologists

Cantabrian Mountains Field Trip.

July 4 - 6, 2022. Oviedo, Spain

Funds to make this geological guide were provided by:

- Projects PGC2018-098272-B-100, CGL2015-70970-P “FALPINO” and PID2020-118228RB-C21 “CANALAB” from the I+D+I Spanish National Plan of the Ministry of Science, Innovation and Universities.

- CANOA-321006500 “PLAN CARTOGRÁFICO 2017–2021” from the Spanish Geological Survey-Instituto Geológico y Minero de España (IGME-CSIC).

ISBN: **978-84-09-42264-7**

Cover Photo: The Pandébano col in the Central Massif of the Picos de Europa (Los Urrieles), formed on early Permian sediments of the Sotres Formation. In the background and from left to right, you can see the Picos Albos, the Neveron de Urriellu and finally the Pico Urriellu tower

Authors, adress and contact:

Nemesio Heredia1; José F. Barrenechea2; Raúl de la Horra3; José López-Gómez4; Fidel Martín-González5; Brais Gonzalo-Guerra1; Bienvenido Diez6; Carlos Galé7; Teresa Ubide8; Violeta Borruel-Abadía3; Joaquín García-Sansegundo9; Luis Buatois10; Pedro Farias9; Javier Martín-Chivelet3; José Carlos García-Ramos11; Laura Piñuela11.

1- Instituto Geológico y Minero de España (IGME-CSIC). C/ Matemático Pedrayes 25, E33005, Oviedo, Spain

2- Departamento de Mineralogía y Petrología, Facultad de Geología, Universidad Complutense, C/ José Antonio Nováis 2, E28040, Madrid, Spain

3- Departamento de Geodinámica, Estratigrafía y Paleontología, Facultad de Ciencias Geológicas, Universidad Complutense, C/ José Antonio Nováis 2, E28040, Madrid, Spain

4- Instituto de Geociencias, CSIC-UCM, C/ Doctor Severo Ochoa 7, 4º, Universidad Complutense de Madrid, E28040 Madrid, Spain

5- Área de geología-ESCET, Universidad Rey Juan Carlos. C/ Tulipán, s/n, E28933 Móstoles, Madrid, Spain

6- Departamento de Xeociencias Mariñas e O.T. Facultade de Ciencias do Mar, Universidade de Vigo. Campus Lagoas-Marcosende. E36310 Vigo, Spain.

7- Universidad de Zaragoza. C/ Pedro Cerbuna 12, E50009 Zaragoza, Spain

8- School of Earth and Environmental Sciences. The University of Queensland. Steele Building. Brisbane QLD 4072 Australia

9- Departamento de Geología. Universidad de Oviedo. C/ Jesús Arias de Velasco s/n, E33005 Oviedo, Spain.

10- Department of Geological Sciences, University of Saskatchewan, 114 Science Place, Saskatoon, SK S7N 5E2, Canada

11- Museo del Jurásico de Asturias (MUJA), Rasa de San Telmo s/n, E33328 Colunga, Asturias, Spain

E-mail addresses: n.heredia@igme.es (Nemesio Heredia), barrenechea@ucm.es (José F. Barrenechea), rhorraba@ucm.es (Raúl de la Horra), jlopez@ucm.es (José T. López-Gómez), fidel.martin@urjc.es (Fidel Martín-González), b.gonzalo@igme.es (Brais Gonzalo-Guerra), jbdiez@uvigo.es (J. Bienvenido Diez), carlos.gale@gmail.com (Carlos Galé), t.ubide@uq.edu.au (Teresa Ubide), vborruel@ucm.es (Violeta Borruel-Abadía), jgsansegundo@uniovi.es (Joaquín García-Sansegundo),), luis.buatois@usask.ca (Luis Buatois), pfarias@uniovi.es (Pedro Farias), j.m.chivelet@ucm.es (Javier Martín-Chivelet), jcgramos.muja@gmail.com (José Carlos García-Ramos), lpinuela.muja@gmail.com (Laura Piñuela)

Participants:

1- Bienvenido Diez, University of Vigo, Spain, jbdiez@uvigo.es

2- Carlos Galé, University of Zaragoza, Spain, carlos.gale@gmail.com

3- Violeta Borruel-Abadía, Complutense University of Madrid, Spain, vborruel@ucm.es

4- José F. Barrenechea, Complutense University of Madrid and IGEO (CSIC-UCM), Spain, barrenechea@ucm.es

5- José López-Gómez, IGEO (CSIC-UCM), jlopez@ucm.es

6- Javier Martín-Chivelet, Complutense University of Madrid and IGEO (CSIC-UCM), Spain, j.m.chivelet@ucm.es

7- Chaim Benjamini, Ben Gurion University of the Negev, Israel, chaim@bgu.ac.il

8- Marc Durand, CNRS, France, mada.durand@orange.fr

9- Ausonio Ronchi, Università degli Studi di Pavia, Italia, ausonio.ronchi@unipv.it

10- Lorenzo Stori, Università degli Studi di Pavia, Italia, lorenzo.stori01@universitadipavia.it

11- Rachid Essamoud, University of Casablanca, Morocco, rachid.essamoud@univh2c.ma

12- Aude Gebelin, University of Plymouth, United Kingdom, aude.gebelin@plymouth.ac.uk

13- Laurent Beccaletto, BRGM, France, l.beccaletto@brgm.fr

14- Guido Roghi, Consiglio Nazionale delle Ricerche, Italia, guido.roghi@igg.cnr.it

15- Tom McCann, Bonn University, Germany, tmccann@uni-bonn.de

16- Sylvie Bourquin, CNRS-University of Rennes, France, sylvie.bourquin@univ-rennes1.fr

17- Marc Poujol, CNRS-University of Rennes, France, marc.poujol@univ-rennes1.fr

18- Annick Chauvin, CNRS-University of Rennes, France, annick.chauvin@univ-rennes1.fr

19- Zhicai Zhu, Bristol University, United Kingdom, nf21124@bristol.ac.uk and Chinese Academy of Geological Sciences, China, zzccugb@126.com

20- Piero Gianolla, University of Ferrara, piero.gianolla@unife.it

21- Luis Buatois, University of Saskatchewan, Canada, luis.buatois@usask.ca

22- Fidel Martín-González, Rey Juan Carlos University, Spain, fidel.martin@urjc.es

23- Nemesio Heredia, IGME-CSIC, Spain, n.heredia@igme.es

24- Joaquín García-Sansegundo, University of Oviedo, Spain, jgsansegundo@uniovi.es

25- Pedro Farias, University of Oviedo, Spain, pfarias@uniovi.es

26- David Pedreira, University of Oviedo, Spain, dpedreira@uniovi.es

27- Brais Gonzalo-Guerra, IGME-CSIC, Spain, b.gonzalo@igme.es

28- José Carlos García-Ramos, Museo del Jurásico de Asturias, Spain, jcgramos.muja@gmail.com

29- Laura Piñuela, Museo del Jurásico de Asturias, Spain, lpinuela.muja@gmail.com

30- Raúl de la Horra, Complutense University of Madrid, Spain, rhorraba@ucm.es<<<

INDEX

	Page
1. INTRODUCTION	
1.1. INTRODUCTION AND ACKNOWLEDGEMENTS	7
1.2. TECTONICS AND STRATIGRAPHY OF THE CANTABRIAN MOUNTAINS	8
1.2.1. Geological setting	8
1.2.2. The stratigraphy and ages of the units	10
2. THE FIELD TRIP STOPS	**17**
2.1. ITINERARY AND LOCATION OF THE STOPS	17
Monday 4th	18
STOP 1:	18
Age of the San Tirso Formation	22
The sedimentary record	22
STOP 2:	24
Petrology of the Permian volcanism of the Acebal Formation	25
Composition and relationship with other Permian magmatism	27
Age of volcanism	28
Relationship with basin evolution	29
STOP 3:	29
The sedimentary record of the Xivares basin	30
Thuesday 5th	34
STOP 4:	34
The Lower Member of the Sotres Formation	39
Sedimentology	40
Mineralogy	42
Paleosols	42
Paleoichnology	44

STOP 5: 45

Stratigraphy. The Permian-Triassic unconformity in the Sotres basin 47

The sedimentary record: the upper Cicera Formation 47

STOP 6: 49

Age of the Middle and Upper members of the Sotres Formation 49

Stratigraphy and sedimentology 49

Paleosols 52

Depositional environmental evolution 52

Mineralogy and fluorite deposits 54

Carbon and oxygen stable isotopes. Climate indicators 55

A common post-Variscan tectono-sedimentary evolution of the Pyrenean-Cantabrian orogenic belt 57

Wednesday 6th 60

STOP 7: 60

Age of the Cicera Formation 62

The sedimentary record of the Cicera Formation 62

The mineralogy of the Cicera Formation 64

STOP 8 64

STOP 9: 65

Age of the Transición Formation 68

The uppermost Triassic sedimentary record. The Transición Formation 69

STOP 10: 71

MUJA (Jurassic Museum of Asturias), near Colunga village, Asturias 71

Pre-Mesozoic hall 71

Triassic hall 71

Jurassic hall 72

Cretaceous hall 72

Introduction to the Asturian Jurassic hall 72

Asturian Jurassic hall 74

The collection of the MUJA 74

The Mesozoic garden 74

Visiting options 75

The MUJA for schoolchildren 75

THE DINOSAUR COAST 75

3. REFERENCES **79**

1. INTRODUCTION

1.1. INTRODUCTION AND ACKNOWLEDGEMENTS

Until very recently, the early Alpine Permian-Triassic tectono-sedimentary phases preserved in the Cantabrian Mountains have suffered from important stratigraphic mismatches and wrong tectonics interpretations. The lack of precise ages and misunderstanding of the stratigraphical units were the main causes behind these problems. In consequence, the beginning of the Alpine cycle in the Cantabrian Mountains has been explained with marked differences depending on the study area, and within a specific geodynamic context far from the general evolutionary phases of the western peri-Tethys basins.

This field trip shows new data based on recent work by the organizing research team. These data show a new stratigraphic chart based on precise ages of each defined unit, a reinterpretation of their sedimentary evolution and the development of a new Variscan-Alpine tectono-sedimentary framework. Furthermore, the new data reveal for the time a similar geodynamic evolution across the Pyrenean-Cantabrian basins at the end of the Variscan cycle and even with those formed within Western and Central Europe during the early-middle Permian. This new obtained information is based on a multidisciplinary work, including geological mapping, sedimentology, mineralogy, petrology of volcanic rocks and new paleontological data.

The topics of the field trip are shown in 10 stops that will be covered in three days. The stops are organized in chronological succession, from the Carboniferous-Permian to the Triassic-Jurassic transitions. The last stop will be at the MUJA (Museo del Jurásico de Asturias).

The organizers want to acknowledge to the institutions that have collaborated to the organization of this field trip, namely Oviedo, Complutense, Rey Juan Carlos, Vigo, Saskatchewan and Zaragoza universities; IGEO and IGME (CSIC); Museo del Jurásico de Asturias (MUJA), and the Association des Géologues du Permien et du Trias (AGPT) for giving us the opportunity of organizing this field trip. We also want to thank MINERSA GROUP for providing all the required borehole data from the Villabona Mine and for facilitating access to the mines for sampling.

1.2. TECTONICS AND STRATIGRAPHY OF THE CANTABRIAN MOUNTAINS.

1.2.1. GEOLOGICAL SETTING

The field trip takes place in the Cantabrian Mountains, located in the western part of the Pyrenean-Cantabrian Alpine Orogen (Figure.1). The Alpine Pyrenean-Cantabrian orogen is the result of the oblique convergence and collision of the Iberian Plate and the Eurasian Plates from Late Cretaceous until early Miocene (Dewey et al., 1989; Srivastava et al., 1990; Jabaloy et al., 2002, among others). The Pyrenean-Cantabrian orogen is made up of the Pyrenees in the east and the Cantabrian Mountains (CM) in the west. Their common origin and cartographic continuity suggest that these mountain ranges are part of a continuous orogen trending E-W extending for more than 800 km (Choukroune et al., 1990; Pulgar et al., 1996; Teixell, 1998; Muñoz, 2002; Gallastegui et al., 2002; Barnolas and Pujalte, 2004; Martin-González and Heredia, 2011a) (Fig. 1).

The field trip area is located between two of the tectonic regions of this orogenic belt: a) the Vasco-Cantabrica Region, in the E and b) the Astur-Galaica Region in the W (Martin-González and Heredia, 2011a, and references therein) (Figure 1a). A) The Vasco-Cantábrica Region is characterized by a thick and complete succession of Mesozoic sediments (Triassic to Cretaceous) (Figure 2). In the north, the extensional Mesozoic structures were partially inverted during the Alpine compressional regime (Garcia-Espina, 1997; Pulgar et al., 1999), while in the south, the Mesozoic succession appears

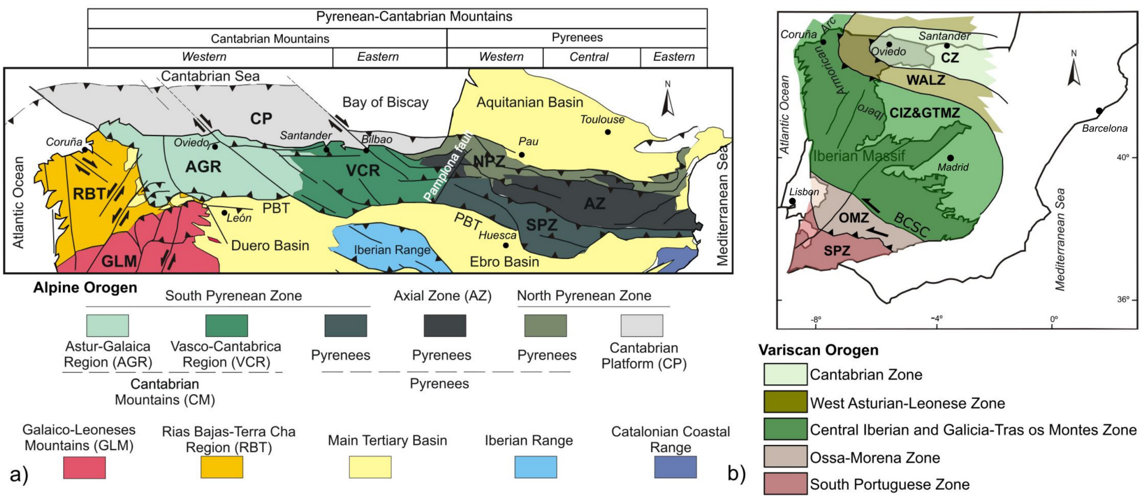

Figure 1. Structural sketch showing the tectono-stratigraphic regions of the Alpine Pyrenean-Cantabrian Orogen in the north of the Iberian Peninsula (modified from Martín-Gonzalez and Heredia, 2011a) and geographical subdivisions (based on Muñoz, 2002). b) Zones of the Variscan Orogen in Iberia and the Ibero-Armorica Arc (Modified from García-Sansegundo et al., 2011).

to be detached, overlapping the Cenozoic synorogenic sediments of the Ebro and Duero foreland basins. B) The Astur-Galaica Region is characterized by the paucity of Mesozoic sediments. Only in the eastern part (Asturian Basin, Figure 2B), a thin and complete sequence is exposed. These deposits are undetached and deformed in a thick-skinned style, affecting here the Alpine orogeny to Paleozoic rocks of the Variscan basement of the Iberian Peninsula (Iberian Massif) (Figure 1b and 2). Cenozoic synorogenic sediments are found in small and isolated depressions (Figure 2B), which formed a broken foreland basin (Martin-González and Heredia, 2011b). The Paleozoic basement of the study area belongs to the foreland of the Variscan Orogen: the Cantabrian Zone (Figure 1b). This zone is a thin-skinned fold and thrust belt (Figure 2C), preserving evidence of the Carboniferous synorogenic sedimentation (Julivert, 1971).

Soon after the end of the Variscan orogeny, in early Permian times, the resulting mountain belt collapsed (Ziegler and Stampfli, 2001). Related to this extensional collapse (not generalized in the Cantabrian Zone), narrow and isolated basins were generated (Figure 2). These basins were controlled by the reactivation of the Variscan and Late Variscan structures, they had close source areas and remained active throughout the Cisuralian (López-Gómez et al., 2019).

The Permian outcrops in the Cantabrian Mountains are in the most external zone of the Variscan orogen (The Cantabrian Zone) (Julivert and Marcos, 1973) (Fig. 1b). In the Carboniferous-Permian transition (late Gzhelian-earliest Asselian), the Late Variscan NW-SE strike-slip faults developed (Julivert, 1971; Arthaud and Matte, 1975; Ribeiro et al., 1990; Merino-Tomé et al., 2009; Heredia et al., 2022) (Figure 2B). The Permian basins in this area were elongated, narrow and isolated, although some of these were very close and may have been connected (López-Gómez et al., 2019). The Permian extensional regime generated a calc-alkaline magmatism (ca. 297-292 Ma, Gallastegui et al., 2004), with the intercalation of volcanic rocks in the sedimentary early Permian sequences and a small plutonic bodies (Suárez-Rodríguez, 1988; Valverde-Vaquero, 1992) (Figure 2B). All these igneous rocks were associated to reactivation of large Variscan and Late Variscan faults (e.g. Liebana fault, León fault) (Gallastegui et al., 1990) (Figure 2B).

The Alpine Cycle continued with generalized extension during the Triassic with the opening of the Bay of Biscay, which was the local result of the Pangea breakup that individualized the Iberian Subplate from the European Plate (e.g. Ziegler, 1988). This extensional event ended in Late Triassic-Early Jurassic times but was reactivated in Late Jurassic-Early Cretaceous (Boillot et al., 1979, García-Espina, 1997). In this way, the lithospheric extension and the subsequent post-rift thermal subsidence were active in two different pulses during the Mesozoic. Later on, a change to a convergent setting between the Iberian subplate and the European plate in the framework of the Alpine Orogeny lead to the generation of the Pyrenean-Cantabrian orogenic belt (Figure 1a). During this orogenic event many of the former Variscan, Late Variscan and Mesozoic faults located in the studied area were inverted. The main episode of crustal uplift (responsible for the present-day relief) was late Eocene-early Oligocene in age, extending to later Miocene times towards the western end of the range (Martin-González et al., 2012, 2014; Martín-González and Heredia, 2011b and references therein).

1.2.2. THE STRATIGRAPHY AND AGES OF THE UNITS

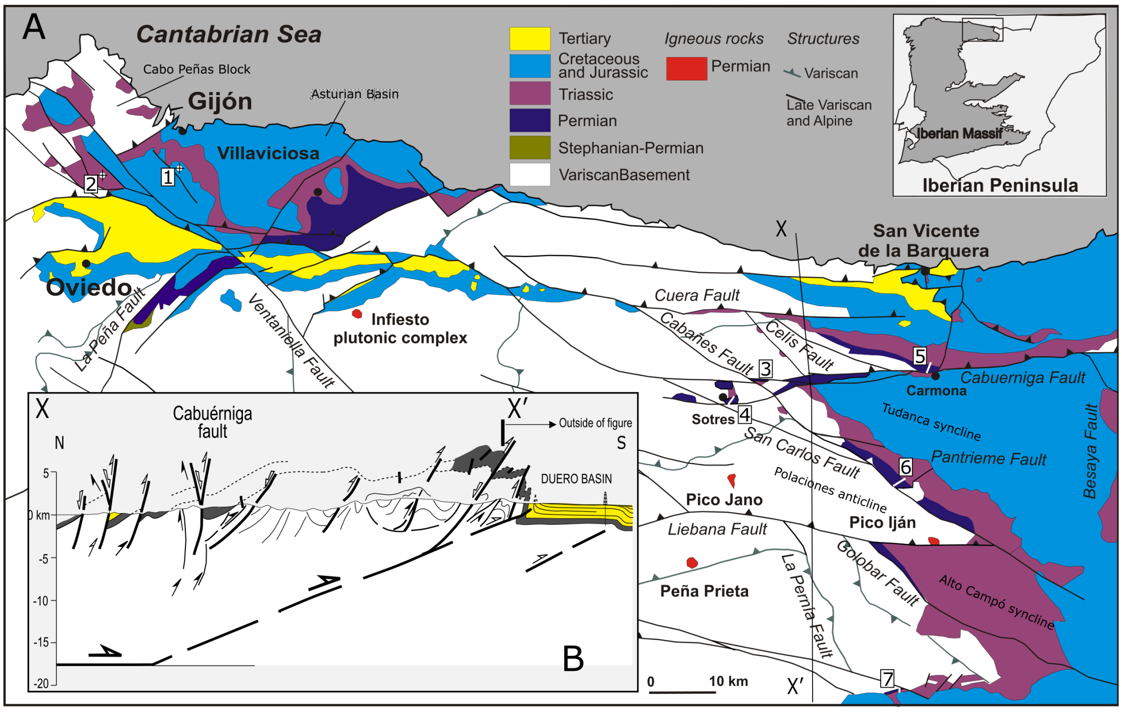

Figure 2. Structural sketch showing the different tectono-stratigraphic regions of the Alpine Pyrenean-Cantabrian Orogen in the north of the Iberian Peninsula (modified from Martín-González and Heredia, 2011a). The main structures and study area are shown. B Simplified geological map of the study area. See Fig. 3 for a more detailed location. Locations of the studied sections are shown: 1.- La Camocha, 2.-Villabona, 3.-Tresviso, 4.- Sotres, 5.- Carmona, 6.- Peña Sagra and 7.- Rueda (1 and 2 represent boreholes, and 3 to 7 are field sections). C Geological cross-section of the Cantabrian Mountains showing the main alpine structures (modified from Pulgar et al., 1999

Up to recent times, the early Alpine, Permian-Triassic tectono-sedimentary phases preserved in the Cantabrian Mountains had been considered independently from the same phases in neighbouring basins of SW Europe, and even from the eastern part of the same orogeny (the Pyrenean Orogeny). In consequence, the beginning of the Alpine cycle in the Cantabrian Mountains had been interpreted within a specific (particular) geodynamic context, far from the general evolutionary phases of the western peri-Tethys basins.

On the other hand, and due mostly to imprecise dates, and misinterpretation of lithological units of these rocks, the stratigraphy of this sedimentary record in this area was many times synthesized as “Permian-Triassic”, without differentiating units. Furthermore, when these units have been differentiated, they were randomly confused, but also interpreted with different ages depending on the authors (see López-Gómez et al., 2019 for details of the nomenclature and ages of the units).

Recent work by our research team (López-Gómez et al., 2019, 2021; Lloret et al., 2022) reinterpreted the early Alpine tectono-sedimentary phases and the Permian-Triassic stratigraphy of the Cantabrian Mountains.

These studies have been based on detailed mapping, new obtained ages, and petrological, mineralogical, paleontological and sedimentological studies, including seismic and borehole data. The results of these studies represent the base of this field guide, including the differentiated units of the new lithostratigraphic succession chart which will be used in the different stops. From base to top these units are: San Tirso, Acebal, Sotres, Cicera, Rueda and transition formations (Figure 3). Contrary to previous work, the lithostratigraphic units are considered representative of the three provinces that constitute the Cantabrian Mountains: the Asturian, Cantabrian and Palentian provinces.

Most of these studies were based on the reconstruction and sedimentary interpretation of eight representative stratigraphic sections in the field. Their selection was based on preliminary detailed geological mapping and tectonic study to avoid repetitions due to fault and thrusts. These sections are shown in Figure 4, and their geographical location is indicated in Figure 2. In Villabona, north of Oviedo city, where the vegetation covers hinders detailed fieldwork, a borehole (cuN-69B) obtained by courtesy of the MINERSA Group, allowed for a detailed study of the Permian-Triassic of this zone.

A detailed sedimentary study of each lithostratigraphic unit was provided in López-Gómez et al. (2019, 2021) and will be summarised in the stops of this guide during the description of the formations. These studies were based on differentiation of facies and facies association, whose main elements will be shown in the different stops.

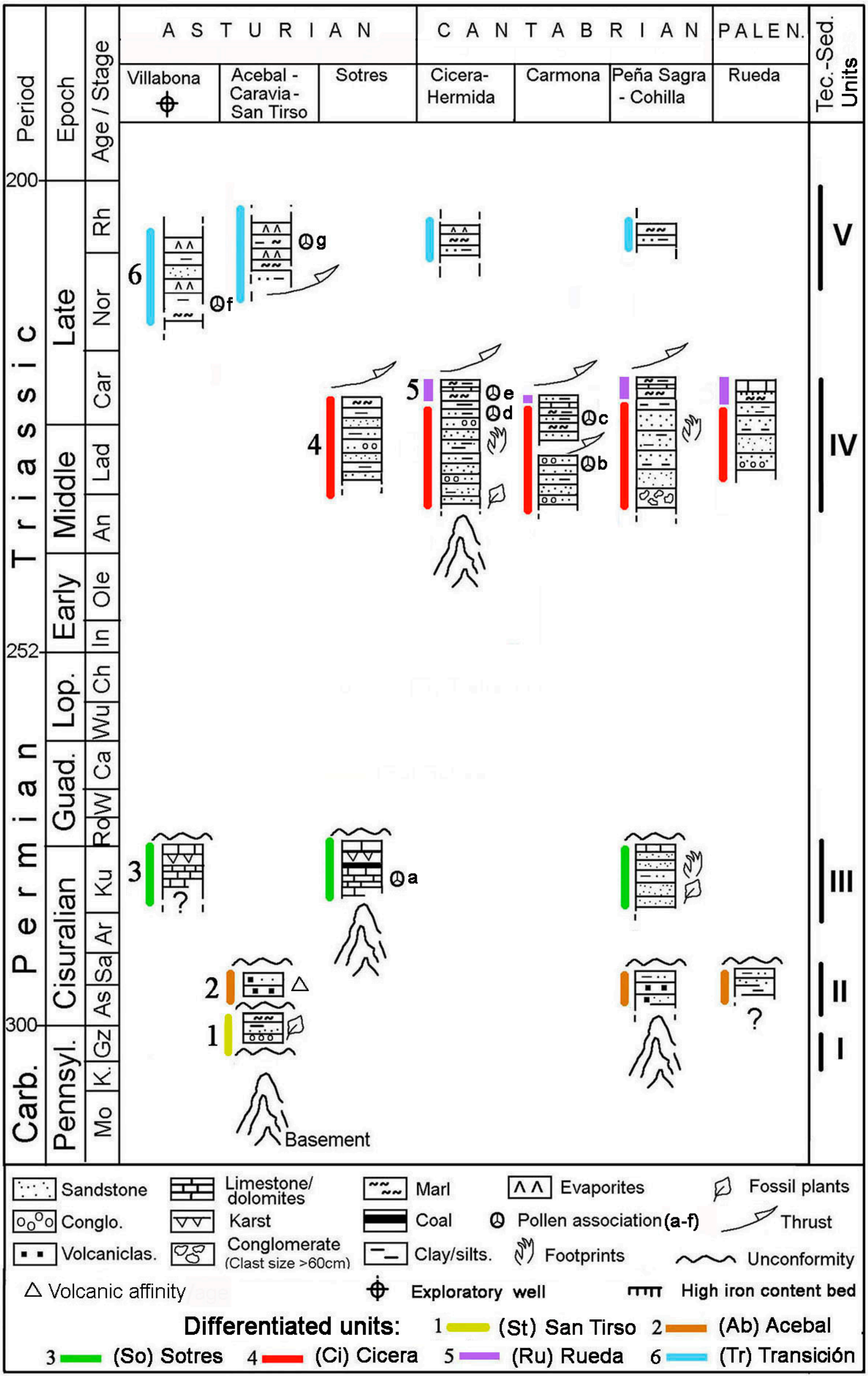

Figure 3. Chronostratigraphical chart of the Permian-Triassic sedimentary record of the Cantabrian Mountains. Modified from López-Gómez et al. (2019).

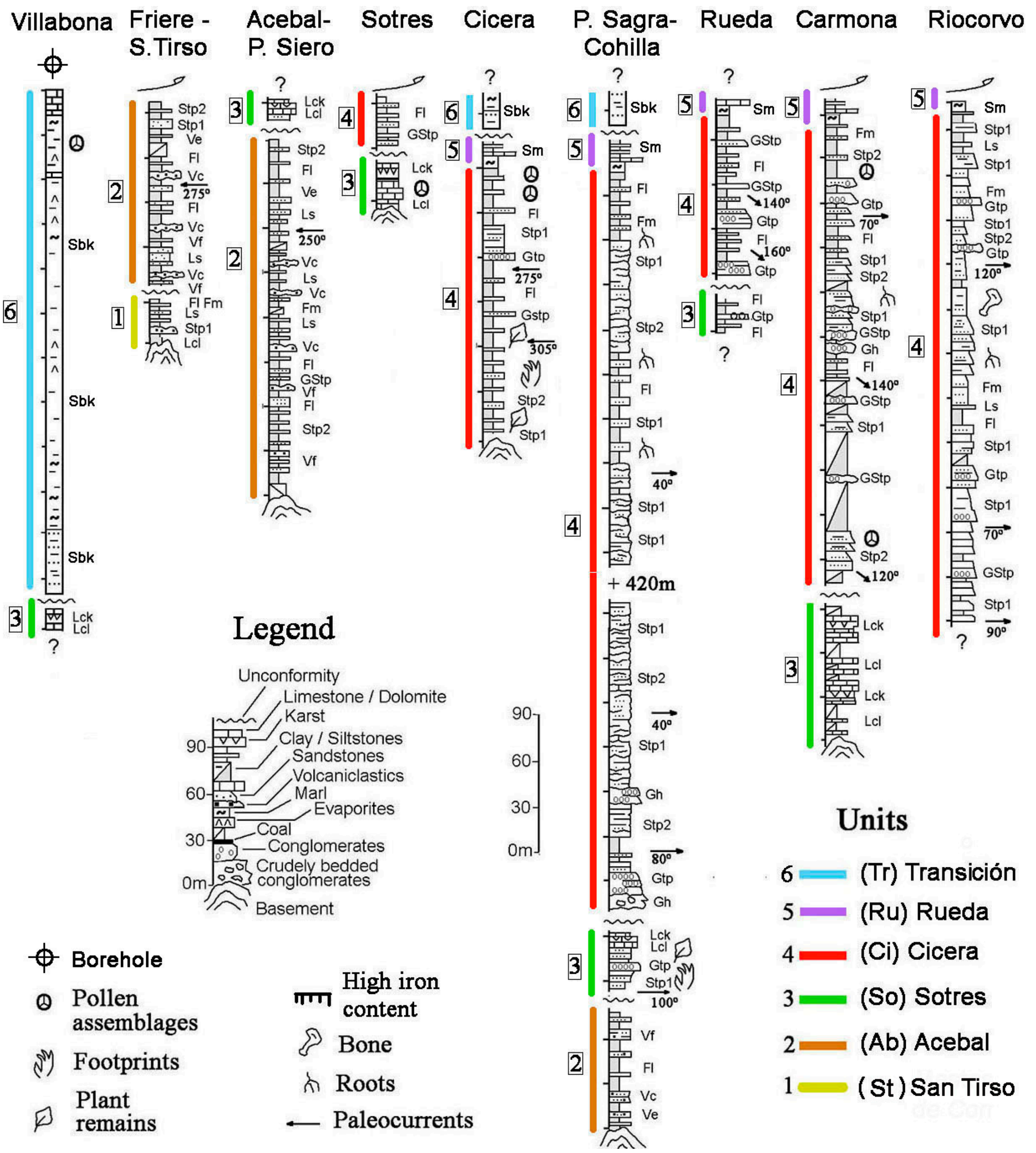

Figure 4. Representative sections, including the Villabona borehole, of the Permian-Triassic record of the Cantabrian Mountains. Modified from López-Gómez et al. (2019).

2. THE FIELD TRIP STOPS

2. THE FIELD TRIP STOPS

2.1. ITINERARY AND LOCATION OF THE STOPS

The different outcrops that will be shown in the field trip are spread over 10 stops which are distributed from the Cantabrian coast to the Cantabrian Mountains (Figure 5). The excursions will start and finish in Oviedo during the three days of the field trip. The order of the stops will be chronological, starting on the first day with the Carboniferous-Permian transition and ending the third day showing the Triassic-Jurassic transition. This order of the stops will also make possible to show the different characteristics between the last stages of the Variscan orogeny and the development of the first Alpine extensional phases. Each day will include three stops, and the last day will also include a visit to the MUJA, which will represent the end of the field trip.

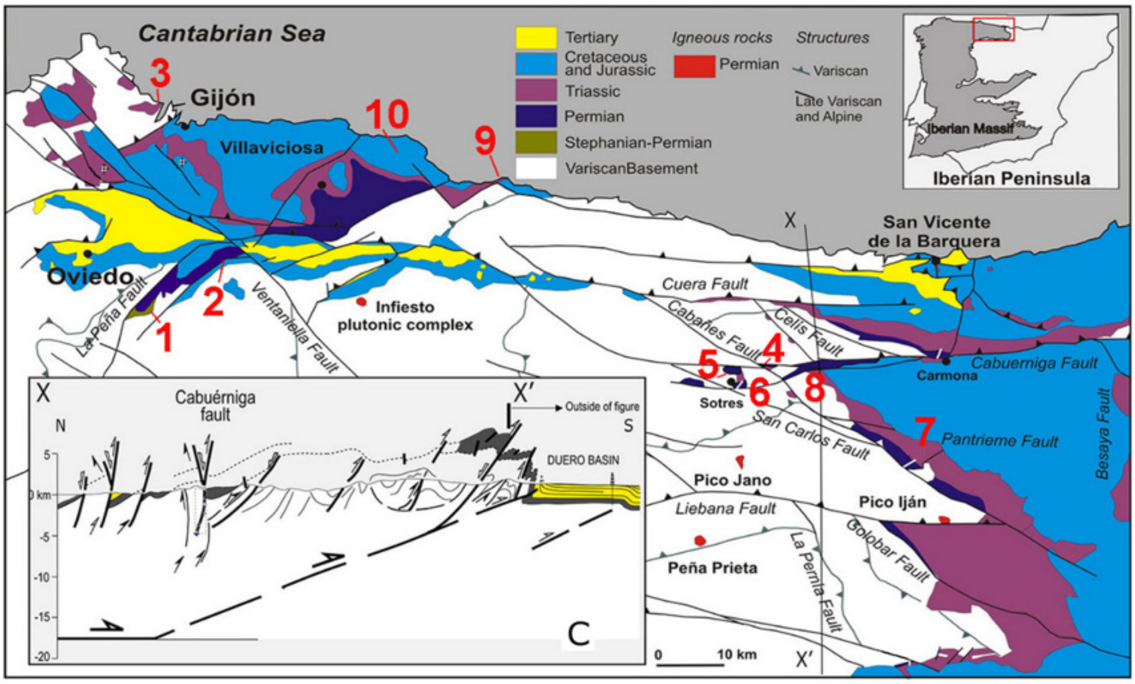

Figure 5. Area of the field trip and location of the stops. 1) San Tirso, 2) Acebal, 3) Xivares beach, 4) Tresviso, 5) Sotres, 6) La Caballar, 7) La Cohilla dam, 8) Linares, 9) Arenal de Morís beach, 10) MUJA.

MONDAY 4TH

It comprises Stops 1, 2 and 3. See figures 5 & 6 for their locations.

STOP 1:

Location:

San Tirso - El Carmen, Asturias (Figure 5).

Objectives:

Introduction to the Pyrenean-Cantabrian Orogen and Variscan-Alpine cycles transition. Late-Variscan faults active in the Carboniferous- Permian boundary. The San Tirso Formation (late Gzhelian-earliest Asselian): Proximal to distal alluvial sedimentation with intercalated coal beds.

The San Tirso Formation (Velando et al., 1975) only appears in the southern part of the La Justa-Aramil synclinorium (Figure 6 and 7), an alpine structure with NE-SW trend, located in the southern end of the Asturian Mesozoic Basin of the Astur-Galaica Region (Alpine Cantabrian Mountains) (Figures 2 and 6). This formation is related to a transpressive step-over (strike-slip duplex), associated with Nalón and Mieres Late Variscan dextral strike-slip faults (Estenssoro, 2021) (Figure 8). The reverse faults associated with the strike-slip duplex (Frieres, La Peña and La Carrera faults) are reactivated Variscan thrusts (Figure 7 and 9).

These faults are located south of the Ventaniella fault, the most characteristic Late Variscan fault of the Iberian Massif (Figure 5). The Late Variscan faults (Arthaud and Matte, 1975) cut the youngest Variscan thrusts and related folds of the Cantabrian Zone (Figure 1b), with Gzhelian ages in Picos de Europa Unit, but do not affect the lower Permian deposits. Taking the aforementioned data into account, it is possible to infer that the development of the Late Variscan faults comprised a short time span (4-5 Myr) between the late Gzhelian and the early Asselian, estimated age also for the related sediments of the San Tirso Formation (Wagner & Martinez-García, 1982). This age is coincident with that estimated for the end of the Ibero-Armorican Arc closure (Weil, 2006), suggesting that these faults accommodated the last Variscan compressional stresses (López-Gómez et al., 2019; Rodríguez Fernández and Heredia, 1987). A review of the continental Carboniferous-Permian sedimentary record in eastern equatorial Pangea has been recently published by Mercuzot et al. (2022).

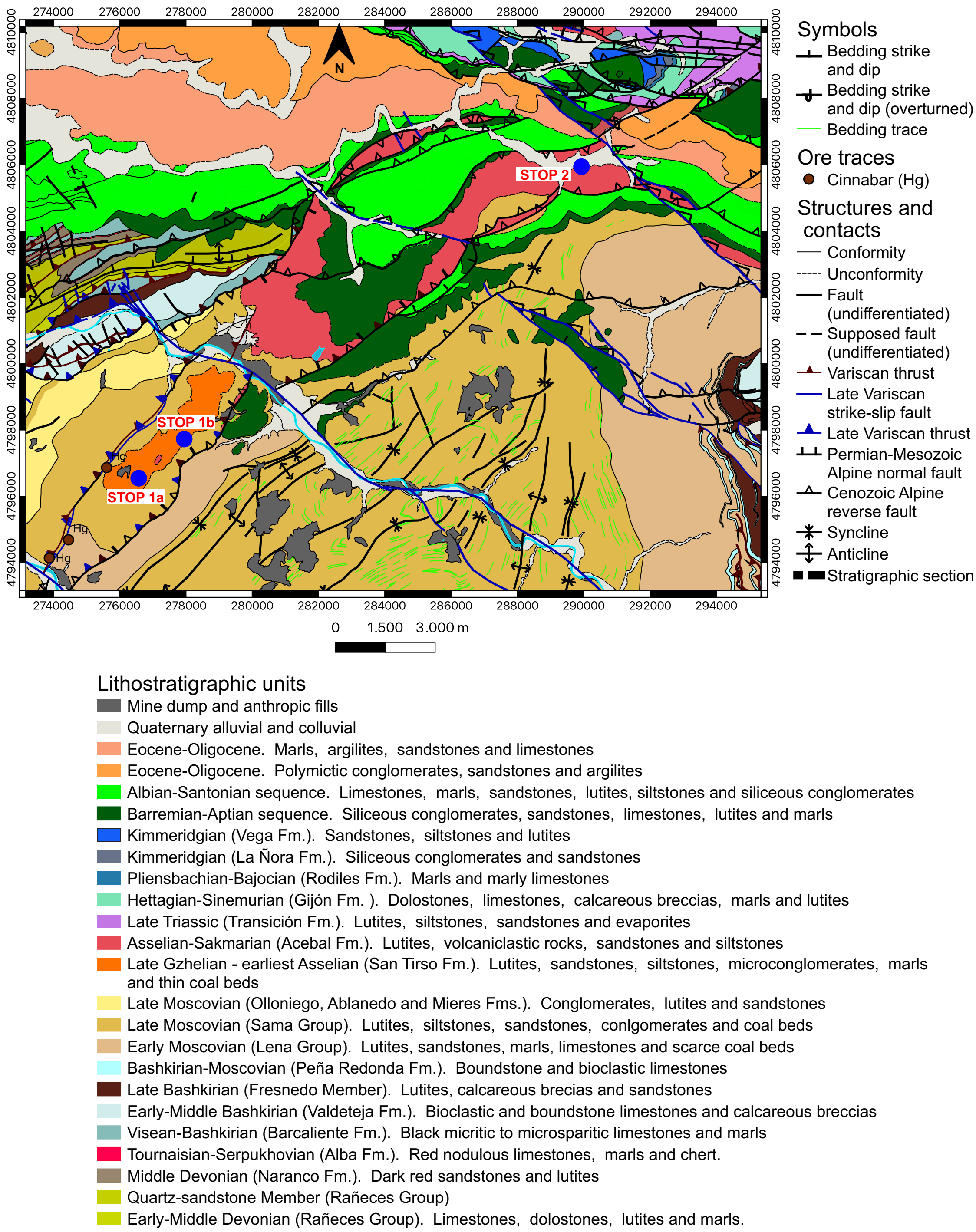

Figure 6. Geological map showing the outcrops of San Tirso (late Gzhelian-lowest Asselian) and Acebal (Asselian) formations in the La Justa-Aramil Alpine syncline. Modified from Merino-Tomé et al. (2011).

All the reverse faults related to Late Variscan Nalón-Mieres strike-slip duplex are Variscan thrusts reactivations: the Frieres, La Peña and La Carrera faults (Figures 8 and 9A). Subsequently, this faults were reactivated as normal faults in Permian times, controlling the deposition of sedimentary and volcanic rocks of this age and the presence of Hg ores (related to Permian volcanism), developed close to their brecciated fault zones (La Peña y La Carrera faults) (Figure 9B). The Permian basin seems to be related to a half-graben south of Nalon fault and a symmetric graben north of this fault, due in the latter case to the overturned position of the reactivated Frieres Variscan thrust (Figure 7). Lastly, some of these faults were reactivated during the Cenozoic Alpine compression, as evidenced by the presence of affected Mesozoic (Frieres fault) and/or Cenozoic rocks (La Carrera fault) (Figures 6, 9A and 11).

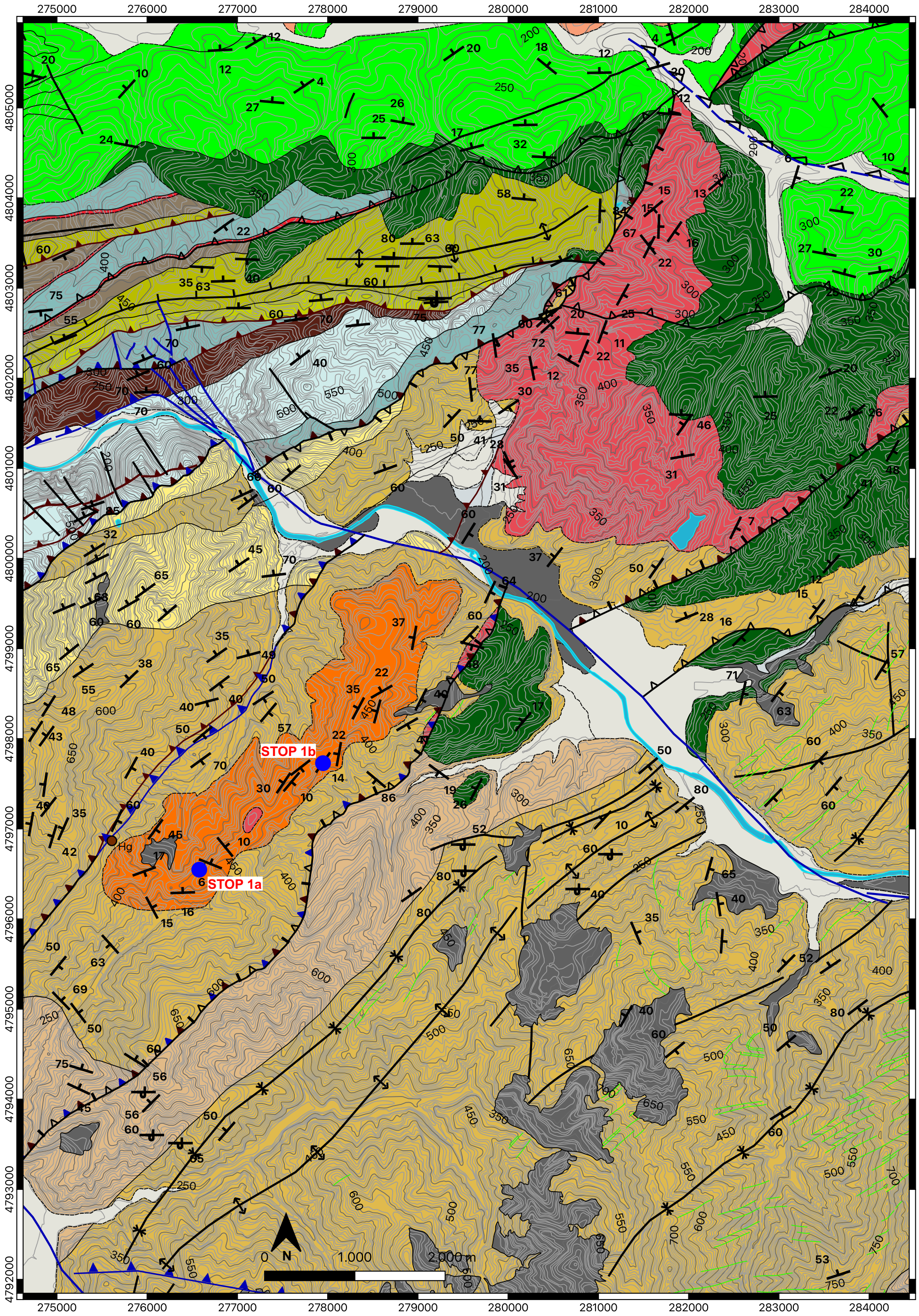

Figure 7. Geological map of the SW end of the La Justa-Aramil synclinorium. Modified from Estenssoro (2021). Legend in Fig. 6.

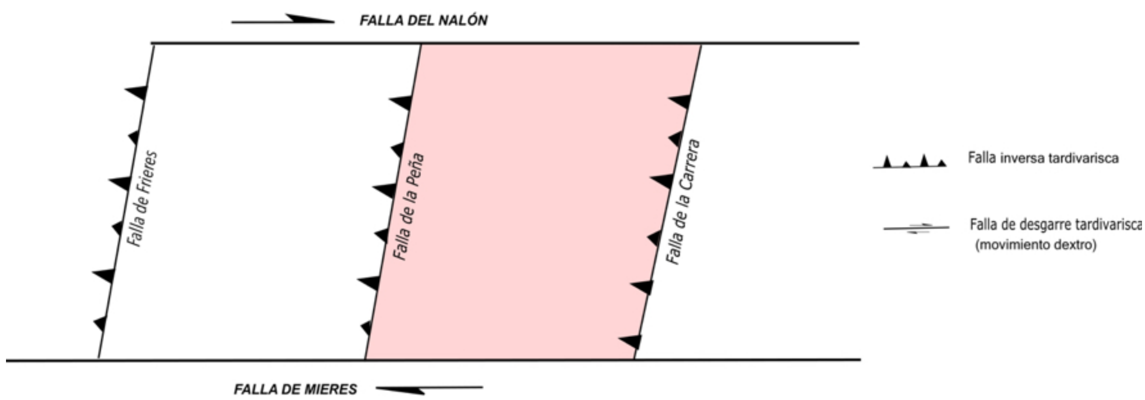

Figure 8. Strike-slip duplex related to Nalón and Mieres Late Variscan faults that produces the reactivation of Frieres, La Peña and La Carrera Variscan thrusts. The red zone shows the conserved depositional area of the San Tirso Fm. (Estenssoro, 2021).

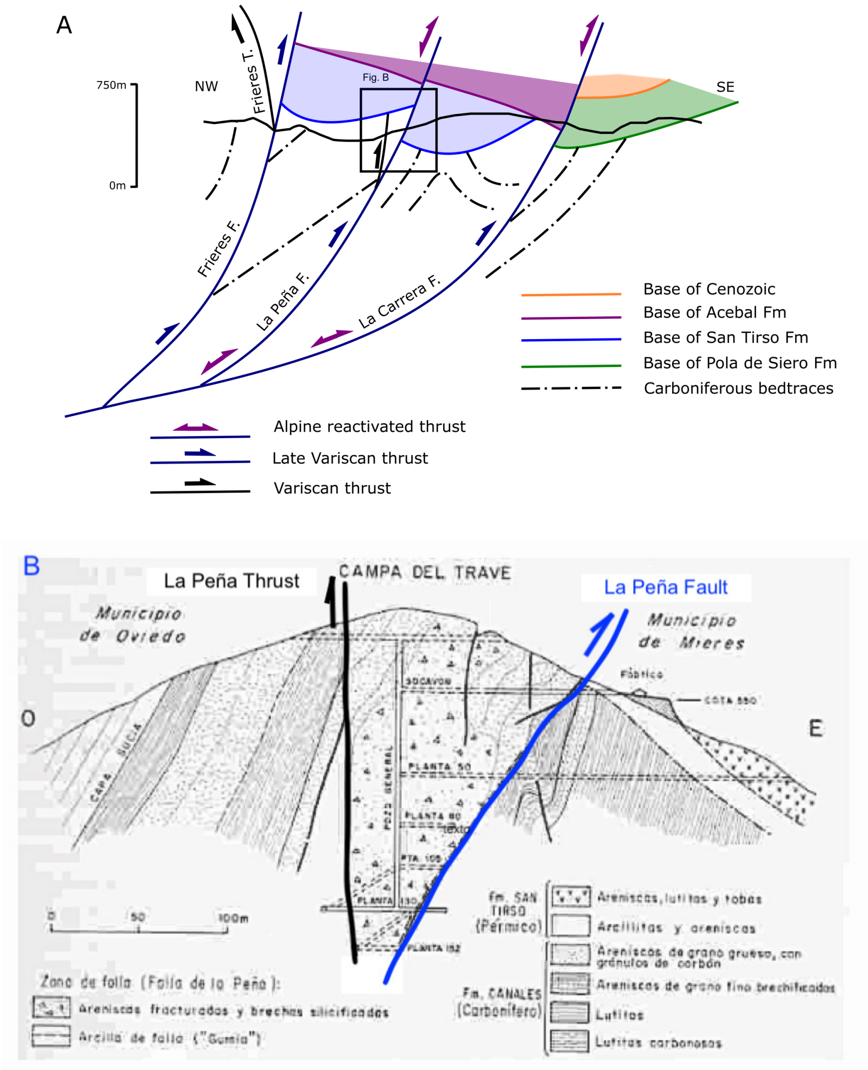

Figure 9. A) Schematic cross section of the La Justa-Aramil synclinorium (modified from Estenssoro, 2021). B) Geological sketch of the Campa del Trave mine (Hg), related to la Peña Fault system. Modified from Luque (1985).

Age of the San Tirso Formation

Wagner and Martínez-García (1982), Martínez-García (1991), and Wagner and Álvarez-Vázquez (2010) described a fossil flora from the lower part of the San Tirso Formation (erroneously "Mestas de Con Formation" for these authors), which could indicate "Stephanian C or lower Autunian". However, this flora is only listed in Wagner and Martínez-García (1982), and reference is made to an ongoing study, which never saw the light so far. An intensive palynological test has been attempted to date the San Tirso Formation but everything has been unsuccessful up to now.

The sedimentary record

The San Tirso Formation outcrops in very few places in the Cantabrian Mountains, and these sections are discontinuous showing partial segments that need to be arranged vertically. Figure 10 shows the vertical succession of the San Tirso Formation in the La Justa-Aramil area. This log is made up of four sections, A to D from base to top, of which the lower two are covered due to local landslides, and only the upper two will be observed.

The lower section (A) is constituted by a 10 m-thick finning-upwards succession of conglomerate beds with red pale sandstone up to 4 m thick at the top (Figure 10, A). Plant fragments and intercalated thin coal beds are common. This lower section is interpreted as proximal to medium alluvial fan deposits developed under humid conditions, similar to examples described by Heward (1978a) in late Carboniferous coal-field deposits of N Spain.

The second section (B) consists of red siltstone up to 18 m thick with root trace fossils and intercalations of cm-thick fine-grained sandstone and limestone beds with flat bases (Figure 10, B). This section is interpreted as overbank deposits with development of ponds probably related to distal alluvial fans environments, similar to examples described by Heward (1978b) from the Stephanian A and B of N Spain.

The third section (C) (Figure 10, C) shows two parts. The lower one is a 12 m-thick succession constituted by dark red poorly organized conglomerate cm-thick beds and some intercalated coarse-grained sandstone cm-thick beds with poorly developed low-angle cross lamination. Thin beds of dark red siltstone may appear intercalated between the sandstone. This lower part is mainly interpreted as proximal (poorly organized and unconfined) deposits related to the basin boundary near areas, with intercalated stages showing more organized sedimentation. The upper part of this section is a 5 m-thick

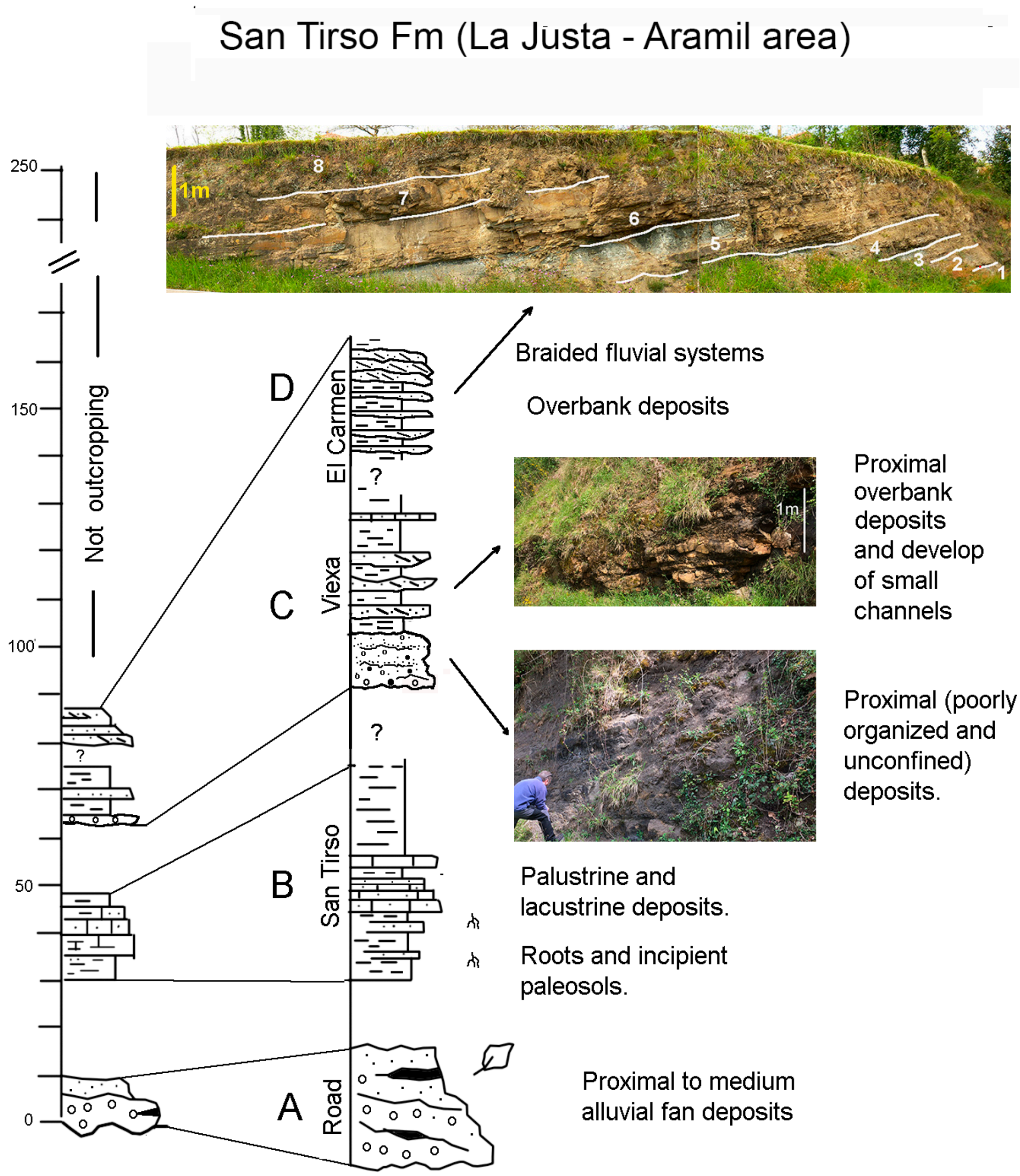

Figure 10. Sedimentological characteristics and interpretation of the San Tirso Formation in La Justa – Aramil area.

succession constituted by cm-thick dark yellow sandstone beds with planar or lightly erosive base, ripples and planar and through cross-stratification. Thin dark red siltstone beds may appear separating the sandstone bodies and constituting finning upwards sequences. This upper part is interpreted as proximal overbank deposits with develop of small channels (Kraus, 1987).

The fourth and upper subsection of the San Tirso Formation (D) outcrops in El Carmen village (Figure 10, D). It is subdivided in two parts. The lower one is 2.5 m thick and constituted by five 0.4-0.8 m-thick finning upwards sequences of ochre sandstone beds with current ripples and low angle planar cross stratification and green siltstone-mudstone at the top. It is interpreted as overbank deposits with incipient soil development.

The upper part, which is 2.3 m thick, is represented by cm-thick ochre sandstone beds with erosive base, planar and trough cross-stratification and current ripples. They are interpreted as the migration of 2D-3D small-medium bars related to braided fluvial systems in multistorey organization (e.g., Ramos and Sopeña, 1983).

The San Tirso Formation sedimentary record shows a succession with clear tectonic control, where reactivation in the alluvial systems are related to frequent fault movements.

STOP 2:

Location:

Near Acebal village, Asturias (Figure 5).

Objectives:

Acebal Formation (Asselian-Sakmarian). Calc-alkaline volcaniclastics. Its relationship with the evolution of the basin.

The Acebal Formation (López-Gómez et al., 2019) outcrop is in the southern part of the La Justa-Aramil Alpine synclinorium, where is unconformably cover by Cretaceous sediments. This synclinorium is located between the Frieres and La Carrera faults, which are reactivations of Variscan faults during the Alpine cycle. In Permian times, la Carrera thrust reactivated as a normal fault and formed the half-graben that constitutes the La Justa-Aramil Basin. This basin is the southern extension of the Villaviciosa Permian basin (Figure 5, 6 and 11), which contains the thickest sequences of the Acebal Formation (up to 600 m). The basal part of the Acebal Formation does not outcrop in this section, due to the presence of an Alpine reverse fault (new reactivation of la Carrera fault) that superimposes this formation on the Cretaceous and also on Cenozoic sediments further to the south (Figure 11). However, more to the south, north of the Nalón Fault (Figures 6 and 7), this basal part is composed by thick polymictic conglomerate beds, which rest unconformably on Carboniferous strata strongly deformed by the Variscan orogeny.

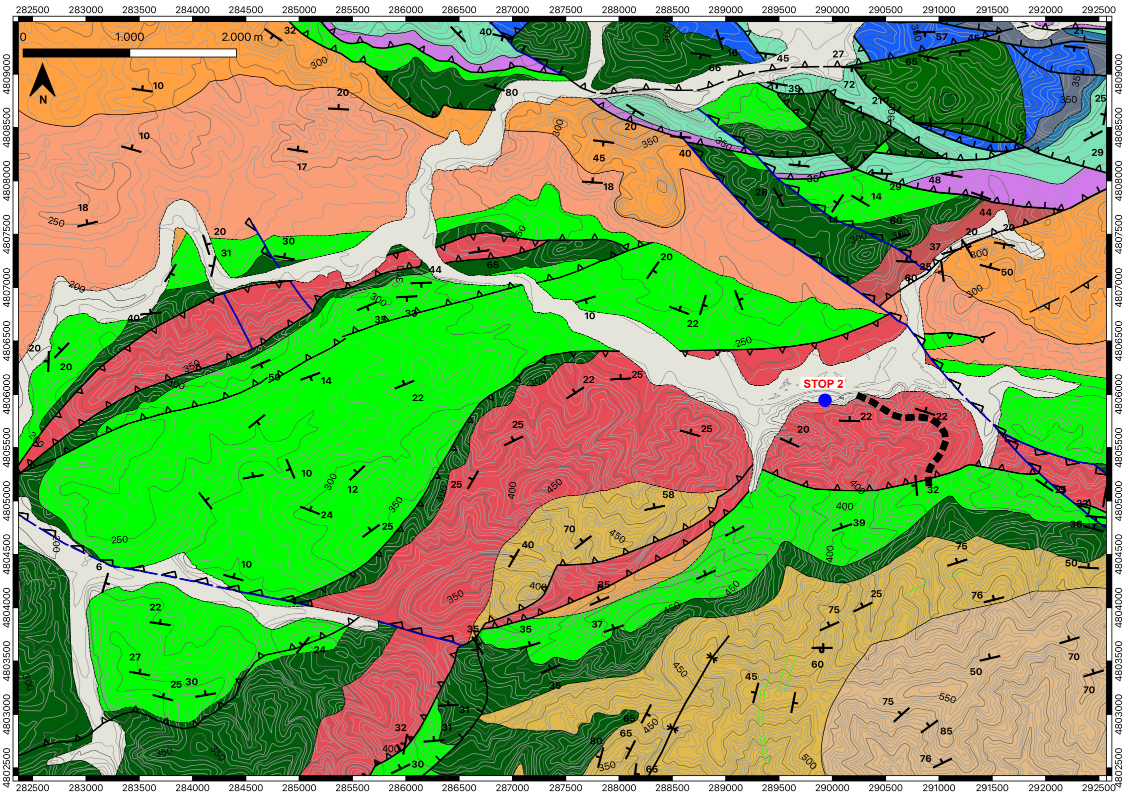

Figure 11. Geological map of the NE end of the La Justa-Aramil Alpine syncline. Modified from Merino et al. (2015). Legend in Fig.6. Modified from Merino-Tomé et al. (2011).

Petrology of the Permian volcanism of the Acebal Formation

Near Acebal village, volcaniclastic rocks are interbedded within the Permian sedimentary succession (Figure 12). Two different types of volcaniclastic deposits are exposed: pyroclastic surge deposits and ash-fall deposits.

Pyroclastic surge deposits include coarse-grained tuff and tuffaceous sandstone ranging in thickness from 5 cm to 5 m. In general, the whole series is characterized by thick bedding with normal grading of pyroclast sizes. Individual beds have internal laminations or show alignments of pyroclasts. Pyroclasts are subangular, equant to elongated, with sizes that can reach up to 2 mm. The deposits are moderately to poorly sorted, heterogeneous with variable proportions of juvenile fragments, cognate lithic pyroclasts, crystals, clastic fragments of sedimentary origin and glass shards. No welded fragments or flame structures have been identified.

Juvenile fragments are vesicle-poor chilled margins ranging in size from 2 µm to 2 mm. They are composed of ferromagnesian or feldspar microphenocrysts embedded in a fine-grained matrix with abundant opaque minerals and glass (Figure 13A).

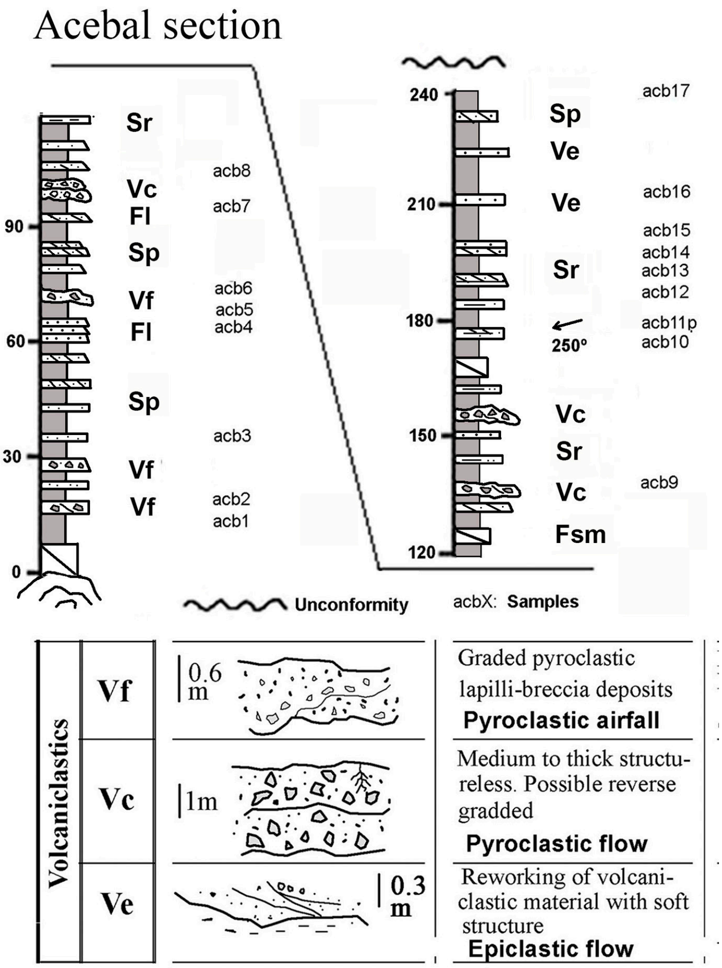

Figure 12. The Acebal section. Volcaniclastic rocks interbedded in the Permian sedimentary succession. To complete facies description, see figure 22.

Cognate lithic fragments are partially altered porphyritic andesites. These fragments contain phenocrysts of plagioclase and minor amphibole and/or biotite. Two subtypes can be identified depending on the modal proportion and composition of the ferromagnesian phenocrysts: a) amphibole andesites with rare pyroxene (Figure 13B), and b) biotite andesites (Figure 13C). Both types also contain feldspar microliths, quartz and magnetite in the groundmass. Apatite and zircon occur as accessory phases. The groundmass varies between felsitic to vitrophyric and usually shows quartz- or chalcedony-filled amygdales.

Isolated and partially broken igneous crystals similar to those included into the cognate lithic fragments are common. Glassy fragments are scarce and have small size. The sedimentary components are subrounded quartz and feldspar and rare mica crystals. Their proportion is variable although it increases towards the top of the Acebal series.

The series ends with a 5 cm-thick ash fall deposit interbedded within the sedimentary succession. This ash fall deposit shows well-defined internal lamination and is composed of crystal shards (Figure 13D).

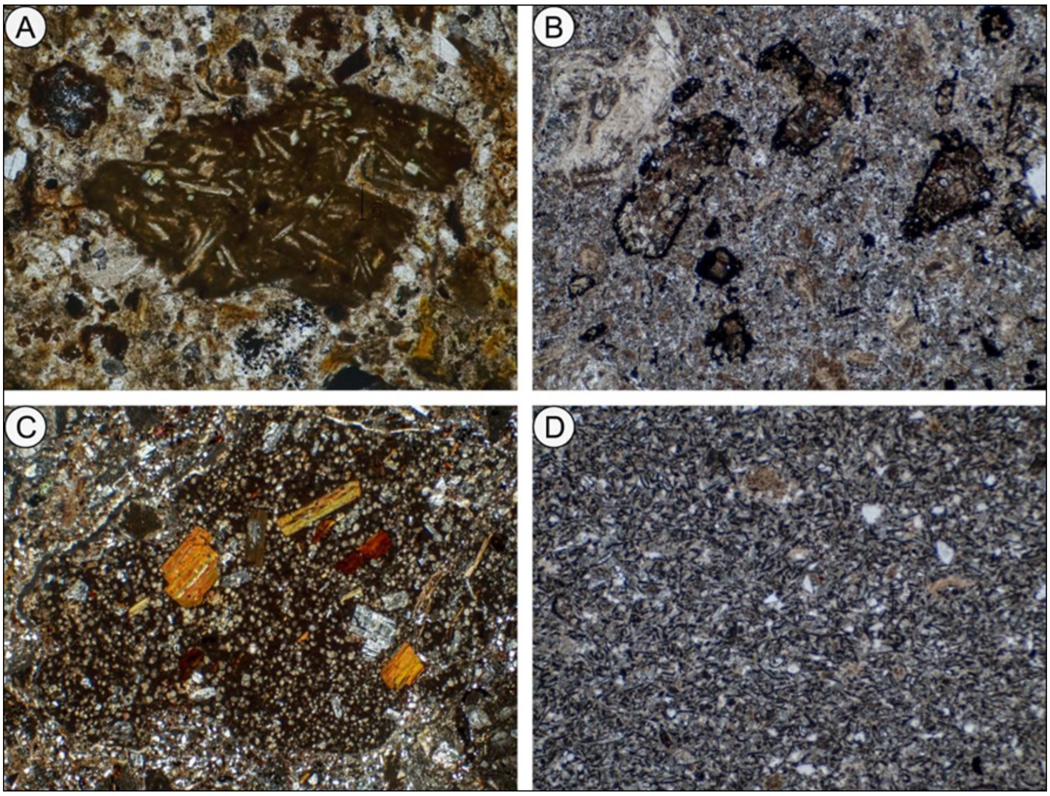

Figure 13. A) Microphotograph (parallel polars) of a juvenile fragment of chilled margin containing feldspar microphenocrysts embedded in a fine grained matrix with glass. B) Microphotograph (parallel polars) of a cognate lithic fragment of amphibole andesite. C) Microphotograph (crossed polars) of a cognate lithic fragment of biotite andesite. D) Microphotograph (parallel polars) of the ash fall deposit composed of crystal shards.

Composition and relationship with other Permian magmatism

This early Permian volcanism has an intermediate composition (andesites to dacites) with typical subalkaline geochemical affinities, but mainly calc-alkaline (Figure 14), showing a subsequent alkaline trend in the Pyrenees (Figure 14) that does not appear in the rest of the areas (e.g., Castro et al., 2002; Pereira et al., 2014). Late-Variscan and post-Variscan calc-alkaline magmatism has been identified in the Paleozoic basement of the Pyrenees, Iberian Chain, and Cantabrian Mountains (Fernández-Suárez et al., 2000; Castro et al., 2002; Corretgé et al., 2004; Gallastegui et al., 2004) and has recently been related to the end of the the Variscan orogen collapse (Lloret et al., 2021), which started in late Carboniferous times. In the western Cantabrian Mountains, located in the hinterland of the Variscan orogen, the plutonic massifs predominate, while in the

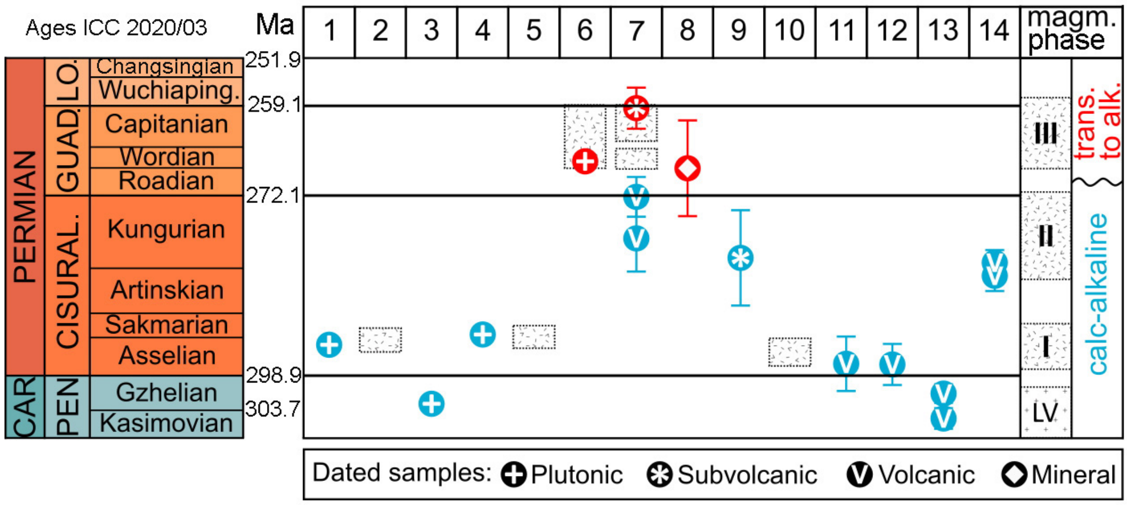

Figure 14. Compilation of age and geochemical data for the Permian magmatism in the Pyrenean–Cantabrian orogen belt. 1: Salas-Belmonte Stock, 2: Acebal-Siero section, 3: Infiesto Plutonic Complex, 4: Peña Prieta Stock, 5: Peña Labra Basin; 6: Cinco Villas Massif, 7: Somport-Anayet Basin, 8: Panticosa Pluton, 9: Lys-Caillouas Massif, 10: Castejón-Laspaúles Basin, 11: Erill Castell-Malpás Basin, 12: Estac-Baró Basin, 13: Cadí Basin, and 14: Castellar de N'Hug Basin. From Lloret et al. (2021).

Axial Zone of the Pyrenees the plutonic rocks alternate with volcanic successions, the latter being predominant in the Central Cantabrian Mountains, located in the foreland to foreland-hinterland transition of the Variscan orogen (Lloret et al., 2021). This magmatism ranged from the Late Pennsylvanian to the Cisuralian (e.g. Fernández-Suárez et al., 2000; Pereira et al., 2014 and references therein) (Figure 14). The dacitic-andesitic volcanism of the Cantabrian Mountains shares physical and compositional features with the Permian calc-alkaline outcrops of the Iberian Chain (Lago et al., 2004 and references therein).

Age of volcanism

There is no radiometric dating of the volcanic rocks of the Acebal Formation yet. However, the age of the post-orogenic Variscan magmatism of the Cantabrian Mountains basement is Asselian-Sakmarian, and it is mainly Asselian in the eastern Astur-Galaica Region (Gallastegui et al., 2004), where the Acebal section is located (Figure 14). López Gómez et al. (2019) proposed a tentative age of the Permian magmatism of the Acebal series as Asselian, being able to reach the Sakmarian. On the other hand, the alkaline magmatism of the Pyrenees is mainly Guadalupian (Figure 14).

<u>Relationship with basin evolution</u>

In the early Permian (Asselian), all the Variscan belt collapsed, leading to the formation of narrow and isolated basins. These basins were controlled by the reactivation of the Variscan and late Variscan structures, had close source areas and remained active throughout most of the Cisuralian. Basins related to the reactivation of Variscan structures are elongated in the direction of these structures, which range from NE-SW, such as La Justa-Aramil basin (Figure 5 and 6) to which stops 1 and 2 correspond. The extensional regime generated a calc-alkaline magmatism that produced the intercalation of volcanic rocks (Acebal Unit) in the Permian sedimentary successions (Suárez-Rodríguez, 1988; Valverde-Vaquero, 1992) and a large number of small plutonic bodies intruded close to the late Variscan faults (Gallastegui et al., 1990), which are Asselian in age. Related to the early Permian extensional collapse, a subhorizontal cleavage is developed, which cut the Variscan structures, and it is best developed in the Carboniferous rocks (mainly slates) of the Pisuerga-Carrión Region (Aller et al., 2004).

During the middle Permian (Guadalupian), the rifting of Pangea started in the Pyrenees, resulting in alkaline magmatism. At this latitude, the Pangea rifting is related to the Bay of Biscay opening, which separated the Iberian and Eurasian plates. This rifting process did not reach the Cantabrian Mountains until the Middle Triassic.

STOP 3:

<u>Location:</u>

Near Xivares beach, Asturias (Figure 5).

<u>Objectives:</u>

Synsedimentary faults, Variscan versus Alpine tectonics, early Permian (Artinskian – Kungurian) debris flow and channelized breccias. Upper Triassic distal fluvial facies with calcretes.

The Xivares beach is located in the Cabo Peñas Block of the Astur-Galaica Region, where the post-Variscan sedimentation is scarce. So, Jurassic sedimentation is absent and Permian, Triassic, and Cretaceous rocks appear in thin and isolated outcrops.

The SW boundary of the Cabo Peñas Block is the Ventaniella Fault, the main Late Variscan fault of the Iberian Massif, while its SE boundary is located in the Veriña fault, an Alpine reverse fault that reactivated a Variscan thrust (Figure 15). The Veriña reverse fault overlaps Ordovician rocks on Triassic and Jurassic rocks of the Gijón-Villaviciosa Unit of the Asturian Mesozoic Basin. The presence of Jurassic rocks in this unit implies a Mesozoic normal fault, currently buried under the Veriña fault, which separates the Cabo Peñas-Block to Gijón-Villavicios Unit: the Musel fault.

In the Xivares beach, the Permian sediments appear in a small basin (750 m wide), bounded by normal faults with Variscan trends (NE-SW), which may be partially inverted during the Alpìne orogen (Figure 15). These rocks probably belong to the upper member of the Sotres Formation (Figure 4). Close to these normal faults, proximal conglomerate facies are present. The Permian rocks rest unconformably on Devonian rocks (Rañeces Group), previously deformed in the foreland of the Variscan orogen (Cantabrian Zone) (Figure 15). In the Permian outcrops minor normal faults, locally synsedimentary, can be observed. Resting unconformably on the Permian rocks and also on the Devonian rocks further east and outside of the Permian basin, Triassic sediments of the Transición Formation (Figure 4) appear. The Triassic sediments are related to normal faults with NW-SE trend (Figure 15), produced by the reactivation of Late Variscan faults that are related to Ventaniella fault (Figure 5). The Transición Formation covers the Permian normal faults and appears folded by an open and asymmetric Alpine syncline. This fold is related to Veriña reverse fault and also with the inversion of the normal fault that limits by the E the Permian basin, where the western flank of this syncline is more upright.

The sedimentary record

The Cantabrian coast is dotted with Permian and Triassic outcrops with reduced lateral continuity. Most of the outcrops are not precisely dated and show significant folding and fracturing. The Xivares beach (Figure 16) is a good example of this sedimentary record. In this area, the different tectonic lineament directions and the support of a pollen dating in the neighboring beach of Moris allow us to clearly differentiate the Permian from the Triassic successions.

The Xivares succession is 38 m thick (Figure 16-1). It is subdivided into seven sections, A to G from base to top respectively, of which the lower five ones (A-E) belong to the Permian and the upper two (F-G) to the Triassic. Although there are not enough data to make a precise temporal attribution, we consider that it may belong to the lower part of the Sotres Formation (Artinskian, early Permian) due to the absence of volcanic material (typical of the Acebal Formation) and carbonate rocks (common in the middle and upper part of the Sotres Formation). The discussion about the age of the

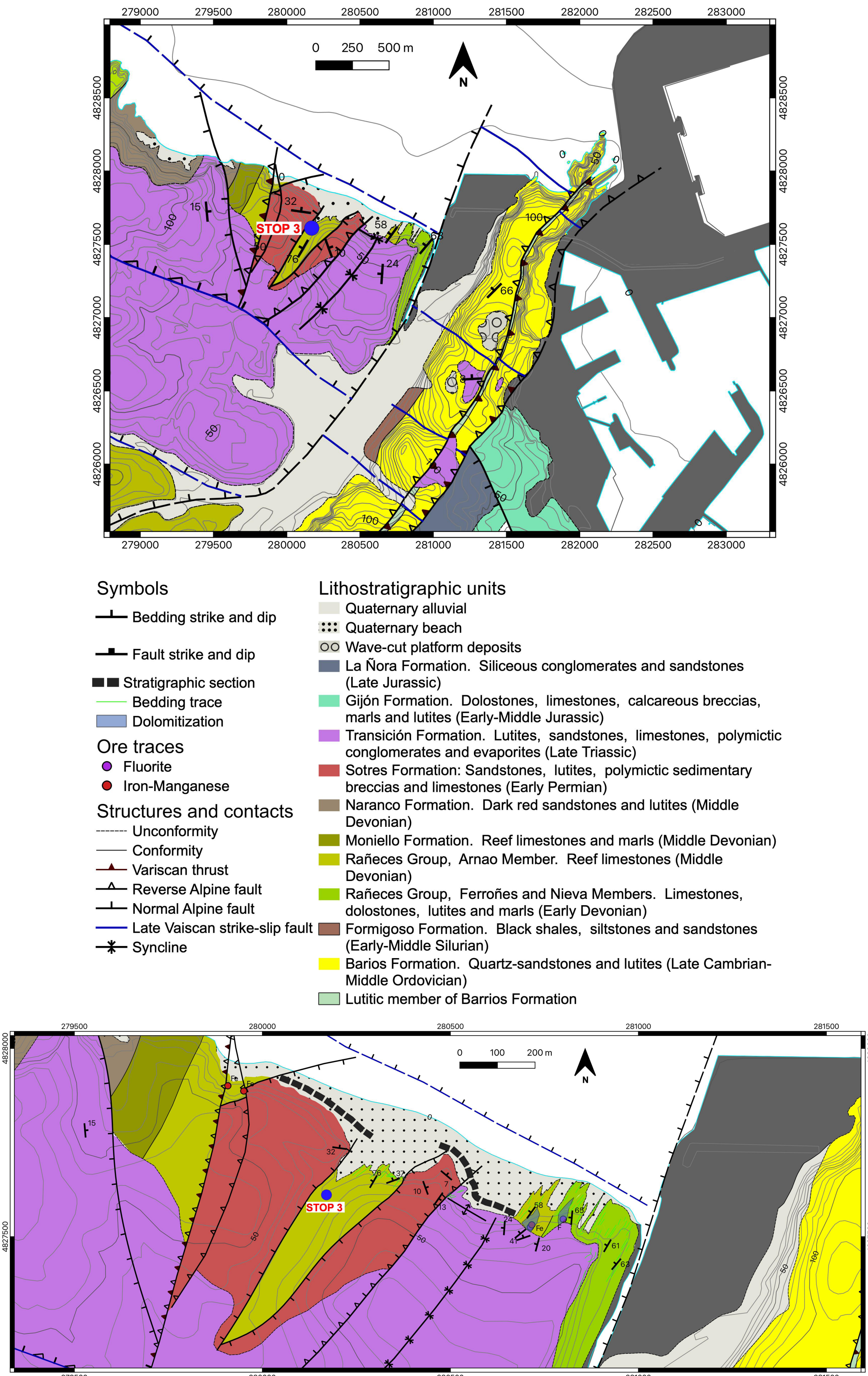

Figure 15. Geological map and detail of the Xivares beach surroundings (Asturias).

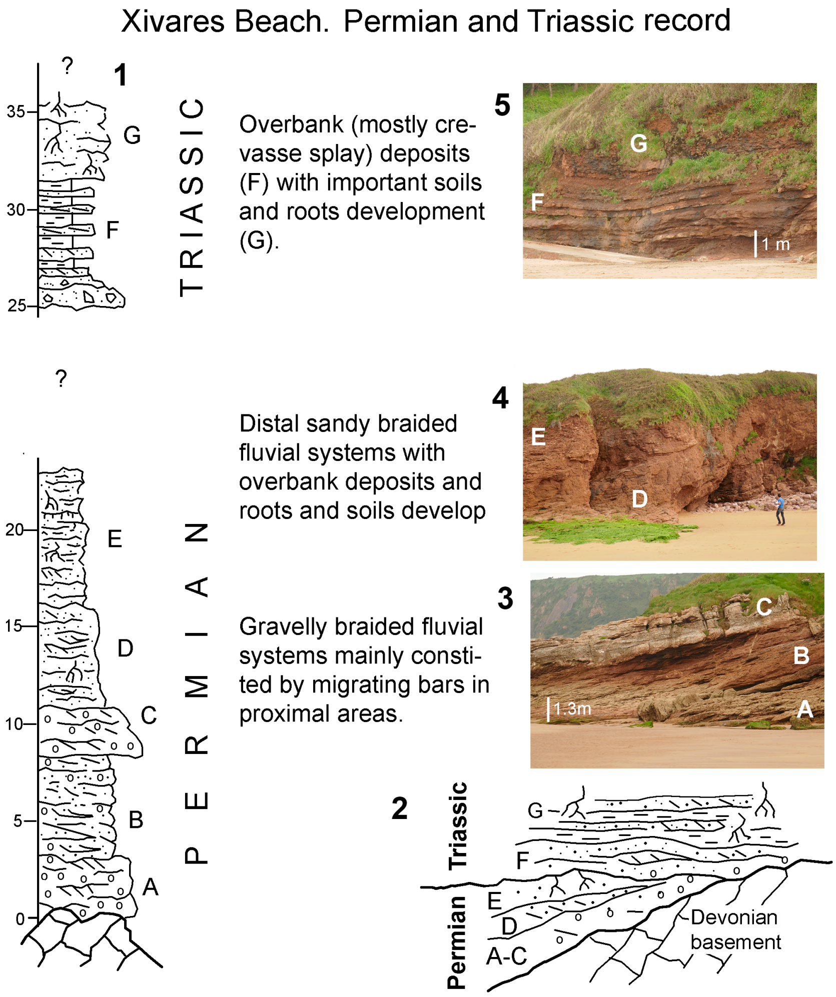

Figure 16. Xivares beach log. It shows two incomplete sections of Permian and Triassic ages, and both of them may rest unconformably on the Devonian basement.

Sotres Formation will be addressed in Stop 4. On the other hand, the age of the Triassic succession is probably Late Triassic, based on the comparison of these rocks with the similar well-dated sedimentary record of the Arenal de Moris beach, as will be explained in detail in the Stop 9 (Figure 5).

The characteristics of the Permian sedimentary succession of the Xivares beach were linked to important fault activity in the basin margin and the later erosion produced by the Triassic sedimentation. As result, the Triassic rocks are unconformable on the Permian rocks, and both are unconformable on the Devonian basement as well (Figure 16-2).

-Sections A to C are constituted by clast-supported (A and C) and matrix-supported (B) conglomerate (Figure 16-3). They constitute 0.7 to 1.6 m thick beds with planar and trough cross-stratification, although the lower part (A) shows beds without clear sedimentary structures. Subsections A and B show finning-upwards trends, while subsection C indicates a reactivation of the sedimentation. They represent gravelly braided fluvial systems mainly constituted by migrating bars in proximal areas (e.g., Owen et al., 2017).

Sections D and E are represented by 0.3 – 0.6 m thick sandy red beds with planar and trough cross-stratification and current ripples (Figure 16-4), although size of the structures decrease in subsection E. Fine and medium-grained beds are intercalated, and all of them are cut by prominent root trace fossils and incipient soil development. They represent distal sandy braided fluvial facies with development of overbank deposits with long periods without sedimentation when vegetation and soils developed dislocating previous sedimentary structures (e.g., Bennett et al., 2016; Gulliford et al., 2017).

Sections F and G represent the Triassic sedimentary record of the Xivares beach log. Subsection F starts with a 0.9 m thick bed of breccia (Figure 16-5). Above this, a succession of dark red 0.2 to 0.5 m thick siltstone and sandstone alternating beds develops. These beds show flat base, low-angle planar and cross-stratification and reach tens of meters of lateral extension. They are interpreted as overbank (mostly crevasse splay) deposits. Section G is probably represented by a similar succession than F subsection, but in this case, it shows bad preservation probably due to roots and soil development, recording more distal and/or less sedimentary accumulation (Kraus and Middleton, 1987; Burns et al., 2017).

THUESDAY 5TH

It comprises Stops 4, 5 and 6. See Figures 5 & 17 for their locations.

STOP 4:

Location:

Tresviso village, Cantabria (Figures 5 and 17)

Objectives:

Variscan tectonics, first stages of the Alpine cycle and fault reactivations. Lower member of the Sotres Formation (Artinskian-Kungurian) constituted by Alluvial (siliciclastics). Includes: Paleosols, paleoichnology, sedimentology and mineralogy.

Tresviso village (Cantabria) is located at an altitude of 907 m, within de Picos de Europa National Park (Eastern Massif). From a geological point of view is located in the Picos de Europa Unit (Figure 18) of the Cantabrian Zone (Figure 1b), the most external of the Variscan Orogen of the NW Iberian Peninsula and also in the western part of the Astur-Galaica Region of the Alpine Cantabrian Cordillera.

The Picos de Europa Unit is a tight imbricate system of Variscan thrust (Figure 18), which mainly affected Carboniferous limestones. These thrusts have a S/SSE tectonic transport and a Kasimovian-Gzhelian age, based on the age of the related synorogenic sediments (Merino-Tomé et al., 2009). The Picos de Europa thrust system is subsequently affected by NNW-SSE dextral strike-slip faults (Figures 17 and 18), which represent the Late Variscan deformation, developed in late Gzelian-earliest Asselian times (Heredia et al., 2022).

In Cisuralian times, the Variscan orogenic collapse took place in this area, developing post-orogenic, narrow and isolated basins, such as the Tresviso-La Hermida-Carmona basin (Figures 2 and 17), where the Sotres Formation was deposited. These basins are related to extensional faults that reactivated Variscan faults.

For the next 30 My, there was no post-orogenic sedimentation in the Picos de Europa Unit, favouring a deep karstification of the Carboniferous limestones of this unit.

In Middle-Late Triassic times, sedimentation resumed with the deposition of the Cicera Formation (Figure 17). During the deposition of this formation, basins expanded and some of the Permian extensional faults became inactive (Figure 17).

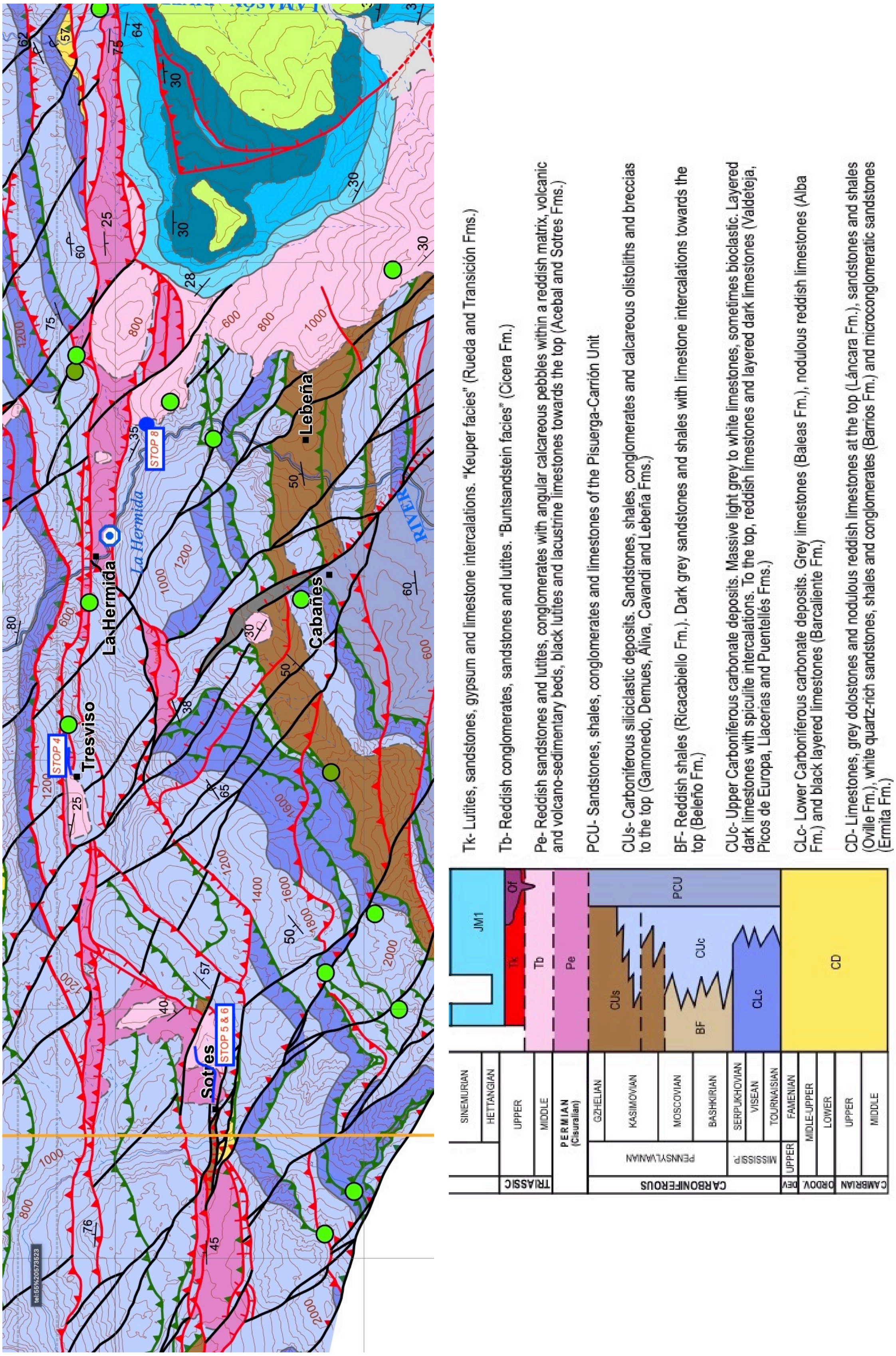

Figure 17. Synthetic geological map of the eastern sector of the Picos de Europa unit, showing the Stops 4, 5, 6 and 8 (4th and 5th of July). Modified from Heredia et al. (2022).

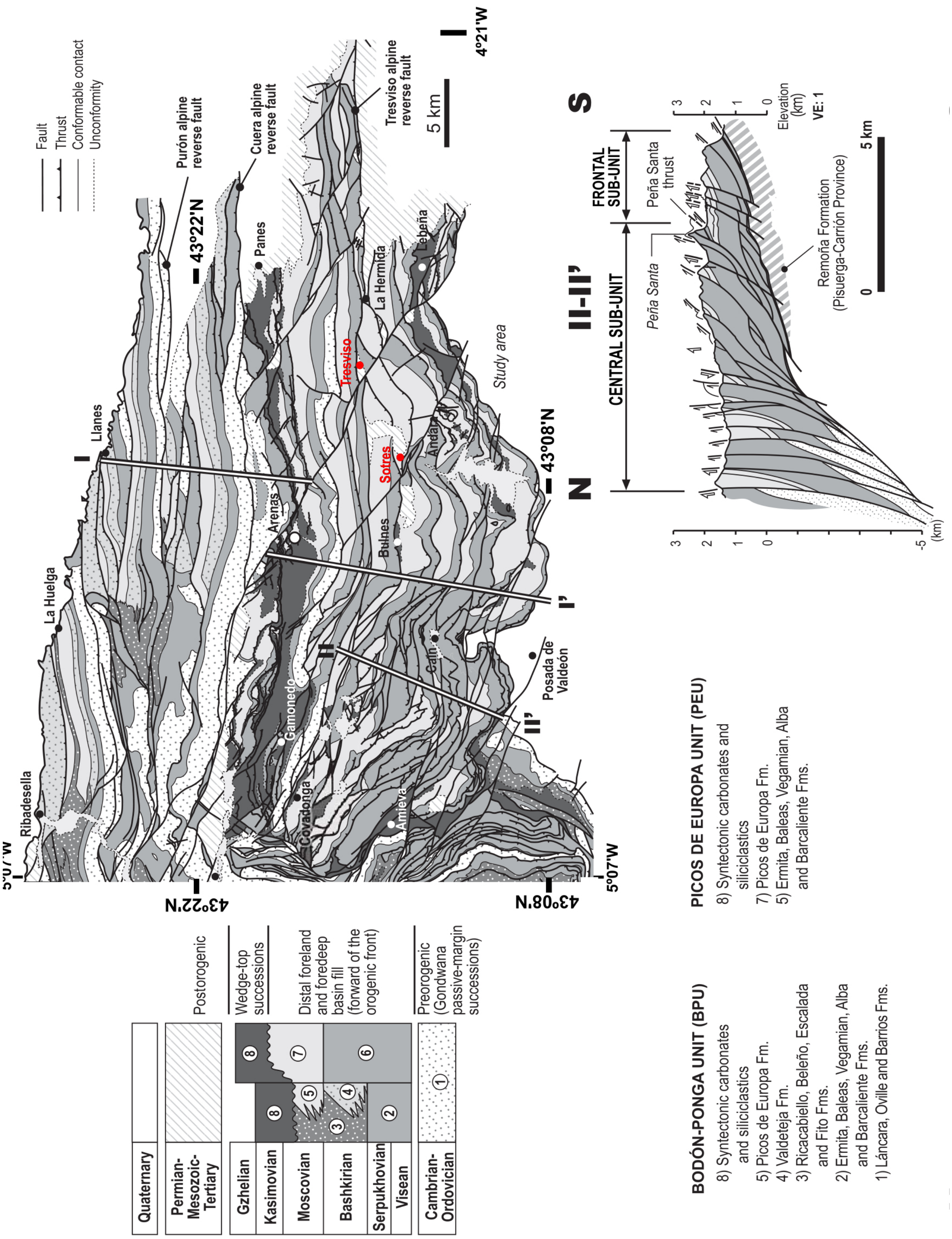

Quaternary
Permian-Mesozoic-Tertiary
Postorogenic
Gzhelian
Kasimovian
Moscovian
Bashkirian
Serpukhovian
Visean
Cambrian-Ordovician
Wedge-top successions
Distal foreland and foredeep basin fill (forward of the orogenic front)
Preorogenic (Gondwana passive-margin successions)
BODÓN-PONGA UNIT (BPU)
8) Syntectonic carbonates and siliciclastics
5) Picos de Europa Fm.
4) Valdeteja Fm.
3) Ricacabiello, Beleño, Escalada and Fito Fms.
2) Ermita, Baleas, Vegamian, Alba and Barcaliente Fms.
1) Láncara, Oville and Barrios Fms.
PICOS DE EUROPA UNIT (PEU)
8) Syntectonic carbonates and siliciclastics
7) Picos de Europa Fm.
5) Ermita, Baleas, Vegamian, Alba and Barcaliente Fms.
Fault
Thrust
Conformable contact
Unconformity
Purón alpine reverse fault
Cuera alpine reverse fault
Tresviso alpine reverse fault
5 km
4°21'W
5°07'W
43°22'N
43°08'N
Ribadesella
La Huelga
Llanes
Panes
La Hermida
Lebeña
Tresviso
Sotres
Andara
Arenas
Bulnes
Gamonedo
Covadonga
Amieva
Cain
Posada de Valdeón
Study area
I
I'
II
II'
N
S
II-II'
CENTRAL SUB-UNIT
FRONTAL SUB-UNIT
Peña Santa
Peña Santa thrust
Remoña Formation (Pisuerga-Carrión Province)
Elevation (km)
VE: 1
5 km
(km)

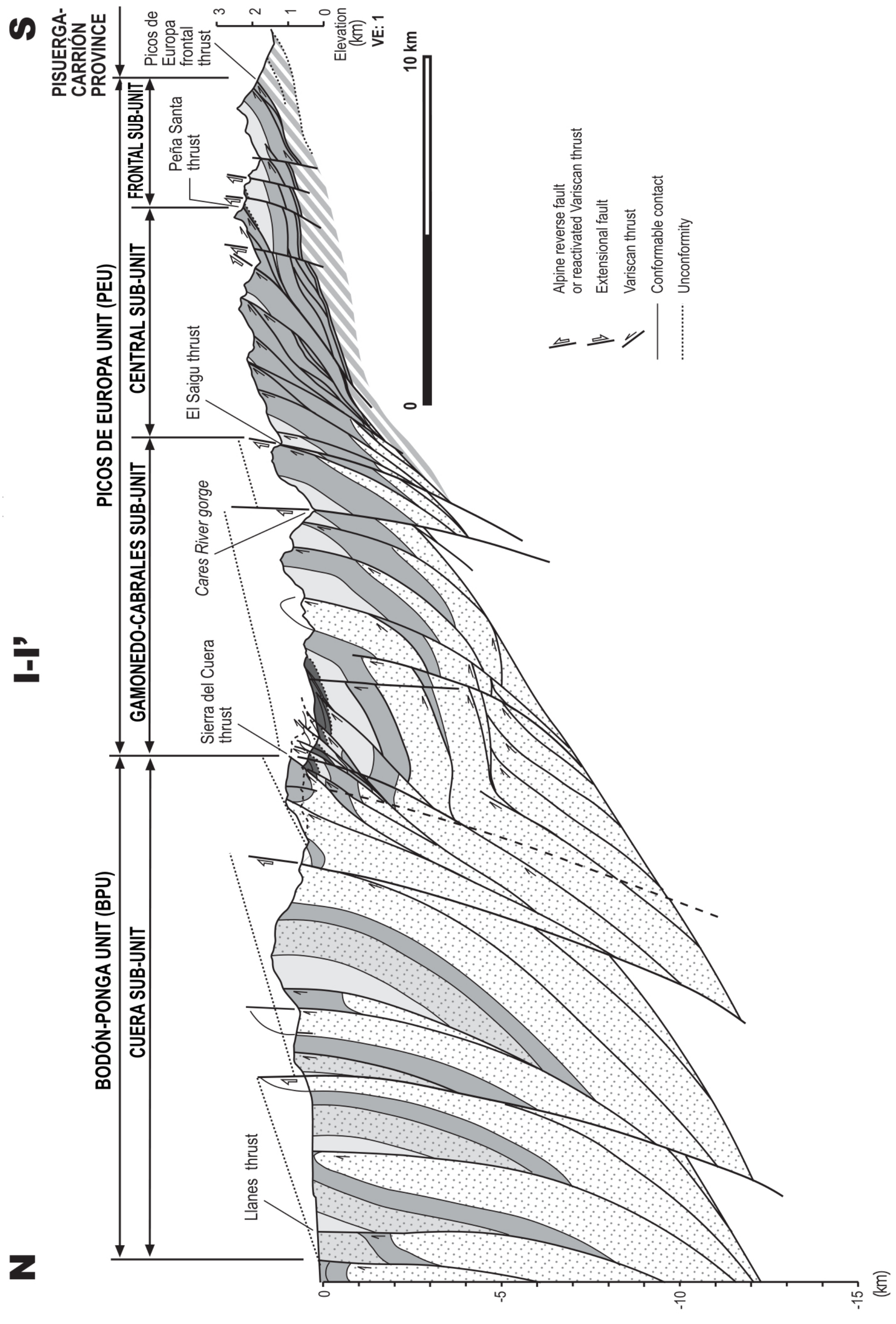

Figure 18. Synthetic geological map and cross sections of the eastern part of the Bodón-Ponga and Picos de Europa units (Cantabrian Mountains, NW Spain). Cross-section I-I' (Merino-Tomé et al., 2009) shows the structure of Cuera Sub-Unit and the central part of Picos de Europa Unit, and II-II' (Farias and Heredia, 1994) lies along the western part of Picos de Europa Unit. VE= Vertical Exaggeration of 1x. Modified from Merino-Tomé et al (2009).

In Cenozoic times (late Eocene-early late Miocene), the Alpine Pyrenean orogeny developed. At this time, the Picos de Europa Variscan Unit was affected by reverse faults, which reactivates, in many cases, Variscan thrusts and Late Variscan faults (Figures 17 and 18). In the Tresviso area, the Cabuerniga Fault System (red faults in Figure 17) is the main Alpine compressive structure (Figures 5, 19 and 20), which produced the fragmentation of the Tresviso-La Hermida-Carmona Permian basin (Figure 17). The Cabuérniga fault system crosses E-W the northern Cantabrian Mountains, close to the Cantabrian sea, for more than 250 km (Heredia et al., 2022) (Figure 5).

In the upper part of the old mining track from Tresviso to Urdón, a small piece of the Tresviso-La Hermida-Carmona basin can be observed (Figure 19). In this section, the Permian sediments are bounded to the S by a normal fault (La Hermida fault) and by a reverse Alpine fault (Cabuérniga fault) to the N, faults that are separated by a few tens of meters. The normal fault is covered by the Triassic rocks located above the Tresviso village (Figure 17).

From a curve of the Urdón track and looking towards the E, the La Hermida sector of this basin can be observed. In this sector, located in the Deva River valley (La Hermida Gorge), the Cabuérniga and La Hermida faults are somewhat more separated and on the latter the La Hermida spa is located (Figure 20). This spa uses the hot waters of one of the thermal springs in the area, which emerges at about 65º C.

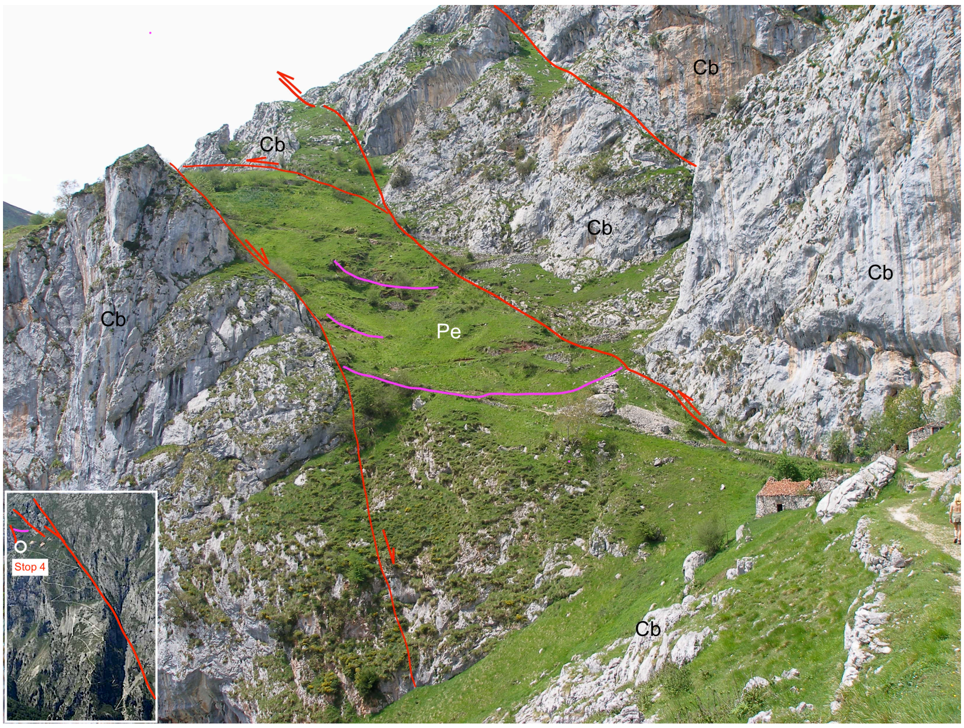

Figure 19. Fragment of the Tresviso-La Hermida-Carmona Permian basin in the upper part of the old mining track Urdón-Tresviso (Urdón Canyon), close to the Tresviso village (Cantabria). Cb- Carboniferous limestones, Pe- Permian Sotres Formation.

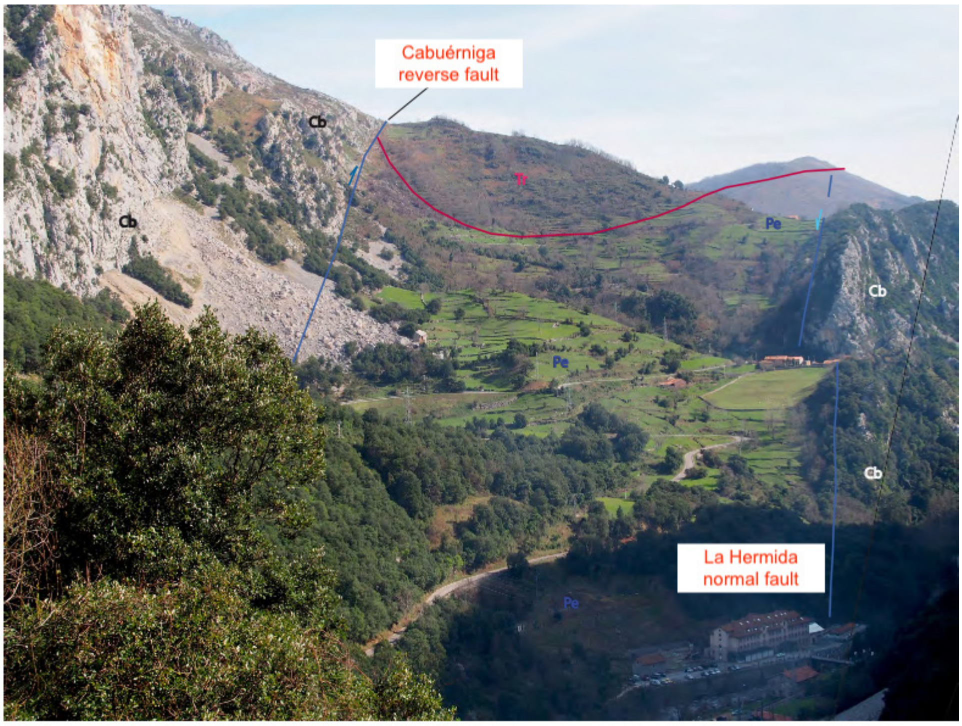

Figure 20. The Tresviso-La Hermida-Carmona Permian basin in the Deva River valley (La Hermida spa sorroundings). Cb- Carboniferous limestones, Pe- Permian Sotres Formation, Tr- Triassic Cicera Formation

<u>The Lower Member of the Sotres Formation</u>

The lower Permian sedimentary record in the Tresviso-Sotres area belongs to the Sotres Formation (Figure 3). This unit, which is Artinskian-Kungurian in age, as will be discussed later, is divided into Lower, Middle, and Upper members (Figure 21). In the Tresviso area, only crops out the Lower member, which is unconformable on the Carboniferous limestone and dolomite of marine origin, and it is truncated in its upper part due to tectonics (Figure 21). The Lower Sotres Formation in this area is constituted by siltstone/claystone with intercalated sandstone, although conglomerate and thick sandstone bodies also appear in other more subsidence areas (e.g., Peña Sagra section, Figure 2).

Near the Pico Paraes site, in the Peña Sagra section, data obtained from footprints allowed Gand et al. (1997) to ascribe the Sotres Formation (section erroneously considered as part of the Caravia Formation by Martínez-García,1991) an Artiskian - Kungurian age (early Permian). These authors also found a fragment of Supaia sp. and recently, López-Gómez et al. (2019) reported a new Supaia sp. specimen in the Lower Member of the Sotres Formation, in the same section of Peña Sagra, and probably in equivalent beds to the ones described by Gand et al. (1997).

Sedimentology

The sedimentary study of the Sotres Formation was carried out in detail by López-Gómez et al. (2021) based on the differentiation of facies and facies associations (Figure 21). The Lower Member of the Sotres Formation is constituted by facies associations B and C (Figure 22), and synthetically their interpretation are:

Facies association B: Migration of 2D and 3D dunes in braided fluvial systems under variable flow conditions (Owen et al., 2017).

Facies association C: Overbank sediments deposited on floodplains in low-energy or distal areas of fluvial systems (Bennett et al., 2016; Gulliford et al., 2017).

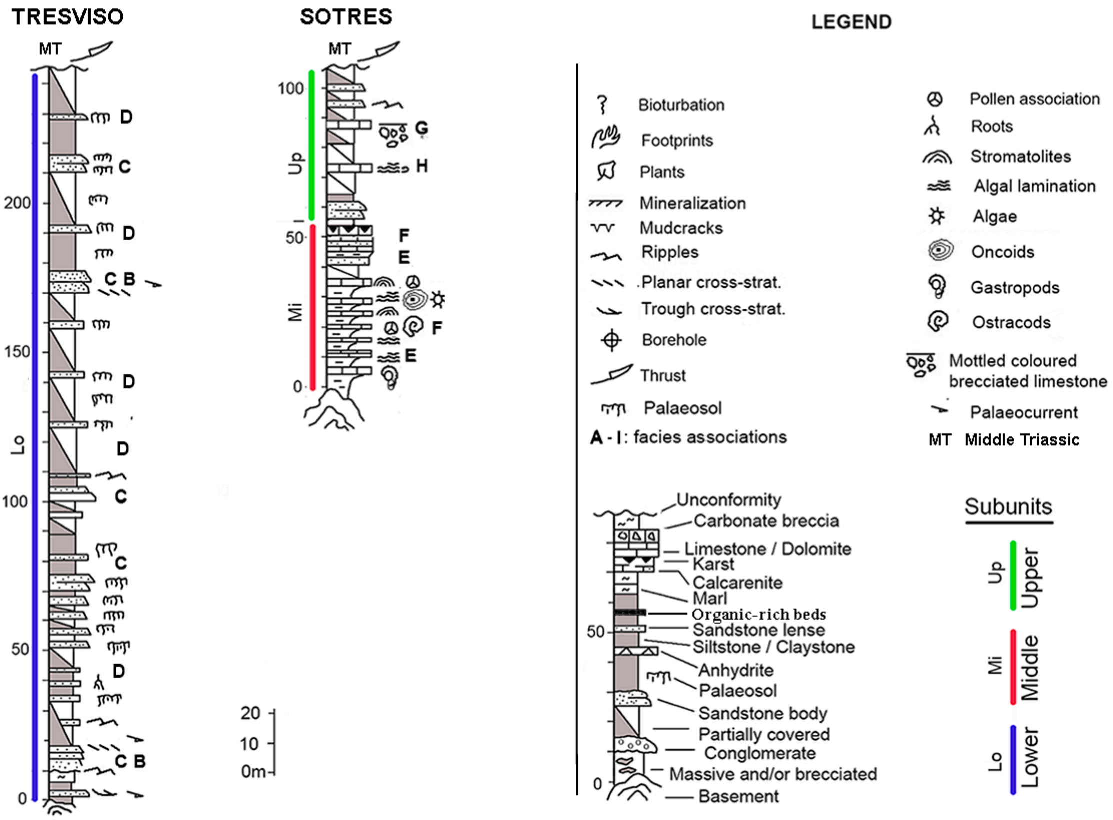

Figure 21. Sotres Formation in Tresviso and Sotres sections. Modified from López-Gómez et al. (2021). See figure i for the descriptions of facies associations A to I.

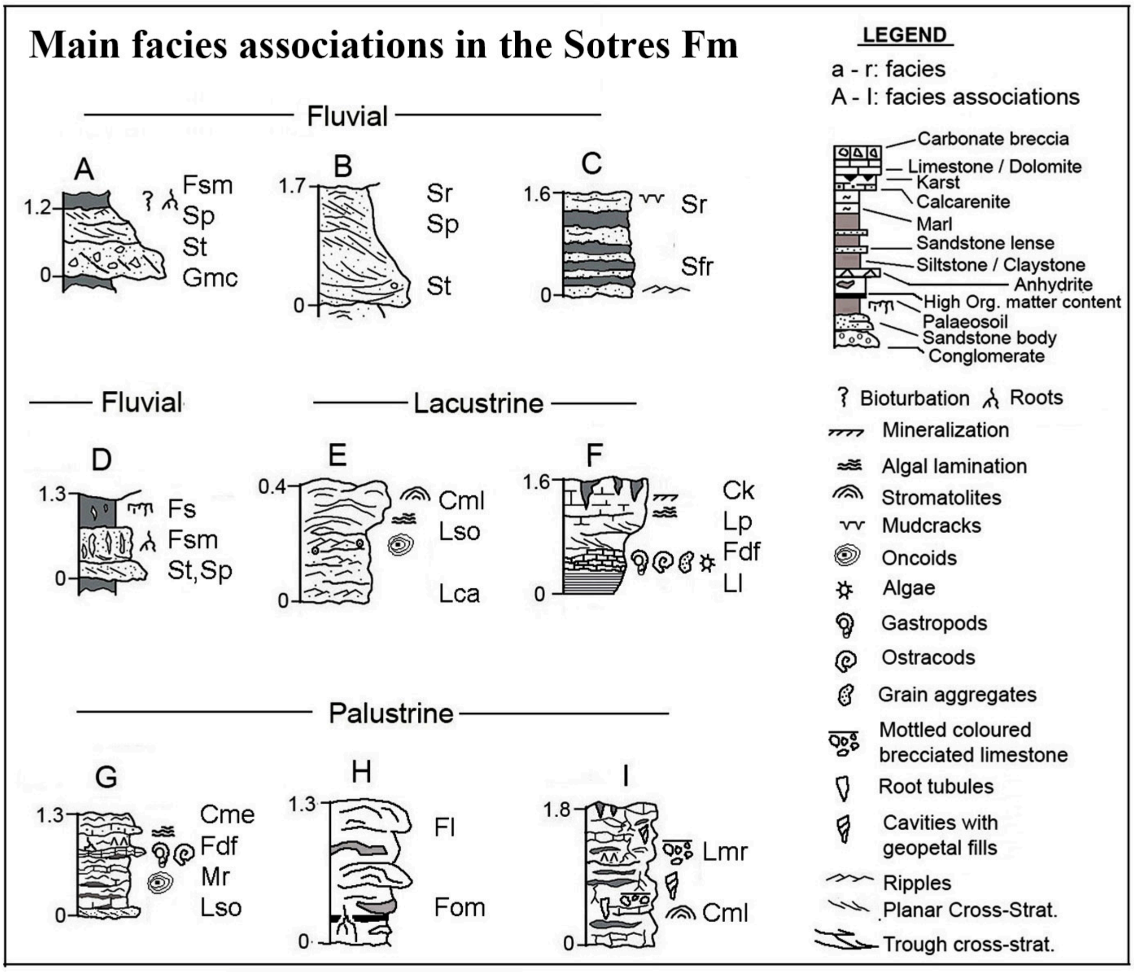

Codes of facies

Gmc: Clast-supported crude organized subangular gravels

St: Fine to coarse-grained sandstones constituting solitary or grouped trough cross-bedding stratification.

Sp: Fine to coarse-grained sandstones with isolated clasts of quartzite constituting solitary or grouped planar cross-bedding stratification.

Sr: Fine to medium-grained sandstones with current ripples, dessication craks and possible plant remains.

Sfr: Alternating medium to fine-grained sandstones and siltstones with fine lamination and ripples.

Fsm: Massive mudstones, siltstones and fine-grained red sandstones deformed by soils development that may show carbonate nodules.

Fs: Massive mudstone with incipient soils.

Fom: Centimetre-thick intercalated beds of massive green marls, red mudstones and gray organic-rich marls disrupted by roots and bioturbation.

Fdf: Poorly rhythmic laminated centimeter-thick mudstone beds with ostracods, gastropods and algae.

Fl: Intercalated mottled siltstones with laminated (dome-like) limestones.

Cml: Carbonate microbial lamination, with possible dome-like structure, constituting millimeter to centimeter-thick beds

Cme: Alternating fine and wavy beds of mottled mudstones, marls, limestones and evaporites that may show biogenic dome-like lamination, bioturbation by roots and coated (pedogenic) grains.

Ck: White massive carbonate beds with karstic surfaces.

Lso: Fine to medium-grained sandy limestone beds with oncoids and small current and oscillation ripples.

Ll: Centimeter-thick beds of laminated dark limestones.

Lp: Well-stratified centimeter-thick gray limestones with small-scale planar cross-stratification and shell fragments.

Lmr: Alternating gray limestones with micobial lamination and mottled marly siltstones. It constitutes centimeter-thick beds that may be disrupted by roots and thin evaporite beds that may constitute dissolution breccia. Coated grains, less than 1mm, and micro karst structures are common.

Lca: White limestones and/or fine-grain calcarenite beds with small-scale planar cross-stratification.

Mr: Centimeter-thick wavy beds of alternating red and green organic-rich marls and structureless or lightly ondulated white limestones disrupted by roots. Intercalated millimeter-thick calcarenite beds may appear.

Figure 22. Facies and facies associations of the Sotres Formation.

Mineralogy

The mineralogical assemblage in samples of the Sotres Formation It is dominated by quartz and clay minerals, along with minor hematite and calcite. Illite is the only mineral present in the clay fraction in samples from the Lower Subunit and is probably the result of a period of very low weathering of the source area. The degree of diagenesis is greater in this subunit than in the rest of the formation, but no traces of kaolinite or smectite were found, suggesting limited chemical weathering during this time frame (Figure 23).

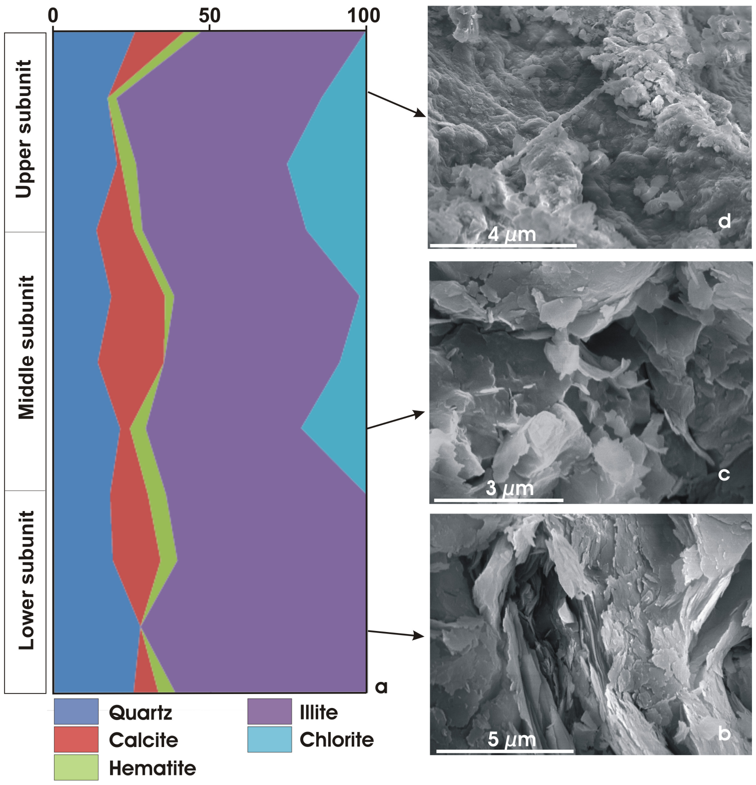

Figure 23. Mineralogical changes in the three members of the Sotres Formation.

Paleosols

Three pedotypes (1-3) were differentiated and classified in the Lower Sotres Formation in López-Gómez et al., 2021). These paleosols show clear vertical distribution when they are detected in a synthetic stratigraphic section (Figure 24).

Pedotype 1: It is developed on sandy materials and is characterized by a subsurface red (10R7/3) horizon with drab-haloed root traces and mottles of drab colours on top of a superficial calcareous horizon (Bk) of purple hue (Figure 24-1A). Carbonate accumulation was classified as Machette's (1985) stage II. The distance from the top of the profile to the Bk horizon does not exceed 12 cm. Drab-haloed root trace fossils are grey in the centre and greenish on the outside. Most likely, they were produced during burial through the reduction of iron around the root (Retallack, 2001). In thin section, pedotype 1 features a compact grain microstructure, with sand-sized grains and fine material between them (Figure 24-2A). Some voids, filled with clay coatings, are pedofeatures indicative of illuviation. Greenish mottling and the purple hue have been interpreted as produced by periodic waterlogging. We classified this pedotype as a gleyed Calcisol (Mack et al.,1993).

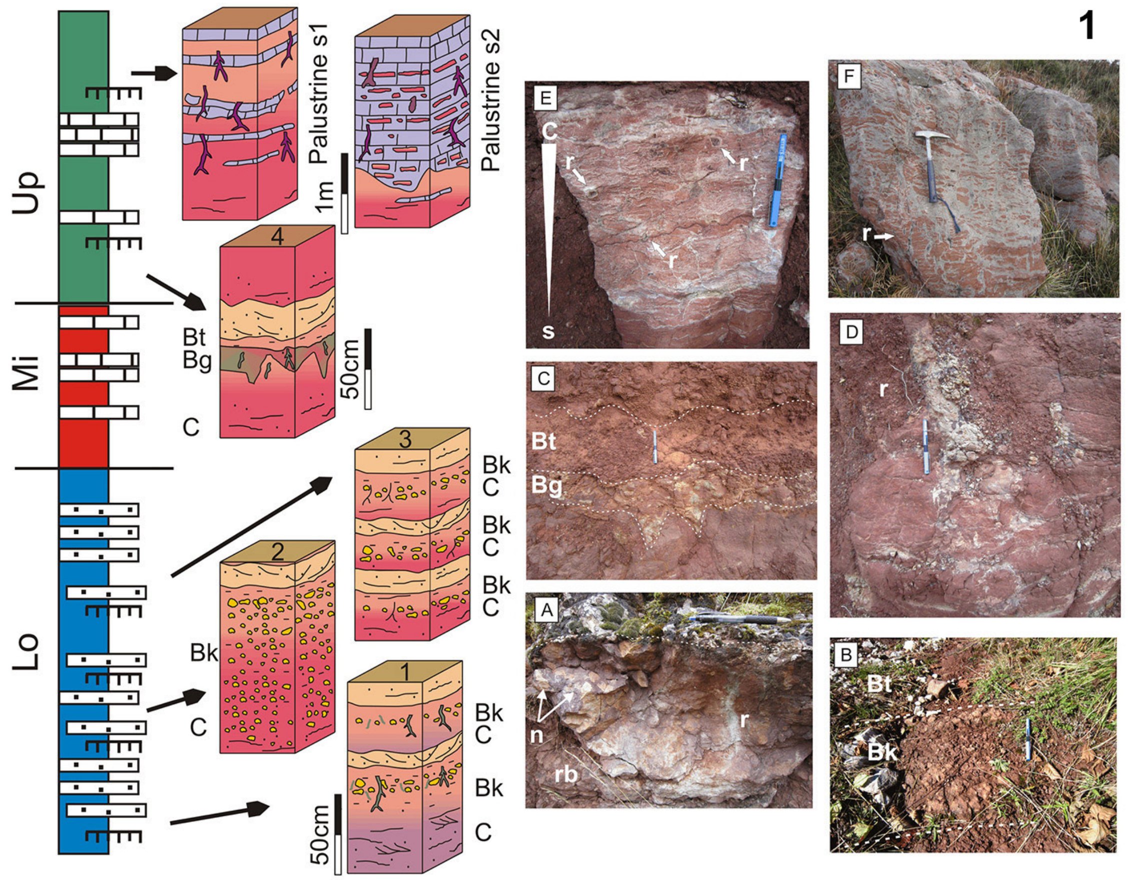

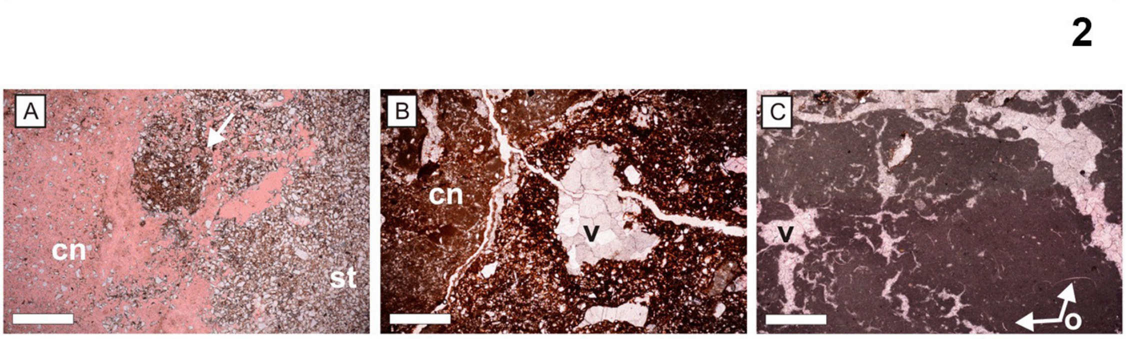

Figure 24. Pedotypes of the Sotres Formation. See text for the description.

Pedotype 2: It shows a very thick Bk horizon, locally reaching 110 cm. This calcareous horizon is composed of nodules of 2-3 cm at stage III of carbonate accumulation developed on red 10R5/8 sandy silt materials below a subsurface clayey horizon of 10-15 cm. Small rhizoconcretions can be also observed. Carbonate is obvious in nodules but also dispersed in the groundmass. Voids filled with euhedral calcite and with a smooth ring of ferruginous material are related to former roots (Figure 24-2B).

Pedotype 3 is also classified as a calcisol, but in this case the Bk horizon is 30-40 cm thick (Figure 24-1B). In the field, this type of pedotype shows a thin (10 cm) and clayey subsurface with root trace fossils on top of the Bk horizon. In places, several levels of this pedotype are repeated one on top of the other (Figure 24-1).

The presence of Bk horizons suggests mean annual rainfall rates lower than 1000–1200 mm (Retallack, 2001). Calcareous horizons are common in arid and semi-arid conditions (up to 600 mm). The calcareous pedotypes described in the Lower Subunit display very shallow Bk horizons (~10 cm) indicating pedogenesis in arid regions. In addition, the thickness of the Bk horizon can be interpreted as a sign of seasonality (Retallack, 2005). While in modern temperate soils, the thickness of the Bk horizon is <50 cm, in tropical monsoon regions of Pakistan and Kenya, this thickness is ~100 cm (Retallack, 2005). Pedotype 2 has a Bk horizon 110 cm thick that is probably the result of strongly monsoon climate conditions, where there are large differences in precipitation between dry and wet seasons.

Paleoichnology

The Sotres Formation is characterised by an extremely low-diversity trace-fossil assemblage comprising Planolites and Palaeophycus. Suites are monospecific and present in overbank mudstone, siltstone, and fine-grained sandstone in the Lower Subunit. The poorly preserved burrow morphologies and the absence of bioglyphs suggest that the traces were emplaced in softgrounds formed in floodplain water bodies. These deposits are locally moderately to intensely bioturbated and are relatively common in the lower interval of the studied unit. Trace fossils are rare in the upper interval, which is characterised by the extensive development of paleosols. The overall trend of a reduced intensity of bioturbation and abundance of ichnofossil-bearing layers may be attributable to palaeoenvironmental or preservation factors. The paucity of bioturbation may reflect a progressive increase in aridity. Alternatively, bioturbation may have been obliterated by soil development.

STOP 5:

Location:

Tresviso-Sotres road (Figure 5), the La Caballar Pass.

Objectives:

The end of the Variscan tectonics activity. Early Permian – Middle Triassic unconformity. The Cicera Formation (late Ladinian – early Carnian).

Sotres village (Asturias, 1050 m.a.s.l.), is located 12 km east of Tresviso (Cantabria) and near the Duje River, that separates the Central (to de W) and Eastern massifs of Picos de Europa (Figure 25).

In the Sotres village sorroundings, on both sides of the Duje River valley (between the Pandébano and Xitu de Escarandi cols), rocks formed in the Permian-Triassic Sotres basin crop-out (Figure 26). The Sotres basin is bounded by Permian normal faults, reactivated in Triassic times. During the Alpine orogeny, the northern edge was affected by a reverse fault, related with the Alpine Cabuerniga fault system (Figures 25 & 26). Between La Caballar col (1253 m) and the Sotres village, the best section of the Sotres basin is found.

Figure 25. The vegetated Permian outcrops (Per) of the Sotres basin in this locality and in the Pandébano col, both separated by the Duje River valley. In the col, the Permian rocks are bounded by the Pandébano Permian normal fault (to the left) and the Cenozoic Cabuérniga reverse fault (both in red lines). An Alpine reactivation of the San Carlos Late Variscan fault (blue line) also affects the Permian rocks. South to the left.

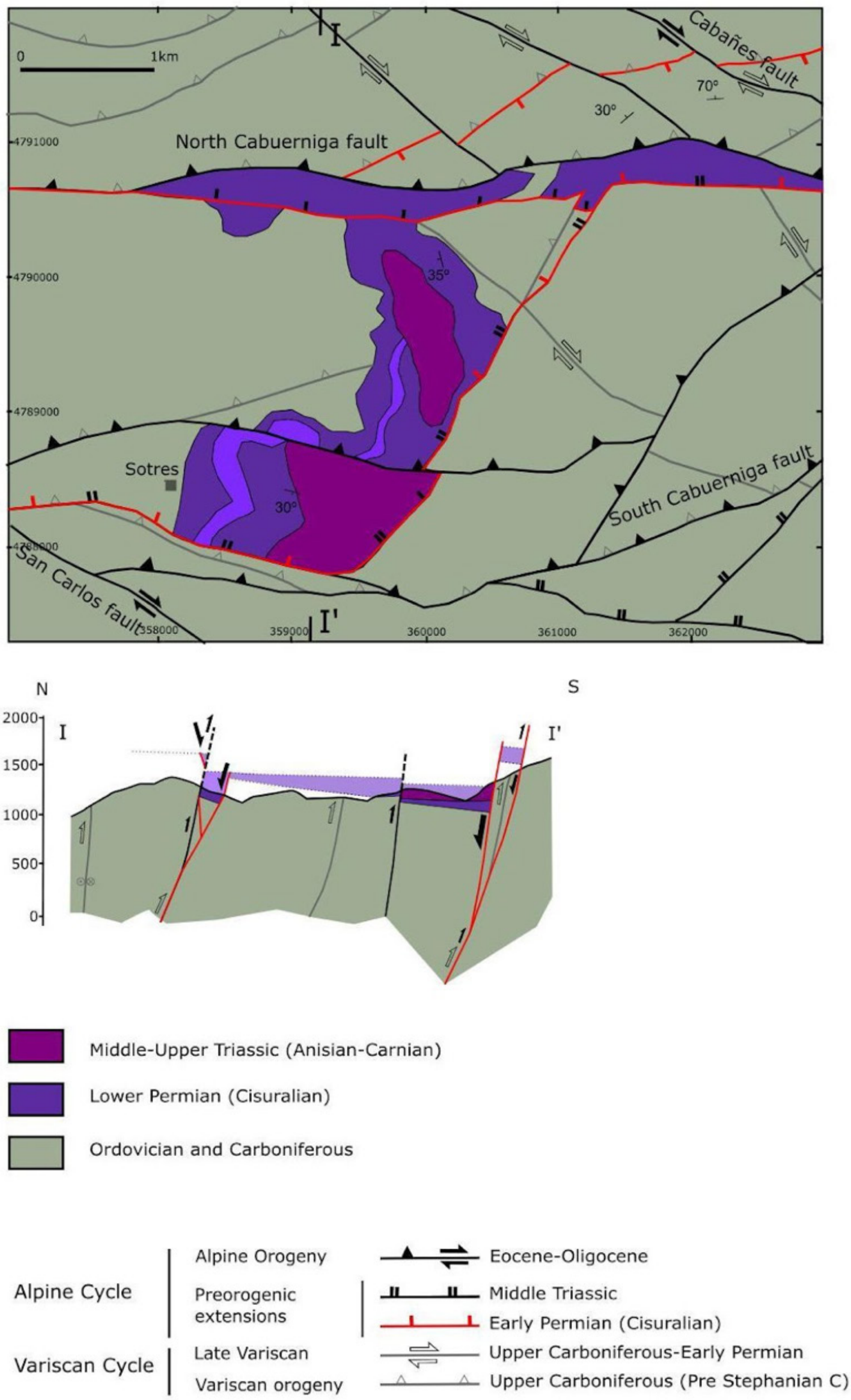

Figure 26. Geological sketch map and cross section of the Permian Sotres basin in the Sotres village surroundings. (Modified from López-Gómez et al., 2021).

Stratigraphy. The Permian-Triassic unconformity in the Sotres basin

The Permian and Triassic sedimentary record in the Cantabrian Mountains is separated by an unconformity (Figure 27). This unconformity separates the Sotres Formation (Artinskian-Kungurian) from the Cicera Formation (Ladinian-early Carnian) (Figure 3). In the Sotres area, the upper Cicera Formation rests unconformably on the middle part of the Upper Sotres Formation, implying a hiatus of more than 35 Ma.

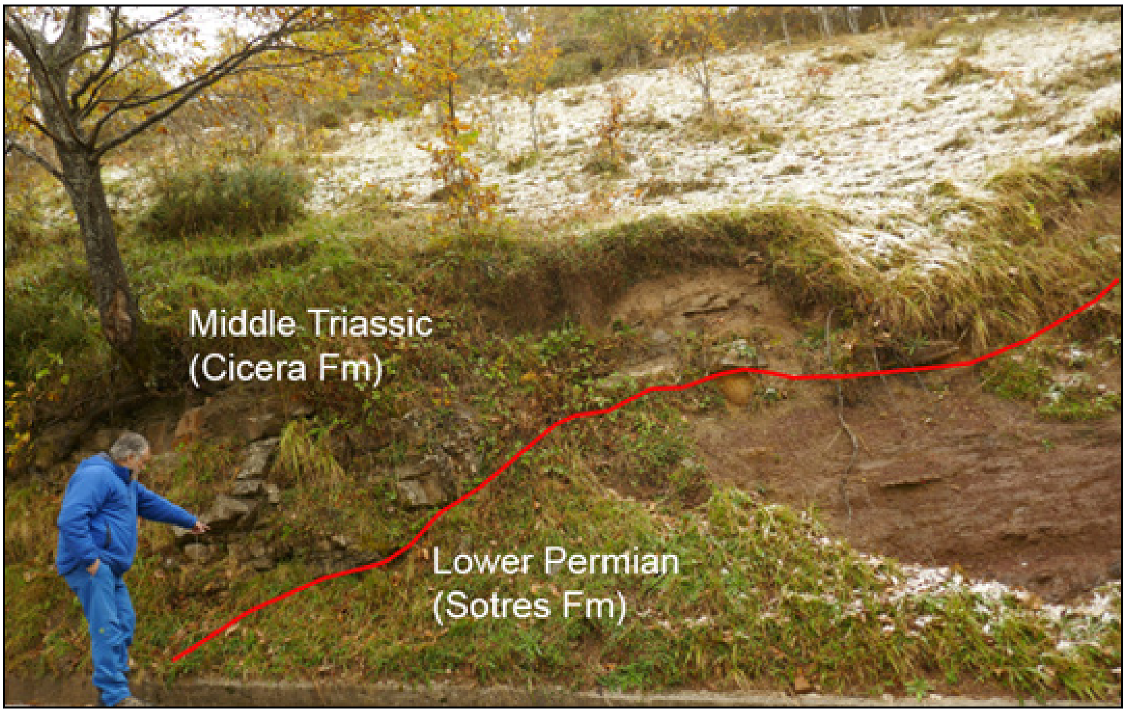

Figure 27. Lower Permian (Sotres Formation) and Middle Triassic (Cicera Formation) unconformity. Sotres-Tresviso road, near La Caballar pass.

The sedimentary record: the upper Cicera Formation.

Although the Middle and Upper Sotres and the Cicera formations will be respectively the focus of stops 6 and 7, here it is possible to observe some of the characteristics of the upper part of the Cicera Formation. The last 430 m of the road before reaching the pass from Tresviso are represented by the Cicera Formation, of Ladinian - early Carnian age (Figure 28). This formation is 35 thick in this area, although the upper part is truncated by faulting (Figure 21). The base of this outcrop is represented by an unconformity on the upper part of the Sotres Formation, of Artinskian-Kungurian (early Permian) age, a sedimentary gap that exceeds 30 Ma.

The Cicera Formation in this area is basically constituted of sandstone with intercalations of siltstone that increase in abundance towards the top, therefore showing a general fining-upward tendency. The section is basically represented by a succession of 4-9 m-thick fining-upward cosets (Figure 28-1 and 2). Sets into the cosets are basically represented by planar and trough structures (2D - 3D, transverse and linguid dunes, respectively) constituting fluvial channel fill successions that may show abandoned deposits at the top of the sets (Figure 28- 3). Gravel bars may represent the lower part of the fining-upward succession and crevasse splay deposits, including crevasse channels, are common in the upper part of the section (Figure 28-4 and 5).

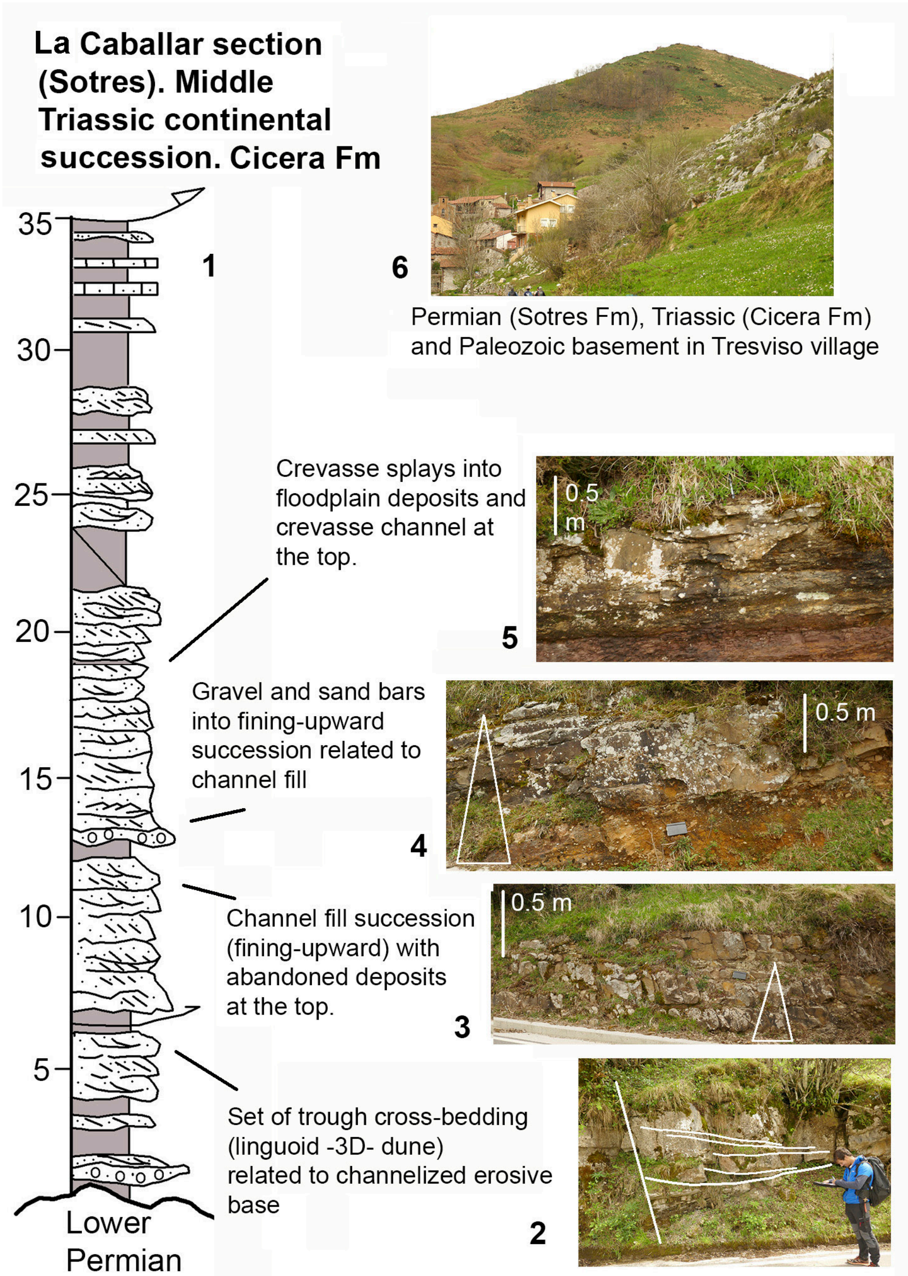

Figure 28. Upper part of the Cicera Formation (late Ladinian-early Carnian) in the Caballar Pass, near Sotres village.

When these facies are compared with other outcrops of this same formation in neighbouring areas, it become apparent that they correspond to the upper part of the Cicera Formation. One of the characteristics of these facies is the increase in carbonate in the uppermost part of the formation, a trend noted in other outcrops and illustrating transition into the overlying Rueda Formation of marine origin (Figure 3).

STOP 6:

Location:

Sotres village, Asturias (Figure 5)

Objectives:

Middle and Upper members of the Sotres Formation (Artinskian-Kungurian). Ages, sedimentology (Carbonate Lakes and palustrine deposits), mineralogy, C and O stable isotopes and paleoclimatology related to the LPIA.

Age of the Middle and Upper members of the Sotres Formation

Spores in the basal shales were attributed to the Autunian (Neves personal communication, in Martínez-García, 1981). This age attribution is not supported by current data. Only one sample yielded a positive result in the Sotres Formation, enabling the adscription of a Kungurian age (early Permian) to this formation (Juncal et al., 2016). This association (SO1) is the only one of Permian age described to date in the Cantabrian Mountains. In fact, the co-occurrence of Potonieisporites novicus and Gardenasporites heisseli leads us to suggest a Kungurian (latest early Permian) age rather than Roadian (earliest late Permian).

These data allow a more accurate duration for the oroclinal bending of the Ibero-Armorican Arc evaluated by Weil et al. (2010). It might be suggested that this deformation was three times slower than previously stated.

Stratigraphy and Sedimentology

As stated before, the Sotres Formation had recently been deeply revisited and modified in its age and sedimentary interpretations, but it was especially in its Middle and Upper members were changed affected more (see details in López-Gómez et al., 2021).

The Middle Member in the Sotres area reaches up to 50 m thick (Figure 21). Sedimentary studies have been carried out based on facies and facies association analysis. Two main facies associations (E and F) have been identified in this member (Figure 21):

Facies association E: It consists of facies Lca, Lso, and Cml. It is mostly represented by a fining-upward sequence up to 0.4 m thick of white limestone or calcarenite with small-scale planar cross-stratification at the base, fine- to medium-grained sandy limestone with oncoids and small current or oscillation ripples in the middle part, and millimetre to centimetre thick-beds of carbonate microbial lamination that may feature dome structures at the top. The succession may represent a higher energy shallow ephemeral lake sequence that would indicate fluvial progradation and shoreline retreat. Vertical repeated sequences suggest pulses related to climate and tectonic controls, which would also condition runoff, erosion and chemical weathering (Platt and Wright, 1991; Jones et al., 2020). Stromatolites may have formed after flooding episodes, as they may have kept pace with the rising water level.

Facies association F: It consists of facies Ll, Fdr, Lp, and Ck (Figure 29-1) in shallowing-upward sequences up to 1.6 m thick. When complete, from bottom to top, they show millimetre-thick laminated dark organic-rich beds, poorly rhythmic laminated succession of centimetre-thick white limestone (wackestone) beds, with variable contents of ostracods, gastropods and algae, and well-stratified centimetre-thick grey limestone with small-scale planar cross-stratification and shell fragments. At the top, the sequence ends with massive carbonate beds showing karst development (Figure 29- 2). The association is interpreted as recording an evolution from deep to subaerial lacustrine environments. Ostracod and gastropod micrite beds are common in relatively deep low energy lakes (Johnson et al., 2009), and small planar cross-stratification trapping shell fragments may develop via currents around the wave base level (Changsong et al., 1991). The presence of karstification features suggests subaerial exposure during low water level periods under a slightly wet climate (Talbot and Allen, 1996).

The Upper Member is not well represented in the Sotres area. Part of this subunit is covered by dense vegetation and faulted in its upper part (Figure 21). It is constituted by facies associations G, H, and I (Figure 22):

Facies association G. This association consists of facies Lso, Mr, Fdf, and Cme (Fig 9, G). It represents a fining-upward sequence up to 1.3 m thick. When complete, from base to top, it consists of millimetre- to centimetre-thick alternating beds of massive white limestone (in places with ostracods and gastropods), red mudstone, and marl which may show root trace fossils, intercalated millimetre-thick beds of clayey limestone containing small current and wave ripples, as well as root mats, and marls, and evaporites. Clayey limestones may contain coated (pedogenic) grains, oncoids, and carbonate microbial lamination within the limestones (Figure 29-3). This succession records palustrine deposition, reflecting changes in the water table, drying of the water body and modification of the primary facies by pedogenic or early diagenetic processes (e.g., Alonso-Zarza and Wright, 2010).

Facies association H. This association is up to 1.3 m thick and includes facies Fom and Fl (Figure 22). It consists of an alternating succession of irregular beds featuring brown mottled siltstone and grey laminated or displacive domal limestones. Massive grey-green marl and red mudstone with some thin intercalated beds of organic-rich material disrupted by roots and bioturbation may appear at the top or bottom of the succession. The association is interpreted as having been deposited within a palustrine environment transitioning to a lacustrine environment. The intercalated rootlet levels correspond to the lowstand stages of the lake and represent periods of pedogenesis (e.g. Détriché et al., 2013).

Facies association I. This association, which is up to 1.8 m thick, contains facies Lmr and Cml (Figure 22). Vertical successions of these facies do not always keep the same order. The association consists of centimetre-thick disrupted beds of alternating, mottled marly siltstone and grey limestone with finer beds of evaporite lenses and/

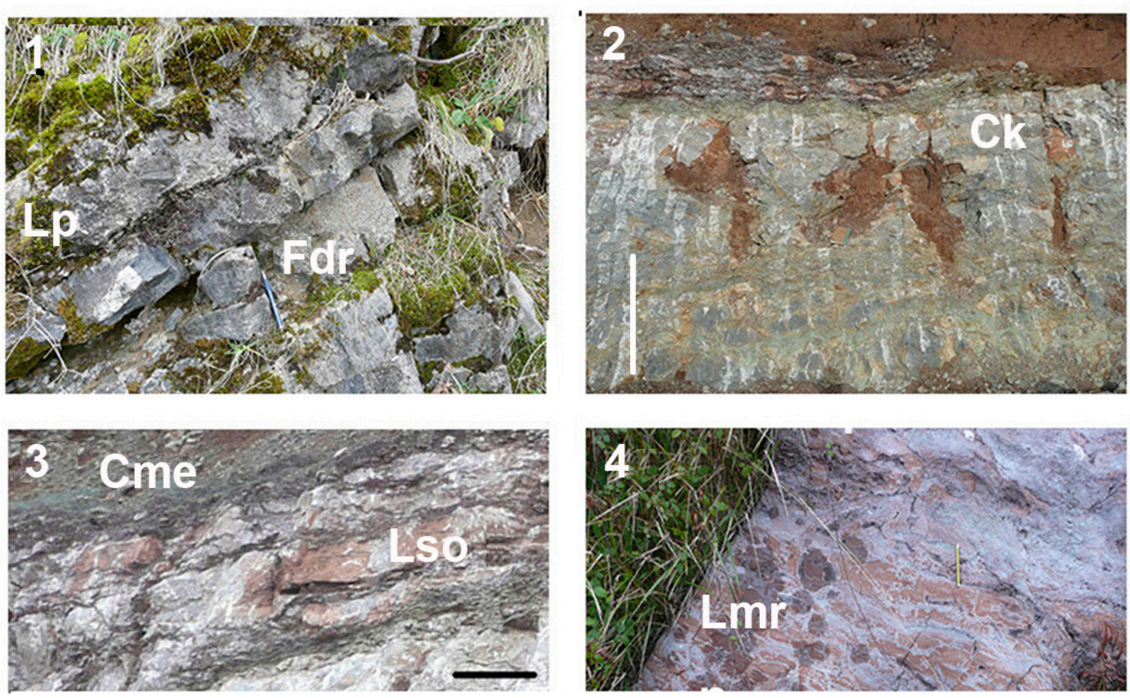

Figure 29. Selected facies from Middle and Upper subunits of Sotres Formation.

or stromatolite-like lamination. Beds are disrupted by root trace fossils, micro-karst and dissolution breccia, and may be affected by different superimposed dissolution structures (Figure 29-4). The succession is interpreted as having been deposited under low-energy conditions subject to frequent water level changes with prolonged exposure periods under arid conditions. Root development, brecciation, and dissolution occurring in such conditions are characteristic features of palustrine environments (Freytet and Plaziat, 1982; Platt and Wright, 1992).

Paleosols

No signs of pedogenesis were found in the lacustrine deposits of the Middle Member of the Sotres Formation; however, pedotype 4 is very common in some sections of the Upper Member (Figure 24-1, 4). Pedotype 4 shows a pale red (10R7/3) horizon with root trace fossils and angular blocky peds on top of a laterally continuous level of greenish coalescing mottles developed on sandy materials (Figure 24-2C). The greenish horizon is classified as a gleyed horizon (Bg), indicating a high water table and probably waterlogging for most of the year. Pedotype 4 occurs vertically intercalated with palustrine carbonates and developed on intermittently flooded silty/sandy materials in non-permanent wetlands, probably related to shores of ponds or lakes. The landscape inferred for the Upper Subunit can be envisioned as a continuous transition between exposed surfaces (pedotype 4) to shallow water bodies in lacustrine areas.

Depositional environmental evolution

A detailed explanation of the depositional environment evolution of the Sotres Formation was carried out by López-Gómez et al. (2021). Figure 30 shows Idealized section of depositional systems related to the three differentiated subunits. A) Asymmetry in deposition and lateral general evolution is a main characteristic of the different subbasins. B) Sketch of an early Permian Sotres subbasin in the Cantabrian Basin and asymmetric sedimentary refill of the subunits controlled by the lateral activity of faults. The Lower Member records a fluvial environment that evolved from proximal to distal areas and may show the transition to the lacustrine environment at the top.

The Middle Member records deposition in various lacustrine subenvironments. It represents the thickest accumulation of sediments in the subbasins, where the presence of permanent standing bodies of waters facilitated the development of stacked, shallowing-upward carbonate sequences, which may include transition from deep anoxic to littoral facies (e.g., Dupraz et al., 2004). An important characteristic of facies association F is the development of karst surfaces mainly at the top of the Middle Member (Figure 21), which indicates general subaerial exposure, probably affecting the whole Cantabrian Basin.

The Upper Member records the development of palustrine subenvironments The fluctuating water table led to the development of a variety of features, including desiccation cracks, dissolution breccias, and evaporite beds and lenses, all of which characterize this stage of basin fill (e.g., Freytet and Plaziar, 1982).

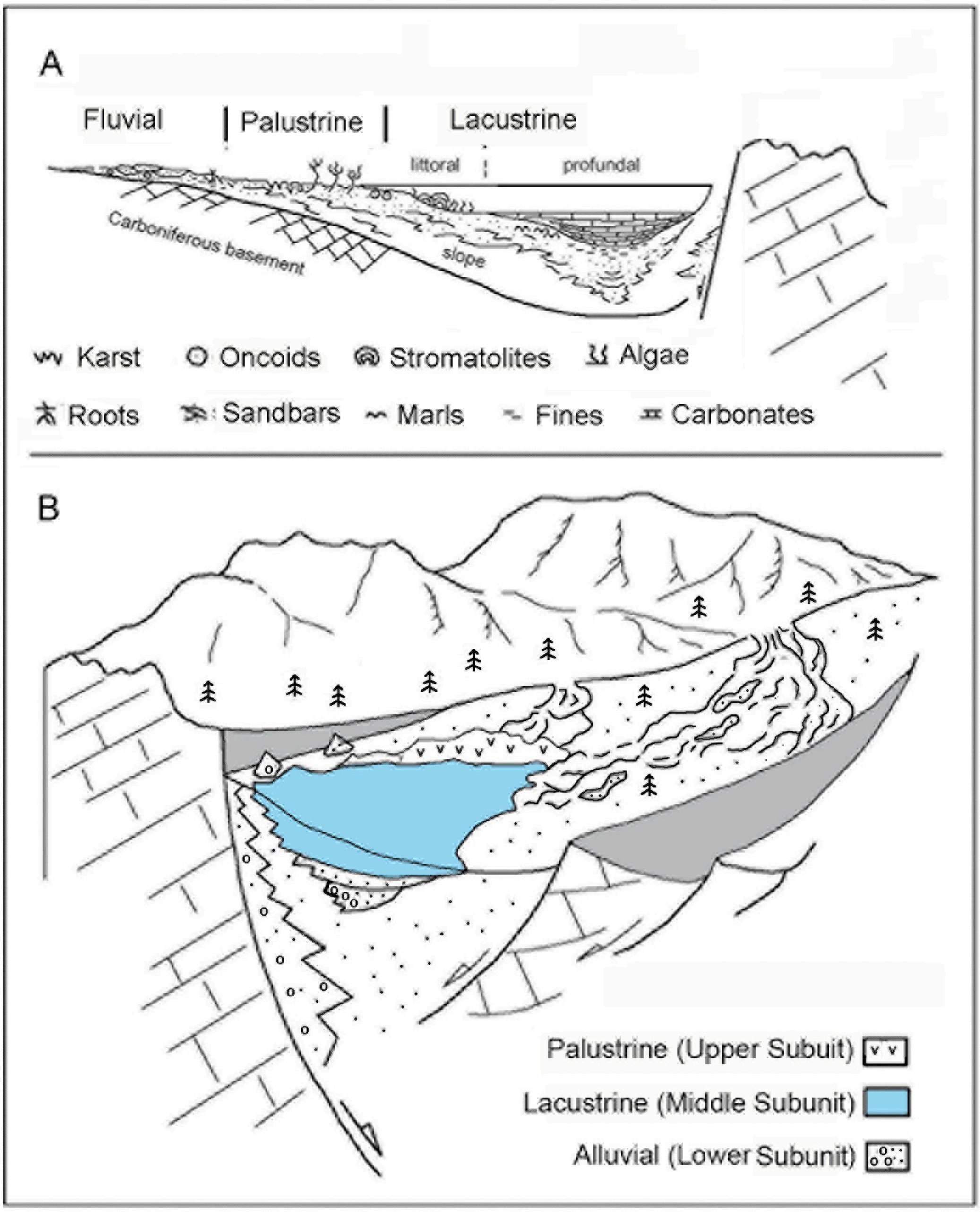

Figure 30. Sketch of the paleoenvironmental evolutions of the Lower, Middle and Upper subunits of the Sotres Formation (Modified from López-Gómez et al., 2021).

Mineralogy and fluorite deposits

The clay mineral composition of the Middle and Upper members of the Sotres Formation contain illite and variable proportions of chlorite and traces of smectite, randomly interstratified with illite (I/S) (Figure 23). López-Gómez et al. (2021) suggested that this composition is indicative of semi-arid conditions as a general trend, with enhanced chemical weathering in those layers which show traces of smectite. Wetter conditions are supported by the development of karstic horizons in these subunits.

Abundant fluorite deposits occur as veins hosted in Carboniferous limestone and as stratabound bodies hosted in the brecciated materials related to these karstified zones that unconformably overlie the Carboniferous limestones (Symons et al., 2017), forming a major producing area in Europe. Fluorite mineralization in the Cantabrian Mountains occurs in the karstified levels at the top of the Middle Member of the Sotres Formation (Figure 29-2) that may constitute productive areas, as is the case of Villabona Mine (Figure 31), North of Oviedo City. Mineralization is controlled by fractures that follow two major structures, the NW–SE-trending Ventaniella Fault (Figure 5), which constitutes the south-western limit of the Jurassic basin, and the E–W-trending Llanera Fault. Mineralization likely formed when F-enriched deep brines (probably of volcanic origin) mixed with the surficial fluids in carbonates, breccias and fractures, resulting in the formation of veins and stratabound bodies of fluorite, barite, calcite, dolomite, and quartz and minor amounts of sulphides. Fluid movement and mineralization occurred between Late Triassic and Late Jurassic times, probably associated with rifting events related to the opening of the Atlantic Ocean (Sánchez et al., 2009).

Figure 31.- Fluorite from Villabona Mine (Courtesy of MINERSA GROUP).

Carbon and oxygen stable isotopes. Climate indicators

Carbonate facies of the Sotres Formation, including lacustrine and palustrine deposits as well as paleosols, were analyzed for δ18O and δ13C to infer palaeoclimatic and paleoenvironmental conditions during deposition (López-Gómez et al., 2021). Both data sets show noticeable changes through time (Figure 32) but no significant covariation (Figure 33), pointing to independent controls for the carbon and oxygen isotopic signals.

The δ13C (‰) data averages −1.74 and shows quite large variability. The most negative values correspond to paleosols, which show a mean of −5.73 ‰ and a low standard deviation of 0.9, probably related with markedly homogeneous input of organic carbon from soil biological activity. δ13C data for lacustrine and palustrine carbonates is heavier, averaging 0.10 ‰ for lacustrine and 0.14 ‰ for palustrine facies, and more variable, with standard deviations of 2.87 and 2.19, respectively. Such variability probably reflects the diverse carbon sources and inputs that commonly characterize shallow lake systems and wetlands. The δ13C series does not show evident trends or patterns and its variability probably reflects changes in local environments over time.

The δ18O (‰) data averages – 5.78 (standard deviation of 1.83), being the mean values of lacustrine (– 6.96), palustrine (– 5.51), and paleosol carbonates (− 5.88) remarkably close to the bulk average. This convergence in the mean values suggests these isotope ratios were mainly determined by factors independent of each environment. López-Gómez et al. (2021) discussed in detail the possible controlling factors of the δ18O variability of the Sotres Formation carbonates, including local changes in temperature and aridity, and changes in rainfall δ18O, all of them potentially associated to supraregional/ global changes in climate. The long-term variations in carbonate δ18O could be reflecting global climate changes in the Artinskian – Kungurian time interval, as they could result of the superposing effects of monsoonal strengthening / weakening (i.e., changes in the “water amount effect”); growth/degrowth of continental ice volume (causing large changes in the overall isotope composition of the ocean, i.e., the moisture source); and regional changes in temperature and hydric balance. Remarkably, a significant δ18O positive excursion is recognized in the Sotres Formation records, which can be tentatively correlated with the “middle” Kungurian positive peak reported from marine records elsewhere (Montañez et al., 2007; Grossman et al., 2008), interpreted as the result of ice-sheet growth and colder global climate.

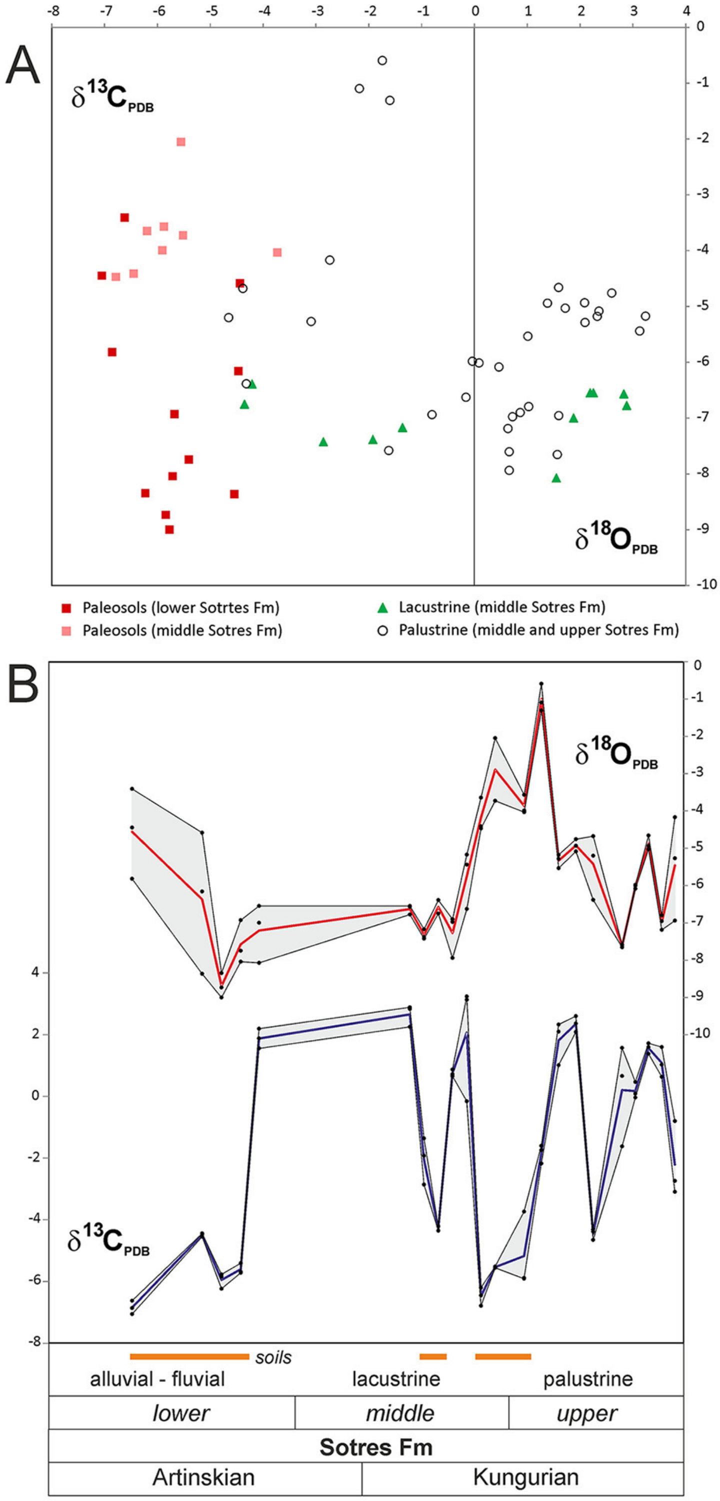

Figure 32. Carbon and oxygen stable isotopes from the Sotres Formation A) δ18O vs. δ13C for the analyzed samples, with indication of the facies type from which the carbonate mineral was extracted. Note the lack of covariation between carbon and oxygen, and the distribution of each group of facies. B) Composite series for carbon and oxygen stable isotopes, constructed by integrating analytical data derived from five stratigraphic sections in the study area. Thick lines represent the average values for each sample (two or three subsamples were extracted from different points of each sample). Black dots represent the analytical values for each subsample. Shaded areas reflect the distribution of all data, between the maximum and the minimum value of the subsamples of each sample. See text for more details and interpretation.

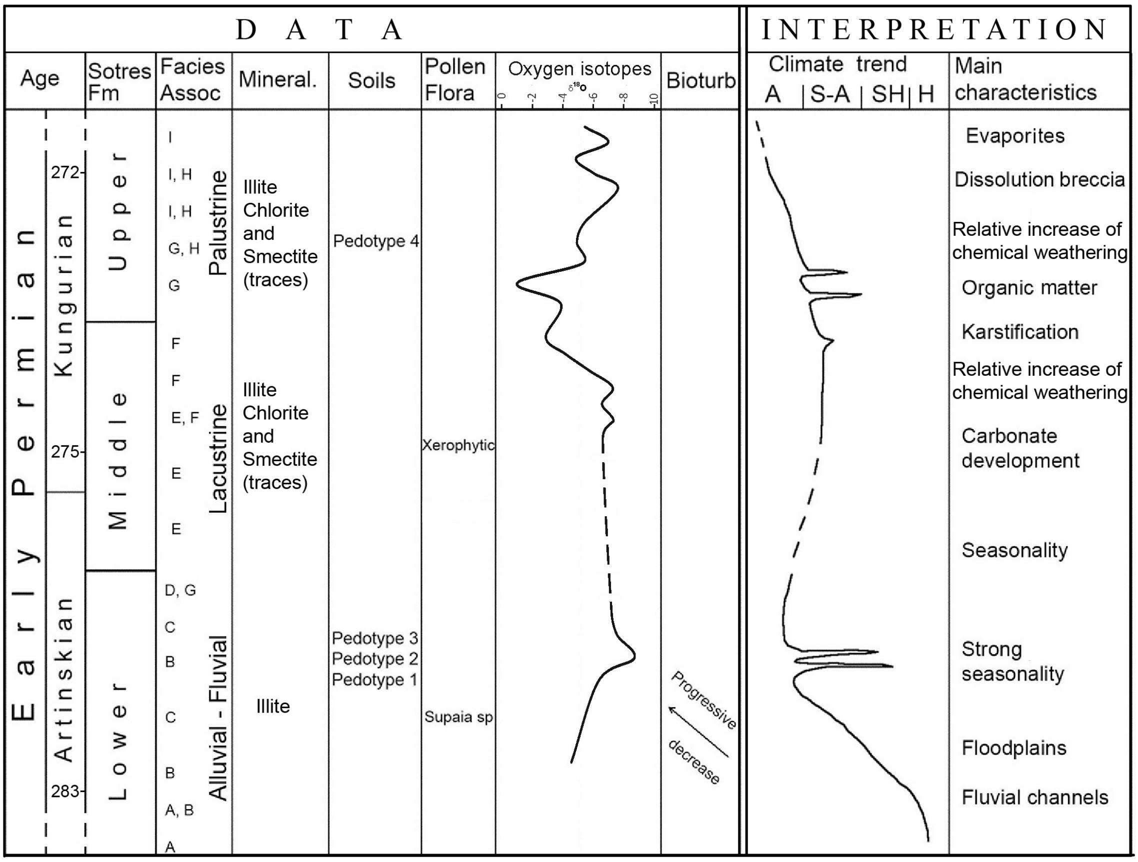

Figure 33. Sketch of the general climate evolution in the Cantabrian Mountains area, W Spanish Pyrenees area during the sedimentation of the Sotres Formation based in different proxies. See the main text for details of the general included data. A- arid, SA- semi-arid, SH- subhumid, H- humid.

A common post-Variscan tectono-sedimentary evolution of the Pyrenean-Cantabrian orogenic belt.

A detailed study of the stratigraphy, sedimentology, paleosols, and volcanism of well-dated early-middle Permian units served to confirm the similar post-Variscan tectono-sedimentary evolution of the Pyrenean-Cantabrian orogenic belt (Lloret et al., 2021).

The collapse of the Variscan orogen started in the hinterland in late Carboniferous times and had reached the foreland and ends in early Permian times. The extensional processes related to the Variscan orogen collapse were not generalized and gave rise to larger basins in the hinterland-foreland boundary during the late Carboniferous (Kasimovian-Gzhelian) than in the foreland, where smaller, thinner, elongated isolated basins developed during the early Permian. During this time, deposits related to this orogen are absent in the collapsed hinterland but a large number of post-orogenic plutonic rocks occur (Figure 34).

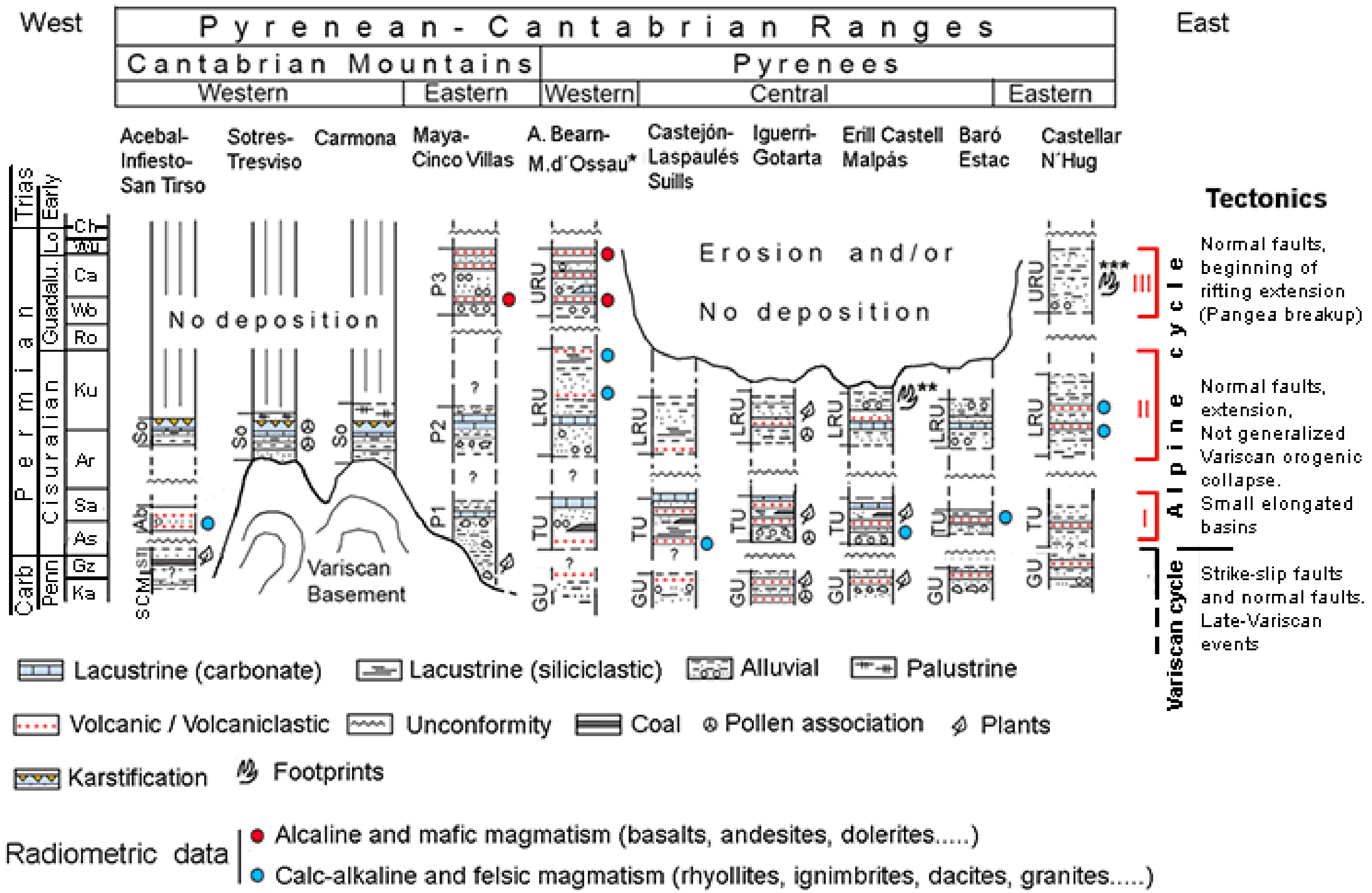

*Figure 34. Sketch of the general evolution of the early-middle Permian (Cantabrian Mountains and Pyrenees) basin showing the three post Variscan extensional tectonic phases of evolution. SCM- Stephanian Cantabrian Mountains. Units: ST- San Tirso, Ab- Acebal, So- Sotres, P1- Permian 1, P2- Permian 2, P3- Permian 3, GU- Gray Unit, TU- Transition Unit, LRU- Lower Red Unit, URU- Upper Red Unit. *Including the surrounding outcrops: Anayet, Sallent de Gallego, Oza and Canal Roya, **Footprints from La Mole d´Amunt (Mujal et al., 2016a), ***Footprints from Noves-La Trava (Mujal et al., 2016b). Modified from Lloret et al. (2021).*

The early Alpine extensional processes took place in three tectono-sedimentary phases (Figure 35):

- The first phase (Asselian-Sakmarian) comprises alluvial sediments and calc-alkaline volcanic rocks.

-The second phase (late Artinskian-early Kungurian) is represented by alluvial, lacustrine and palustrine sediments with intercalations of calc-alkaline volcanic beds, with a clear aridification tendency.

-The third phase (Wordian-Capitanian) essentially is not represented by sedimentation in the Cantabrian Mountains and underwent significant erosion in the Pyrenees. In the latter area, the succession consists of alluvial deposits with intercalations of alkaline and mafic beds. This last Permian extensional phase marks the transition to the early-middle Triassic rifting stage, related to the Pangea break-up at these latitudes.

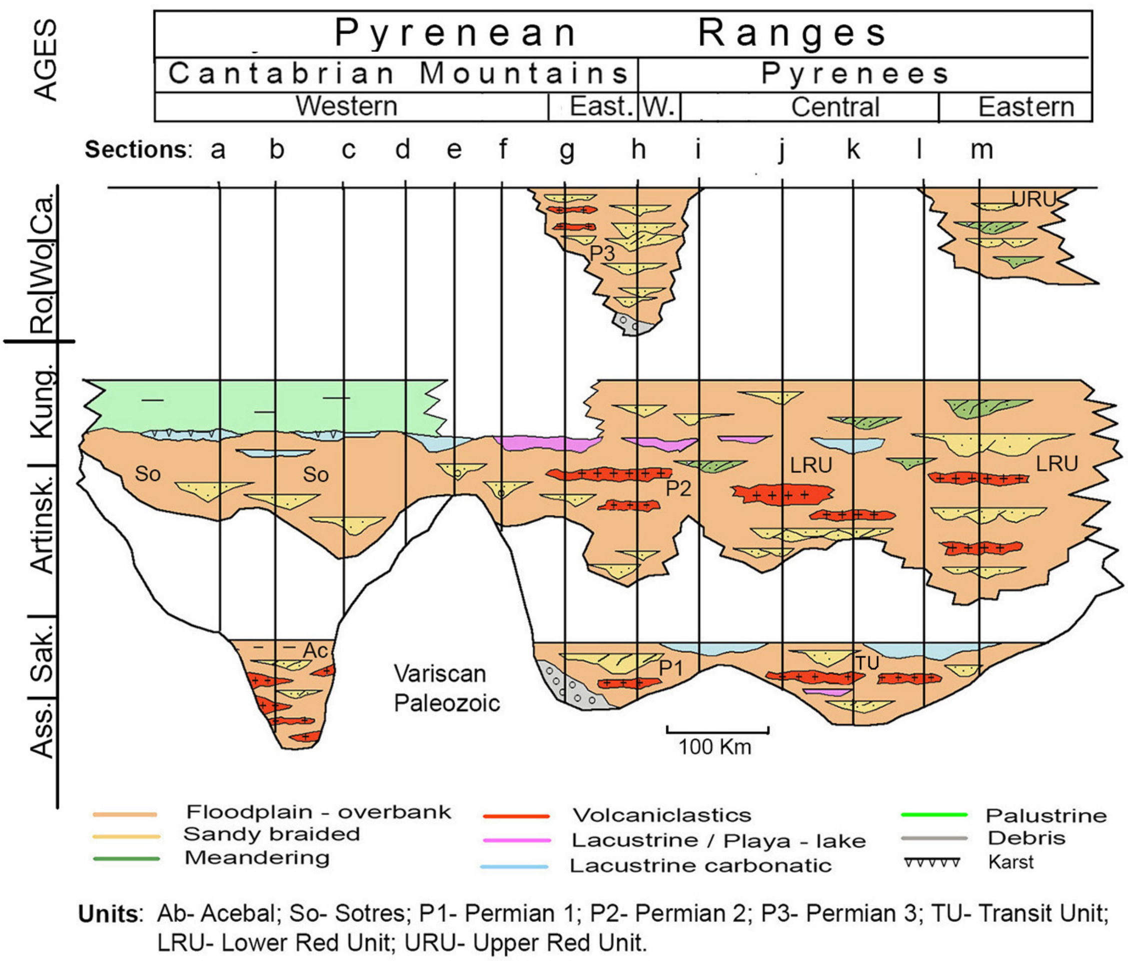

Figure 35. Time-space reconstruction of vertical and lateral development of the studied units and their depositional systems in the Pyrenean–Cantabrian orogenic belt. The interval lacking sedimentation and/or erosion is also shown. Modified from Lloret et al. (2021).

WEDNESDAY 6TH

It comprises Stops 7, 8, 9 and 10. See Figures 5 & 17 (Stop 8) for locations.

STOP 7:

Location:

La Cohilla section, near La Cohilla Dam, Cantabria (Figure 5).

Objectives:

Chenge of depocentres related to the Alpine tectonjics. First Mesozoic sedimentary record in the Cantabrian Mountains. The Cicera Formarion (Ladinian-early Carnian), its age, mineralogy and sedimentary evolution.

The La Cohilla dam section (Nansa River, Cantabria) is in the Vasco-Cantábrica Region (Figures 1 and 2), in the southern flank of the Tudanca Alpine syncline, close to the Pisuerga-Carrión Unit of the Variscan Cantabrian Zone, which crops-out in the Polaciones anticline (Figure 2). This anticline separates the Tudanca and Alto Campoo Alpine synclines and is affected by several faults, mainly in its northern flank. The Pisuerga-Carrion unit is composed by Carboniferous siliciclastics related to the emplacement of all major tectonic units of the arcuated Cantabrian Zone (Figure 1b), occupying the internal part of this arc (Ibero-Armorican Arc). The Triassic Cicera Formation rests unconformably on the lower Permian (Acebal and Sotres formations) and also on the Carboniferous deposits of the Pisuerga-Carrión Unit (Potes and Remoña groups) (Figure 36), the latter deformed by the Variscan orogeny.

Deposition of the Sotres and Cicera Formations in this area is related to the NW-SE San Carlos Late Variscan fault (Figures 2 & 36), which was reactivated as a normal fault in early Permian and Middle-Late Triassic times (García-Espina, 1997) (Blue lines in Figure 36). This reactivation allowed the Triassic deposits to be thicker in the N block (Tudanca Syncline) than in the S block (Alto Campoo syncline) of this Late Variscan fault. In addition, lower Permian deposits are absent in this southern block.

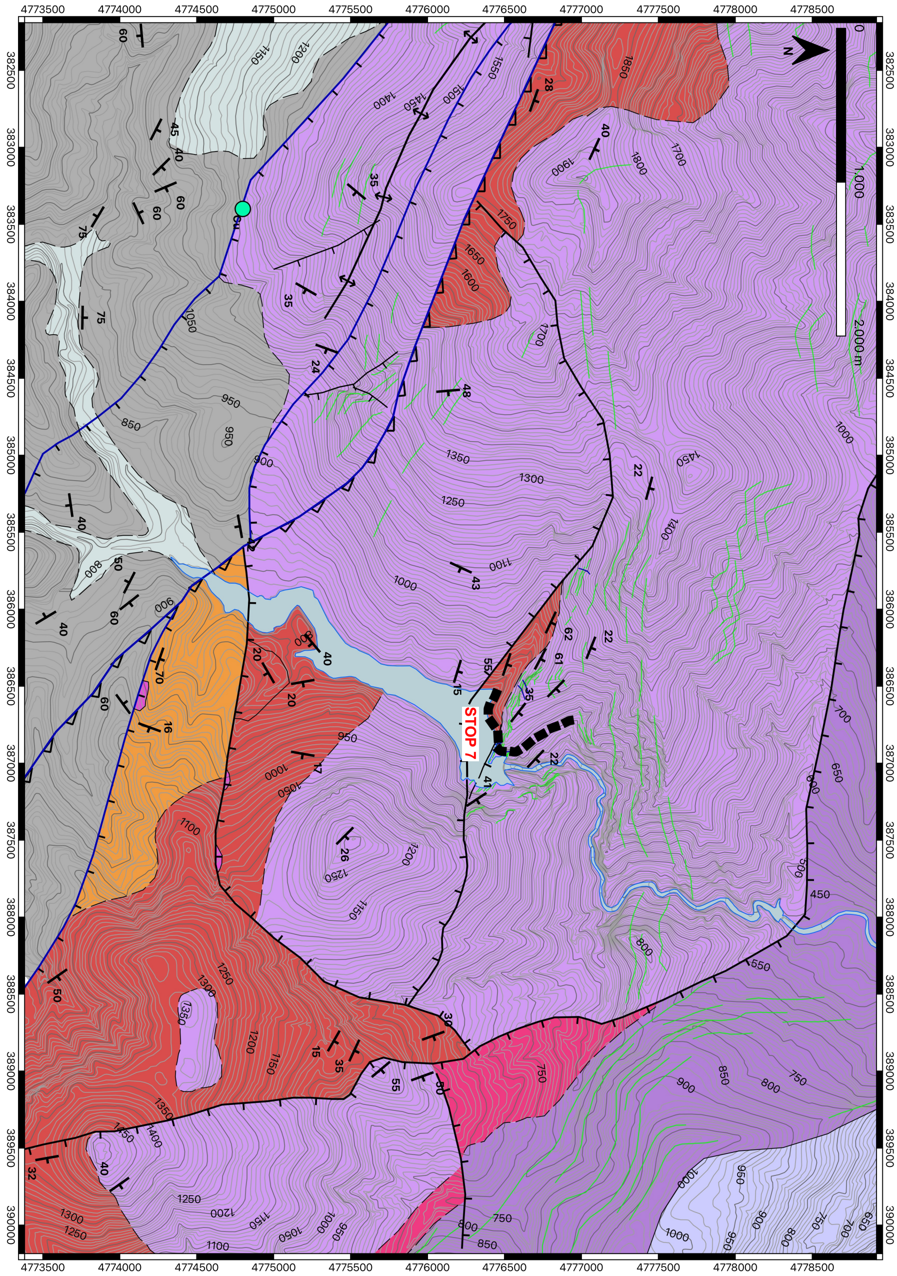

Symbols
- Bedding strike and dip
- Bedding trace
- Stratigraphic section

Structures and contacts
- Conformity
- Unconformity
- Variscan thrust
- Late Variscan strike slip fault
- Permian-Mesozoic Alpine normal fault
- Cenozoic Alpine reverse fault
- Anticlyne

Ore traces
- Malachite, Azurite, Chalcopyrite (Cu)

Lithostratigraphic units
- Rodiles Formation (Pliensbachian-Bajocian). Marls and marly limestones
- Gijón Formation (Hettangian-Sinemurian). Dolostones, limestones, calcareous breccias, marls and lutites
- Transition from Transición to Gijón formations (Rhaetian-Hettangian). Vuggy yellowish dolostones
- Cicera Formation (Anisian-Carnian). Siliceous conglomerates, sandstones, siltstones and lutites.
- Sotres Formation (Kungurian). Calcareous angular sedimentary breccias, sandstones, lutites and laminated limestones
- Calc-alkaline intrusive igneous rocks (Asselian)
- Remoña Formation (Late Kasimovian-Early Gzhelian). Lutites, sandstones, conglomerates, calcareous breccias and olistoliths
- Potes Group (Bashkirian-Early Moscovian). Lutites, sandstones, siltstones and olistostromes

Figure 36. Geological map and detail of the La Cohilla dam surroundings (Peña Sagra range, Cantabria).

Age of the Cicera Formation

The oldest Triassic palynological assemblages were obtained from the Cicera Formation in the Cicera section (samples SP5 and Ca1, López-Gómez et al., 2019) (Figures 3 and 4). These two samples show very similar associations. The presence of typical Middle Triassic taxa as Lunatisporites noviaulensis, Illinites chitonoides, Microcachryidites doubingeri, and Michrocachryidites fastidioides, together with circumpollen species, that diversified during late Ladinian all indicate a Longobardian age (late Ladinian).

Samples Cic11 and Cic12 were obtained near the sample collected from the Cicera Formation. The presence of Chordasporites singulichorda, Triadispora spp. and the circumpollen species together with Patinasporites densus and Vallasporites ignacii, that have their first appearance in the base of early Carnian would indicate a Longobardian - Cordevolian transition (Ladinian - early Carnian).

The sedimentary record of the Cicera Formation.

The aforementioned tectonic context allowed for the accumulation of a much thicker Triassic succession here than in any other area of the Cantabrian Mountains. The Cicera Formation (Ladinian-early Carnian, Middle-early Late Triassic Figure 3) was first described in López-Gómez et al. (2019), where the sedimentary interpretation and the age of formation are detailed. This formation reaches almost 1 km thick in this area and shows an extensive development of different fluvial sedimentary record (Figure 37). Schematically, the Cicera Formation in the La Cohilla area shows three sedimentary records: conglomerate in the lower part, an important succession of sandstones (>600m) in the middle and upper part, and interbedded sandstone and siltstone in the upper part.

The basal conglomerates are on the unconformity that separates the Cicera Formation from the Lower Permian deposits (Sotres Formation). These conglomerates are clast-supported crudely bedded gravel (Gh) (Figures 3 & 37) and represent longitudinal bedforms and/or sieve deposits (Tanner and Hubert, 1992). These conglomerates tend to organize themselves in the immediately higher levels, constituting clast-supported cm-thick bedded gravels with planar and through cross-stratification (Gpt) (Figures 4 & 37) that represent gravel bars and bedforms developed into small channels (Colombi et al., 2017).

The sandstone beds are mostly represented by fine to coarse sand with planar and trough cross-beds (Sp1) (Figure 5, 10 & 37). They represent planar and sinuous crested (2d-3D) dunes in channel fill (Ramos and Sopeña, 1983; Owen et al., 2017). Due to the well of the outcrops, these sandstone beds allow to differentiate Miall´s (1996) minor and major boundary surfaces. They show 5-6 m thick successions of beds separated by 6th order major boundary surfaces (flat regionally surfaces that represent 104-105 years) that include minor order surfaces of 5th order (channel base surface that represents 103-104 years) and 4th order (process of development of micro to macroforms that represent less than 103 years). These successions are related to the development of braided fluvial systems mostly represented by multistory processes (Miall, 2014).

The upper part of the log mostly shows alternating sandstone and siltstone beds. Sandstones are constituting by Spt1 facies and similar facies that also include fine deposits

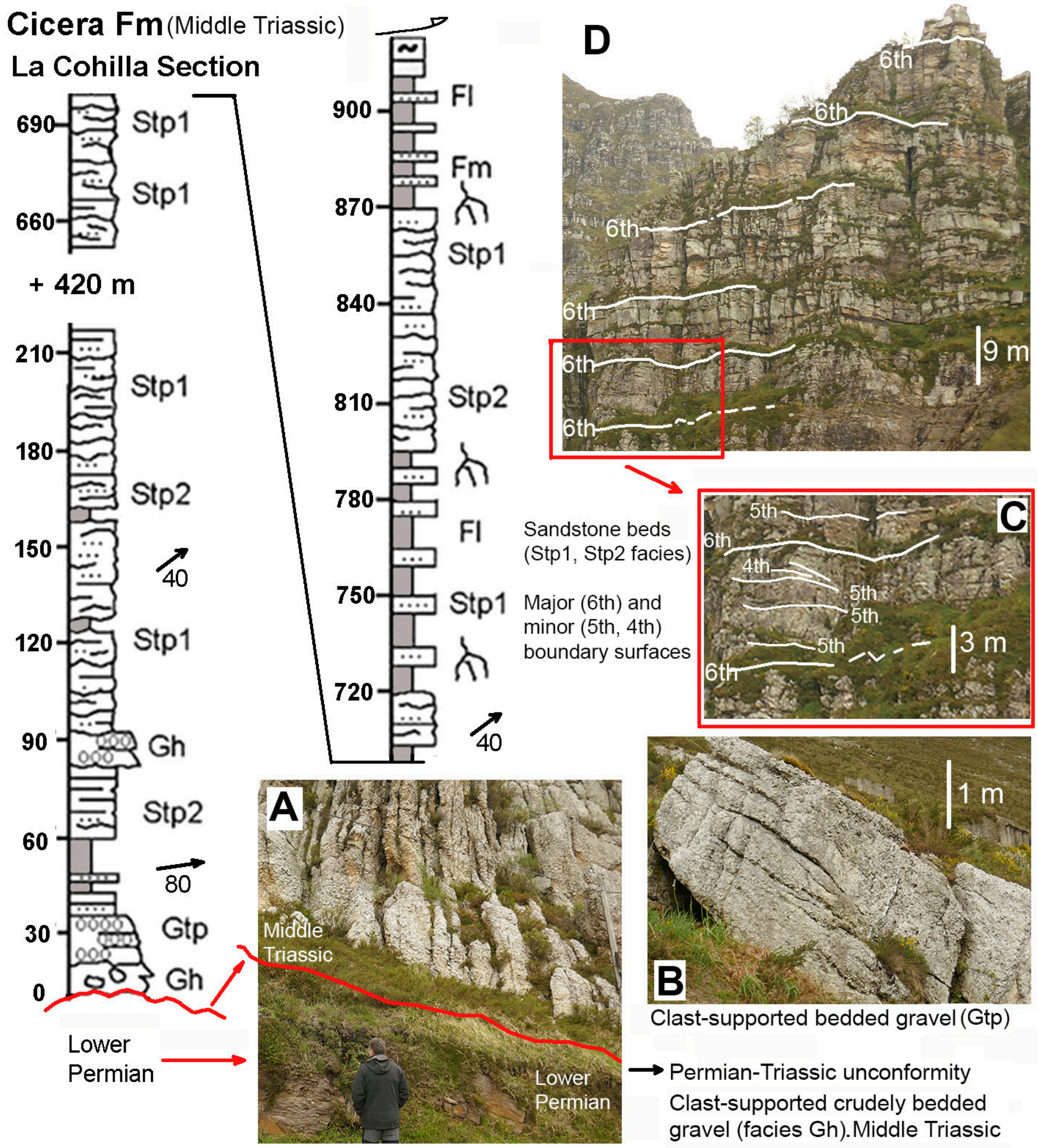

Figure 37. The Cicera Formation (Ladinian – early Carnian) in La Cohilla section. A- Permian (Sotres Formation) – Triassic (Cicera Formation) unconformity. B- Conglomerates of the lower Cicera Formation. C and D- Middle and upper parts of the Cicera Formation indicating some Major Boundary Surfaces (MBS 6th) and minor boundary surfaces (mbs 5th and 4th). See figure 22 for the facies codes.

with bioturbation at the top (Spt2). Siltstones include mud-silt deposits with roots with thin fine sand levels with parallel lamination (facies Fl) or desiccation cracks (facies Fm). This upper part is interpreted as the evolution of fluvial systems into floodplain with fine-sand deposits related to exceeded bankfull dischargue (Burns et al., 2017; Gulliford et al., 2017).

The Rueda Formation, lower Carnian in age (Figure 3A) and shallow marine in origin (López-Gómez et al., 2019), is transitionally above the Cicera Formations, although due to faulting, this unit does not crop out in this area.

It is important to note that none of the different Tethys transgressive pulses during the Middle Triassic reached this area of Iberia.

<u>The mineralogy of the Cicera Formation</u>

The mineralogical composition of the Cicera Formation includes, quartz, clay minerals, minor hematite, and variable proportions of calcite, albite, or orthoclase. The clay mineralogy is dominated by illite in most of the samples, but abundant smectite has been recognized towards the top of the unit, together with traces of chlorite or kaolinite. This mineralogical variation is probably related to marine influence in the uppermost part of the unit.

STOP 8

<u>Location:</u>

Linares village, Cantabria. Puente Nansa-La Hermida road (Figure 5)

<u>Objective:</u>

Upper Carboniferous (marine) / Middle Triassic (braided fluvial systems) unconformity. The paleoreliefs and their significance in the basin evolution.

Near of the Linares village (Cantabria), in the Puente Nansa-La Hermida road, Middle Triassic red rocks unconformably cover grey Carboniferous limestones of the Picos de Europa Unit (Figure 38). These limestones were karstified for almost 60 my, from the uplift of the Variscan Cordillera to deposition during the Triassic, since the post-orogenic Permian deposits only covered a small part of this orogenic chain. Karstic cavities filled by Permian and Triassic sediments, tilted by the Alpine orogeny, appear along the Picos de Europa Unit.

At this stop, you can also see the Triassic sediments covering the La Hermida normal fault that limits the Tresviso-La Hermida-Carmona basin to the south, a fault that we already recognized in the Tresviso section (Stop 4) and that gave rise the La Hermida thermal springs.

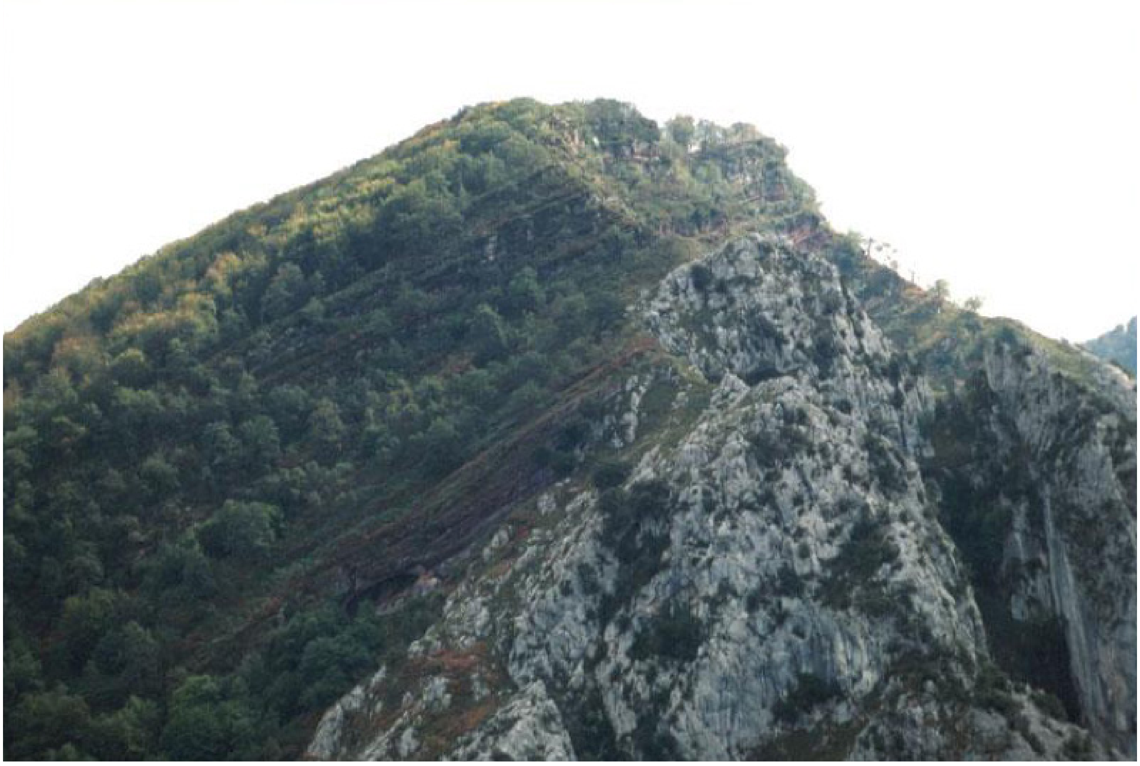

Figure 38. Middle Triassic red rocks unconformably covering grey Carboniferous karstified limestones. Linares village (Cantabria) surroundings (La Hermida-Puente Nansa road).

STOP 9:

Location:

Arenal de Moris beach, near Caravia village (Figure 5)

Objectives:

Age, mineralogy and sedimentary evolution of the Transición Formation (Norian – Early Jurassic transition), and syn-sedimentary fault activity.

In the Arenal de Moris beach, the transition between the Triassic and Jurassic crop-out. The sedimentary record of this transition was defined as the Transición Formation by Suarez-Vega (1974). This outcrop is located in the eastern end of the Asturian Mesozoic Basin, near to Bodon-Ponga Unit of the Variscan Cantabrian Zone, constituted by Cambria-Ordovician siliciclastics and Carboniferous carbonates, deformed by thrusts with large displacements and some related folds (Figure 39). The Triassic rocks outcrop is bounded at the east by a NW-SE normal fault (probably a Late Variscan fault reactivation), which puts the Triassic rocks in contact with Lower-Middle Jurassic rocks (Vega Formation) (Figure 39), out of the scope of this guide.

Symbols
- Bedding strike and dip
- Bedding trace
- Stratigraphic section

Mineral and water resources
- Fluorite (F) and Barite (Ba)
- Iron-Manganese (Fe-Mn)
- Galena-Sphalerite (Pb-Zn)
- Thermal spring

Structures and contacts
- Conformity
- Unconformity
- Variscan thrust
- Late Variscan strike slip fault
- Late Variscan thrust
- Permian-Mesozoic Alpine normal fault
- Cenozoic Alpine reverse fault

Lithostratigraphic units
- Lamprophyre dikes (Jurassic?)
- Tereñes and Lastres Formations (Kimmeridgian-Tithonian): bioclastic grey marls, limestones, sandstones and lutites
- Rodiles Formation (Pliensbachian-Bajocian). Marls and marly limestones
- Gijón Formation (Hettangian-Sinemurian). Dolostones, limestones, calcareous breccias, marls and lutites
- Transición Formation (Norian-Rhaetian). Lutites, siltstones, sandstones and evaporites
- Sotres Formation (Kungurian). Calcareous angular sedimentary breccias, sandstones and lutites
- Fito Formation (Middle-Late Moscovian). Lutites, siltstones, sandstones, marls, limestones and coal beds
- Escalada Formation (Early-Middle Moscovian). Micritic and bioclastic limestones, lutites and marls
- Beleño Formation (Bashkirian-Moscovian). Lutites, sandstones, siltstones, marls and limestones
- Valdeteja Formation (Bashkirian). Bioclastic and micritic boundstone limestones and calcareous breccias.
- Lower Member of Valdeteja Formation (Early-Middle Bashkirian). Calcareous breccias, bioclastic limestones and spiculites
- Barcaliente Formation (Serpukhovian-Bashkirian). Black micritic to microsparitic laminated limestones
- Alba Formation (Tournaisian-Visean). Nodulous red limestones, marls and chert
- Sueve Formation (Early-Middle Silurian). Black shales and lutites
- Ligüeria Member of Barrios Formation (latermost Cambrian). Conglomerates and lutites
- Barrios Formation (Late Cambrian-Ordovician). Quartz-sandstones, conglomerates and lutites
- Oville Formation (Middle Cambrian). Lutites, siltstones and sandstones

Figure 39. Geological map and Triassic section of the Arenal de Morís beach surroundings (Asturias). Modified from Merino-Tomé et al. (2011).

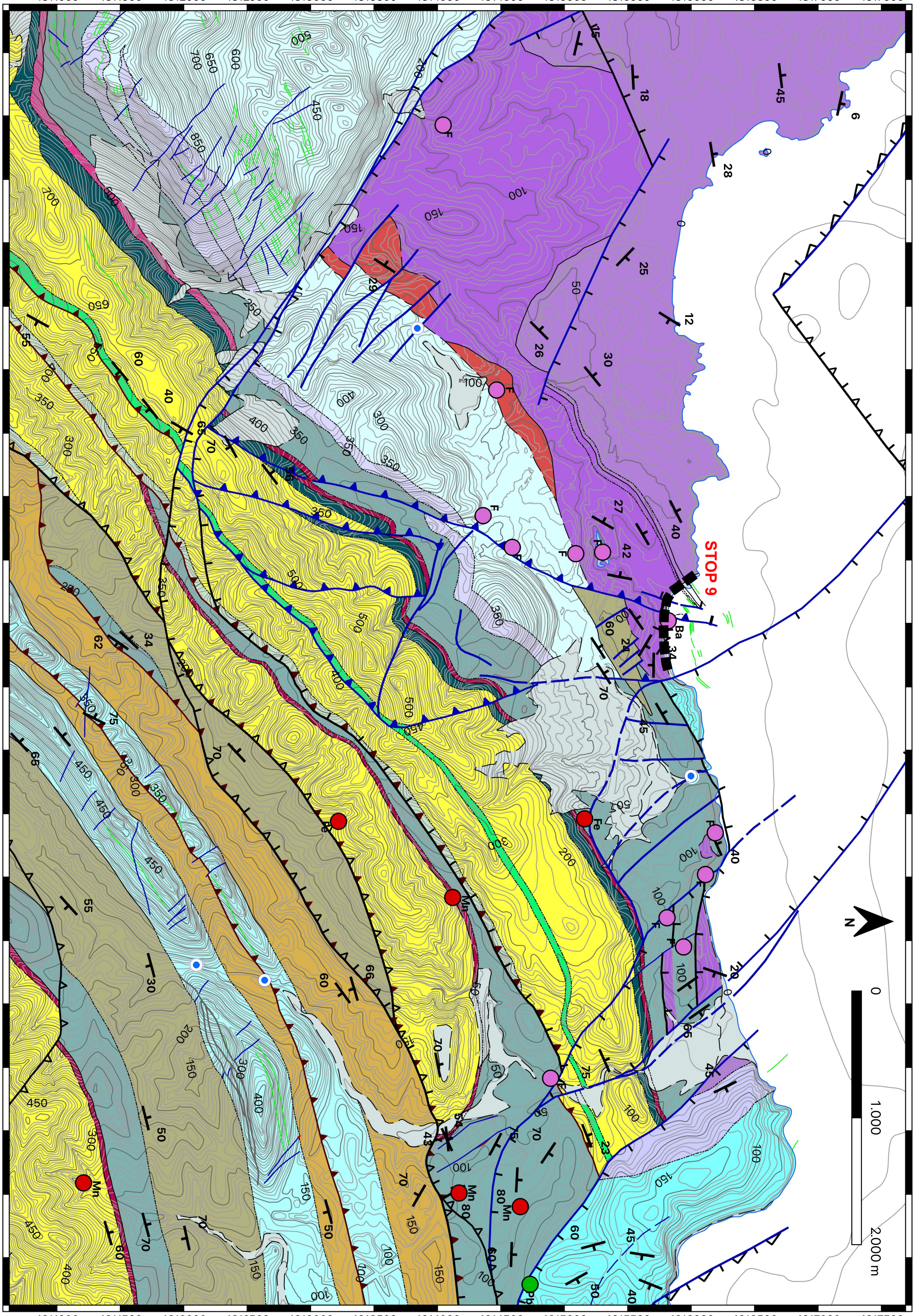
STOP 9
N
0
1.000
2.000 m
4811000
4811500
4812000
4812500
4813000
4813500
4814000
4814500
4815000
4815500
4816000
4816500
4817000
4817500
319500
320000
320500
321000
321500
322000
322500
323000
323500
324000
324500
325000
325500
326000
326500
327000
327500
328000
328500
329000

Age of the Transición Formation

In the westernmost zone of Arenal de Moris, sample AS-05 was collected in the transition levels between the red sandstone and the carbonates of the upper part. The resulting palynological assemblage is not very diverse and is poorly preserved.

Alisporites sp., Clasopollis spp., Ovalipollis ovalis (Krutzsch) Scheuring, and trilete spores have been identified (Figure 40). The genus Ovalopollis is present until the base of the Hettangian, and the genus Classopollis begins in the Rethian, suggesting that the sample can be circumscribed to the Rhaetian to basal Hettangian interval. As this corresponds to the upper part of the Transición Formation and its lower part was dated as Norian (López-Gómez et al., 2019), we can assume that the Transición Formation has a Norian-Rhaetian age (Figure 3).

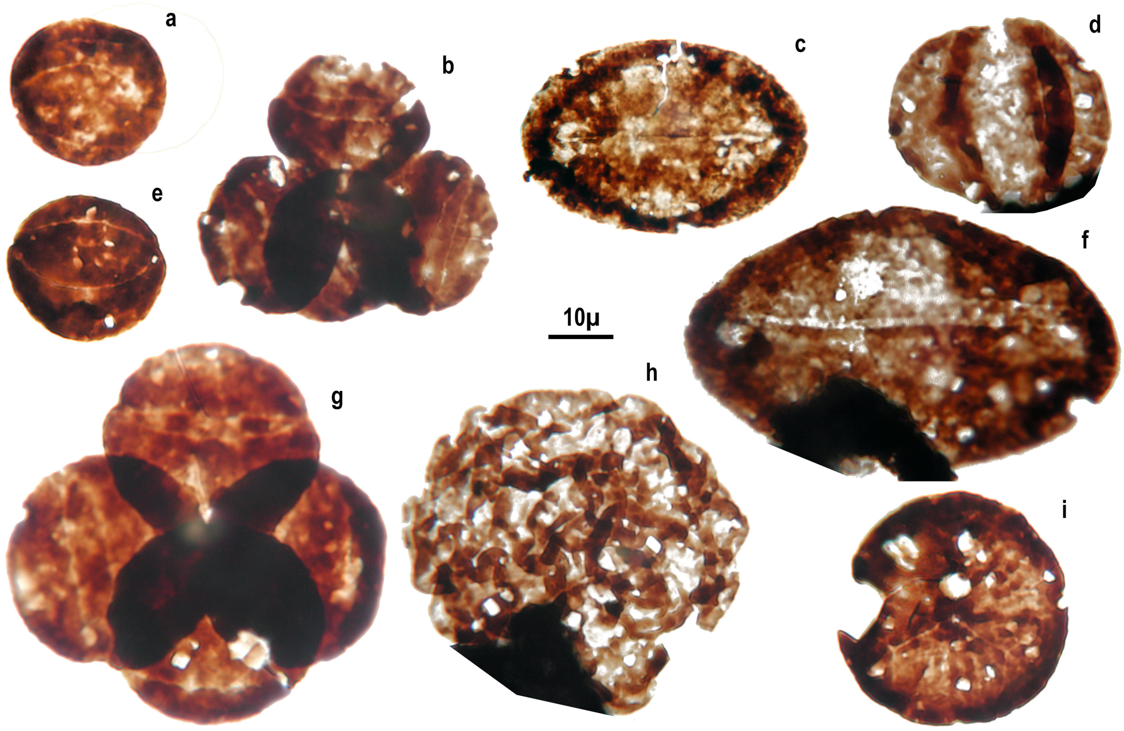

Figure 40. Palynological assemblage AS-05 Arenal de Moris W: a) Classopollis sp., AS-05/1/C364, b) tetrad Classopollis sp., AS-05/1/F494, c) Ovalipollis ovalis, AS-05/1/D300, d) Alisporites sp., AS-05/2/Q504, e) Classopollis sp., AS-05/1/D452, f) Ovalipollis ovalis, AS-05/2/L482, b) tetrad Classopollis sp., AS-05/1/T441, h) Cerebropollenites sp., AS-05/1/K294, i) Trilete spore, AS-05/1/J440.

The uppermost Triassic sedimentary record. The Transición Formation.

The Moris beach sedimentary record is essentially constituted by the Transición Formation (Figures 3 & 41). This unit was defined by Suárez-Vega (1974) as the “sediments just below the Lias” in the Asturias province. Although this definition lacked precision in age, it nevertheless indicated that this was a “transition” from Ladinian - early Carnian (now Cicera Formation) sediments of continental origin to those of marine origin of Early Jurassic age. This formation has been recently dated in López-Gómez et al. (2019), and new information is now presented here as well. these new studies indicate that the Transition Formation ranges from Carnian to Rhaetian. However, the dolomitic levels at the top of this formation (Gijón Formation, Figure 41E) may range into the Hettangian (e.g., Barrón et al., 2006).

The Transition Formation is essentially exposed in the present-day Cantabrian coast and neighbouring areas. However, this unit is strongly deformed. This unit is 330 m thick in the Villabona borehole, North Oviedo city (López-Gómez et al., 2019), but it never exceeds 150 m in the coast.

The outcrop of the Moris beach is interrupted by many faults, mainly of short displacement. Here, the Transición Formation is about 135 m thick, albeit representing only the upper half of the unit. The Moris beach succession can be divided in five intervals (A to E from base to top respectively, Figure 41) and display a transition towards fully marine dolomite and limestone of Jurassic age (Figure 41E). Interval A of the Transition Formation is made up of shale with thin levels of marl, fine-grained sandstone, and evaporite (Figure 41A). It shows incipient edaphic processes in its upper part. Interval B is mainly constituted by siltstone beds intercalated with anhydrite and marl. Soil development and plastic deformation is apparent (Figure 41B). Anhydrite-bearing beds become dominant in interval C (Figure 41C), being interbedded with green marl and affected by plastic deformation. Interval D represents the upper part of the Transition Formation and is constituted by mudstone that passes upwards to grey limestone (Figure 41D), just below prominent Lower Jurassic interval (Figure 41E) constituted by dolomite and limestone beds.

The lower intervals (A-C) of the Transition Formation have a clear marine influence that becomes more evident in the uppermost part. It represents deposits accumulated in supratidal and sabkha zones that show alternating submerged and exposed periods. Sector D is mostly represented by sub- and intertidal deposits. Similar sedimentary transitions were defined by Warren and Kendall (1985) in modern and ancient examples.

Figure 41. Triassic (Transición Formation, A to D) and Jurassic outcrops (Gijón Formation, E) of the Arenal de Moris beach, with the five sectors described in the text. A-E) Details of these sectors.

STOP 10:

Location:

MUJA (Jurassic Museum of Asturias), near Colunga village, Asturias (Figure 5).

Objectives:

Visit to the museum and end of the field trip.

The Jurassic Museum of Asturias (MUJA), a singular building with the shape of a three-toed dinosaur footprint, opened its doors in 2004, and since this date, it is the best-known and most-visited museum in Asturias. Design of the Asturian Architect Rufino García Uribelarrea, with a copper roof, the MUJA rises in a spectacular location between Colunga and Lastres villages, with a panoramic view of part of "The Dinosaur Coast" (central-eastern littoral of Asturias) (Figure 42,1).

With an exhibition area of more than 2000 m2, the Museum shows what our planet was like during the "Age of Dinosaurs". The visitor can travel back in time and observe which creatures dominated Mesozoic ecosystems, specially, during the Jurassic Period.

The exhibition, structured in a chronological sequence, includes three large exhibition halls: Triassic, Jurassic, and Cretaceous (the digits of a large footprint) and offers extensive information on different aspects of dinosaurs. The visit is completed by three more additional rooms: Pre-Mesozoic, Introduction to the Asturian Jurassic, and Jurassic of Asturias (Figure 42, 2).

Pre-Mesozoic hall

This hall provides information about the age of the Earth, the first organisms, the magnitude of geological time, the dynamics of the continents, the dating methods, the type of fossils, as well as on the classification of vertebrates and their relationships. It also refers to the extinction event that took place at the end of the Paleozoic, the most devastating in the history of our planet.

Triassic hall

The Triassic is the period in which the dinosaurs appeared (230 ma). This room offers information about the varieties of dinosaur fossils that can be found (bones, footprints, skin impressions, gastroliths, coprolites, bitemarks, eggs, and nests). The main anatomic differences between dinosaurs and other reptiles are also shown. Several images of relevant researchers in the study of dinosaurs can be seen on the "Gallery of Dinosaurologists". Plateosaurus, the largest and best-known prosauropod in Europe, is displayed in the center of the room.

Jurassic hall

The information furnished in this space include the classification of these singular reptiles in two groups, according to the arrangement of the hip bones: saurischian (lizard-hipped) and ornithischian (bird-hipped) dinosaurs. References to the features of the main groups are made: sauropods (quadrupedal herbivorous with long necks and tails), theropods (bipedal carnivorous), ornithopods (bipedal and/or quadrupedal herbivorous), stegosaurs (quadrupedal herbivorous with plates along the back and spines at the end of the tail), ankylosaurs (quadrupedal herbivorous with dermal armor), and ceratopsians (quadrupedal horned herbivorous). The central part of the hall is occupied by a Camarasaurus skeleton, a large-sized sauropod dinosaur, common in the deposits of central and western United States (Figure 42, 3).

Cretaceous hall

This space offers information on the biology of dinosaurs (some aspects of their reproduction or their social behaviour). Other issues presented in this hall are the relationship between non-avian dinosaurs and birds, these latter considered by the scientific community as avian dinosaurs, specifically theropods, and an explanation on the diverse theories on the extinction of non-avian dinosaurs by the end of Cretaceous (66 ma). Occupying the central circle there is also a couple of Tyrannosaurus skeletons, one of the greatest terrestrial predators in the history of the Earth (Figure 42, 4).

Introduction to the Asturian Jurassic hall

This place offers information about Asturian Jurassic by means a stratigraphic log and its formations: Gijón (muddy carbonate coast rich in salts), Rodiles (shallow open sea), Vega (meandering rivers and ponds), Tereñes (muddy coast to shelf lagoon) and Lastres (deltas, swamps and marshes). It also shows the palaeogeographic evolution of the Asturian Basin during the Jurassic, first covered by the sea and rich in marine invertebrates as well as ichthyosaurus and plesiosaurs, and subsequently represented by

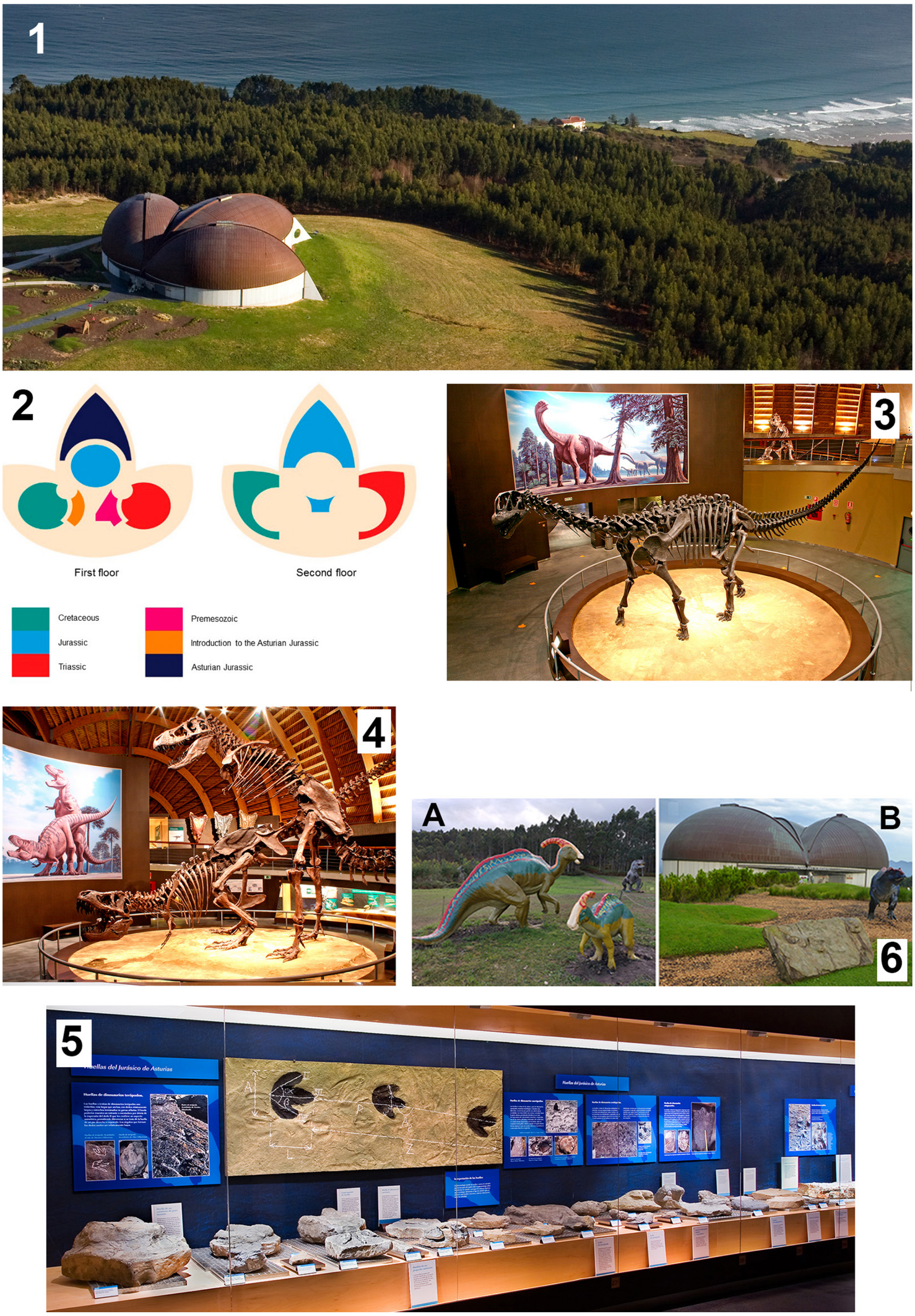

Figure 42. MUJA Museum. 1. The Jurassic Museum of Asturias located between Lastres and Colunga villages. Image: Álvaro García-Ramos. 2. Distribution of the spaces in the large footprint. 3. Jurassic room with Camarasaurus skeleton. Image: Álvaro García-Ramos. 4. Cretaceous room with two skeletons (female and male) of Tyrannosaurus rex. Image: Álvaro García-Ramos. 5. Asturian Jurassic area with some dinosaur tracks preserved as sandstone casts. Image: Álvaro García-Ramos. 6. Display of dinosaurs in the garden of MUJA. A, Two ornithopods: Parasaurolophus in the foreground and a theropod Tyrannosaurus in the background. B, Sandsonte block with two theropod footprints and the theropod Allosaurus.

terrestrial and coastal environments dominated by fishes and diverse varieties of reptiles (dinosaurs, pterosaurs, crocodiles, turtles, and lizards).

Asturian Jurassic hall

This room exhibits the varieties of rocks and fossils more representative of the diverse environments took place throughout the Asturian Basin during the Jurassic. In addition, this place shows also multiple footprints and skeletal remains of fish, dinosaurs, and other reptiles (turtles, crocodiles, etc.) (Figure 42, 5). In another space, the industrial application of some Jurassic materials is shown such as jet (fossilized wood) and the varieties of Jurassic rocks used in the region for the construction of buildings. Finally, a panoramic aerial photography of “The Dinosaur Coast” shows the location in the present-day sea cliffs of the nine dinosaur tracksites indicated.

The collection of the MUJA

Of the 5200 samples housed at MUJA, up to now, only 5% are in permanent exhibition. The dinosaur footprints collection is the most complete and diverse in Europe and the third worldwide. Other remarkable peculiarities of the museum collection are: 1) The best set of stegosaur tracks. 2) The largest theropod (78 cm long) and stegosaur (58 cm long) footprints ever known. 3) The pterosaur (flying reptiles) footprints best preserved. 4) Multiple dinosaur and some pterosaur footprints with skin impressions. 5) The unique lizard trackway known from the Jurassic. 6) The most complete skeletons of ichthyosaurs and plesiosaurs (marine reptiles) of the Iberian Peninsula. 7) The most abundant and diverse collection of Jurassic plant remains and invertebrate trace fossils from Spain.

The Mesozoic garden

The garden of the Jurassic Museum of Asturias, with more than 7000 m2, offers to visitors a tour through the Mesozoic displaying more than 20 replicas of different Jurassic and Cretaceous dinosaurs (Allosaurus, Brachiosaurus, Camptosaurus, Carnotaurus, Dacentrurus, Deinonychus, Diplodocus, Euoplocephalus, Pachycephalosaurus, Parasaurolophus, Stegosaurus, Triceratops and Tyrannosaurus, as well as several reproductions of flying reptile Pterodactylus (Figure 42, 6). Moreover, this outer area exhibits some fossils from the Jurassic of Asturias, such as theropod footprints and the trunk of a conifer, as well as, replicas of theropod and ornithopod trackways from the

Tereñes tracksite in Ribadesella and a sauropod trackway from La Griega beach tracksite in Colunga.

Visiting options

There are different ways for visiting the Museum, in an individual manner or organized groups, in both, there are several options: 1) On your own, with a hand guide. 2) With an audioguide, available in Spanish, English, French, and German. 3) With a free guided visit, lasting for one hour. 4) Guided visit and didactic workshop. In addition, the Museum also offers accessible visits, tailored to people with a physical, sensory or mental disability.

The MUJA for schoolchildren

The visit to the Museum is an activity that must be planned in advance. Teachers and monitors have the opportunity to prepare the school activities during the open days. For this kind of visits, the Museum provides didactic and pedagogic material. The didactic units, called MUJA in the classrooms, are adapted to different formative cycles and they are available in Spanish and English.

THE DINOSAUR COAST

The most spectacular outcrops of Jurassic rocks in Asturias extend practically continuously along the central-eastern coast, from Gijón to Ribadesella, and is known as "The Dinosaur Coast". This area was declared as Natural Monument by the Government of the Principality of Asturias, in 2001. The visit to the Museum is complemented by nine tracksites along this coast. The brochure "The Dinosaur Coast" is available on the MUJA and its pdf on the Museum´s website (museojurasicoasturias.com).

3. REFERENCES

3. References

Aller, J., Alvarez-Marrón, J., Bastida, F., Bulnes, M., Heredia, N., Marcos, A., Pérez-Estaún, A., Pulgar, J.A., Rodríguez-Fernández, L.R. (2004). Zona Cantábrica: Estructura, Deformación y Metamorfismo. In: Vera, J.A. (ed.), Geología de España, SGE-IGME, pp. 42-47.

Alonso-Zarza, A. M., Wright, V. P. (2010). Palustrine carbonates. Carbonates in Continental Settings: facies, environments and processes. Developments in Sedimentology 61, 225-267.

Arthaud, F., Matte, P. (1975). Les decrochements tardi-hercyniens du sud-ouest de l'Europe; geometrie et essai de reconstitution des conditions de la deformation. Tectonophysics 25, 139-171.

Barnolas, A., Pujalte V. (2004). La Cordillera Pirenaica. In: Vera, J.A. (ed.), Geología de España, IGME-SGE, Madrid, pp. 233–343.

Barrón, E., Gómez, J.J., Goy, A., Pieren, A.P. (2006). The triassic–jurassic boundary in Asturias (northern Spain): palynological characterisation and facies. Review of Palaeobotany and Palynology 138, 187-208.

Bennett, A.E., Kearsey, T.I., Davies, S. J., Millward, D., Clack, J. A., Smithson T. R., Marshall, J. E. A. (2016). Early Mississippian sandy siltstones preserve rare vertebrate fossils in seasonal flooding episodes. Sedimentology 63, 1677–1700.

Boillot, G., Dupeuble, P.A., Malod, J. (1979). Subduction and Tectonics on the continental margin of northern Spain. Marine Geology 32, 53–70.

Burns, C. E., Mountney, N. P., Hodgson, D. M., Colombera, L. (2017). Anatomy and dimensions of fluvial crevasse-splay deposits: Examples from the Cretaceous Castlegate Sandstone and Neslen Formation, Utah, U.S.A. Sedimentary Geology 351, 21–35.

Castro, A., Corretgé, L.G., de la Rosa, J., Enrique, P., Martínez, F.J., Pascual, E., Lago, M., Arranz, E., Galé, C., Fernández, C., Donaire, T., López, S. (2002). Palaeozoic magmatism. In: Gibbons, W., Moreno, T. (eds.), The Geology of Spain. Geological Society, London. pp. 117-153.

Changsong, L., Qi, Y., Li, S. (1991). Structural and depositional patterns of the Tertiary Baise Basin, Guang Xi Autonomous Region (southeastern China): a predictive model for fossil fuel exploration. Lacustrine Facies Analysis, International Association of Sedimentologists, Spec. Publ. 13, pp. 75-92.

Choukroune, P., Roure, F., Pinet, B., ECORS Pyrenees Team (1990). Main results of the ECORS Pyrenees profile. Tectonophysics 173, 411-423.

Colombi, C. E., Limarino, C. O., Alcober, O.A. (2017). Allogenic controls on the fluvial architecture and fossil preservation of the Upper Triassic Ischigualasto Formation, NW Argentina. Sedimentology 362, 1-16.

Corretgé, L.G., Suárez, O., Galán, G., Fernández-Suárez, J. (2004). Zona Asturoccidental-leonesa: Magmatismo. In: Vera, J.A. (ed.), Geología de España, SGE-IGME, 63–68.

Dewey, J. F., Helman, M. L., Turco, E., Hutton, D. H. W., Knott S. D. (1989). Kinematics of the western Mediterranean. In: Coward, M. P., Dietrich, D., Park, R. G., (eds.) Alpine tectonics, Geological Society Special Publications, London, 265-283.

Dupraz, C., Visscher, P. T., Baumgartner, L. K., Reid, R. P. (2004). Microbe-mineral interactions: early carbonate precipitation in a hypersaline lake (Eleuthera Island, Bahamas. Sedimentology 51, 745-765.

Estenssoro, P. (2021). Control estructural de las sucesiones del Carbonífero superior-Pérmico inferior en la terminación suroccidental del Sinclinorio de La Justa-Aramil (zona central de Asturias). MSc Thesis, Universidad de Oviedo, 38 pp.

Farias, P., Heredia, N. (1994). Geometría y Cinemática de los dúplex de Pambuches (Unidad de Picos de Europa, Zona Cantábrica, NO de España). Revista de la Sociedad Geológica de España 7(1–2), 113–120.

Fernández-Suárez, J., Dunning, G.R., Jenner, G.A., Gutiérrez-Alonso, G. (2000). Variscan collisional magmatism and deformation in NW Iberia: constrains from U-Pb geochronology and granitoids. Journal Geological Society, London 157, 565–576.

Freytet, P., Plaziat, J. C. (1982). Continental carbonate sedimentation and pedogenesis–Late Cretaceous and Early Tertiary of Southern France. In Purser, B. H. (ed.), Contributions to Sedimentology 12, 217 pp.

Gallastegui, G., Heredia, N., Rodriguez Fernandez, L.R., Cuesta, A. (1990). El stock de Peña Prieta en el contexto del magmatismo de la Unidad del Pisuerga-Carrión (Zona Cantábrica, N de España). Cadernos do Laboratorio Xeolóxico de Laxe 15, 203-217.

Gallastegui, G., Suárez, O., Cuesta, A. (2004). Zona Cantábrica: Magmatismo. In Vera, J.A. (ed.), Geología de España, SGE-IGME, pp. 47–49.

Gallastegui, J., Pulgar, J. A., Gallart, J. (2002). Initiation of an active margin at the North Iberian continent ocean transition. Tectonics 21, 1501-1514.

Gand, G., Kerp, H., Parsons, C., Martínez-García, E. (1997). Palaeoenvironmental and stratigraphic aspects of the discovery of animal traces and plant remains in Spanish Permian red beds (Peña Sagra, Cantabrian Mountains, Spain). Geobios, 30, 295– 318.

García-Espina, R. (1997). La estructura y evolución tectonoestratigráfica del borde occidental de la Cuenca Vasco-Cantábrica (Cordillera Cantábrica, NO de España). PhD Thesis, Universidad de Oviedo, 230 pp.

García-Sansegundo, J., Poblet, J., Alonso, J.L., Clariana, P. (2011). Hinterland-foreland zonation of the Variscan orogen in the Central Pyrenees: comparison with the northern part of the Iberian Variscan Massif. Geological Society of London, Special Publication 349, 169–184.

Grossman, E. L., Yancey, T. E., Jones, T. E., Chuvashov, B., Mazzullo, S. J., Mii, H-S (2008). Glaciation, aridification, and carbon sequestration in the Permo-Carboniferous: the isotopic record for low latitudes. Palaeogeography, Palaeoclimatology, Palaeoecology 268, 222–233.

Gulliford, A. R., Stephens, S. F., Hodgson, D.M. (2017). Crevasse splay processes and deposits in an ancient distributive fluvial system: The lower Beaufort Group, South Africa. Sedimentary Geology 358, 1-18.

Heredia, N., Martín-González, F., Farias, P., García-Sansegundo, J., Pedreira, D., Gonzalo-Guerra, B, García-Davia, G., Mateos-Herrero, G., A.G. Flórez. (2022). Geology of the Cabuérniga fault system: evolution of a large Alpine structure with Variscan inheritance. Journal of Maps 18,

Heward, A. (1978a). Alluvial fan sequence and megasequence models: with examples from Westphalian D – Stephanian B coalfield, Northern Spain. In: Miall, A.D. (ed.): Fluvial Sedimentology. Canadian Society of Petroleum Geologists. Memoir 5, 669-702.

Heward, A. (1978b). Alluvial fan sequence and lacustrine sediments from the Stephanian A and B (La Magdalena, Ciñera and Sabero) coalfields, northern Spain. Sedimentology 25, 451-488.

Jabaloy, A., Galindo-Zaldívar, J., González-Lodeiro, F. (2002). Paleostress evolution of the Iberian Peninsula (Late Car- bonferous to present-day). Tectonophysics 357, 159-186. Julivert, M. (1971). Décollement tectonics in the Hercynian cordillera of NW Spain. American Journal of Science 270 (1), 1–29.

Johnson, C. R., Ashley, G. M., De Wet, C. B., Dvoretsky, R., Parks, L., Hover, V. C., Owen, R. B., McBrearty, S. (2009). Tufa as a record of perennial fresh water in a semi-arid rift basin, Kapthurin Formation, Kenya. Sedimentology 56, 1115-1137.

Jones, S. M., Prave, A. R., Raub, T. D., Cloutier, J., Stüeken, E. E., Rose, C. V., Linnekogel, S., Nazarov, K. (2020). A marine origin for the late Mesoproterozoic Copper Harbor and Nonesuch Formations of the Midcontinent Rift of Laurentia. Precambrian Research 336, 105510.

Julivert, M., Marcos, A. (1973). Superimposed folding under flexural conditions in the Cantabrian Zone (Hercynian Cordillera, NW Spain). American Journal of Science 273, 353-375.

Juncal, M., Diez, J.B., Broutin, J., Martínez-García, E. (2016). Palynoflora from the Permian Sotres Formation (Picos de Europa, Asturias, Northern Spain). Spain Journal of Palaeontology 31 (1), 85–94.

Kraus, M. J. (1987). Integration of channel and floodplain suites, II. Vertical relations of alluvial palaeosols. Journal of Sedimentary Petrology 57, 602–612.

Kraus, M., Middleton, L. (1987). Contrasting architecture of two alluvial suites in different structural settings. Recent developments in Fluvial Sedimentology, Soc. Econ. Paleont. Min. Spec. Publ. 39, 253–262.

Lago, M., Arranz, E., Pocovi, A., Galé, C., Gil-Imaz, A. (2004). Lower permian magmatism of the Iberian Chain, Central Spain, and its relationship to extensional tectonics. In: Wilson, M., Neumann, E.-R., Davies, R.R., Timmerman, M.J., Heeremans, M., Larsen, B.T. (eds.), Permo-Carboniferous Magmatism and Rifting in Europe. Vol. 223. Geological Society, London, Special Publications, pp. 465–490.

Linol, B., Bercovici, A., Bourquin, S., Diez, J. .B., López-Gómez, J., Broutin, J., Durand, M., Villanueva-Amadoz, U. (2009). Late Permian to Middle Triassic correlations and palaeogeographical reconstructions in south-western European basins: New sedimentological data from Minorca (Balearic Islands, Spain). Sedimentary Geology 220, 77–94.

Lloret, J., López-Gómez, J., Heredia, N., Martín-González, F., de la Horra, R., Borruel-Abadía, V., ..., Lago, M. (2021). Transition between Variscan and Alpine cycles in the Pyrenean-Cantabrian Mountains (N Spain): Geodynamic evolution of near-equator European Permian basins. Global and Planetary Change 207, 103677.

López-Gómez, J., De la Horra, R., Barrenechea, J.F., Borruel-Abadía, V., Martín-Chivelet, J., Juncal, M., Martín-GGonzález, F., Heredia, N., Biez, J.B., Buatois, L. (2021). Early Permian during the Variscan orogenen collapse in the equatorial realm: insights from the Cantabrian Mountains (N Iberia) into climatic and environmental changes. International Journal of Earth Sciences 110, 1355-1387.

López-Gómez, J., Martín-González, F., Heredia, N., De la Horra, R., Barrenechea, J.F., Cadenas, P., Juncal, M., Diez, J.B., Borruel-Abadia, V., Pedreira, D., García-Sansegundo, J., Farias, P., Galé, C., Lago, M., Ubide, T., Fernández-Viejo, G., Gand, G. (2019). New lithostratigraphy for the Cantabrian Mountains: a common tectonostratigraphic evolution for the onset of the Alpine cycle in the W Pyrenean realm, N Spain. Earth-Science Reviews 188, 249–271.

Luque, C. (1985). Las mineralizaciones de mercurio de la Cordillera Cantábrica. PhD Thesis, Universidad de Oviedo, 1531 pp.

Machette, M. N. (1985). Calcic soils of the southwestern United States. Soils and Quaternary Geology of the Southwestern United States. Special Paper of the Geological Society of America 203, 10–21.

McCann, T., Pascal, C., Timmerman, M., Krzywiec, P., López-Gómez, J., Wetzel, A., Krawczyk, C.M., Rieke, H., Lamarche, J. (2006). Post-Variscan (end Carboniferous –Early Permian) basin evolution in Western and Central Europe. In: Gee, D.G., Stephenson, R.A. (eds.), European Lithosphere Dynamics. Geological Society London Memoirs 32 (1), pp. 355-388.

Mack, G. H., James, W. C., Monger, H. C. (1993). Classification of paleosols. Geological Society of America Bulletin 105, 129–136.

Martín-González, F., Freudenthal, M., Heredia, N., Martín-Suárez, E, Rodríguez-Fernández, L. R. (2014). Palaeontological age and correlations of the Tertiary deposits of the NW Iberian Peninsula: the tectonic evolution of a broken foreland basin. Geological Journal 49 (1), 15-27.

Martín-González, F., Heredia N. (2011a). Complex tectonic and tec- tonostratigraphic evolution of an Alpine foreland basin: The western Duero Basin and the related Tertiary depressions of the NW Iberian Peninsula Tectonophysics 502. 75-89.

Martín-González, F., Heredia, N. (2011b). Geometry, structures and evolution of the western termination of the Alpine-Pyrenean Orogen reliefs (NW Iberian Peninsula). Journal of Iberian Geology 37, 102-120.

Martínez-García, E. (1991). Hercynian syn-orogenic and post-orogenic successions in the Cantabrian and the Palentian zones (NW Spain). Comparison with other western European occurrences. Giornale di Geologia 53, 209–228

Mercuzot, M., Bourquin, S., Pellenard, P., Beccaletto, L., Schnyder, J., Baudin, F., Ducassou, C., Garel, S., Gand, G. (2022). Reconsidering Carboniferous–Permian continental paleoenvironments in eastern equatorial Pangea: facies and sequence stratigraphy investigations in the Autun Basin (France). International Journal of Earth Sciences, 1-34.

Merino-Tomé, O. A, Bahamonde, J. R., Colmenero, J. R., Heredia, N., Villa, E., Farias, P. (2009). Emplacement of the Cuera and Picos de Europa imbricate system at the core of the Iberian-Armorican arc (Cantabrian zone, north Spain): New precisions concerning the timing of arc closure. Geological Society of America Bulletin 121 (5–6), 729–751.

Merino-Tomé, O., Suárez Rodríguez, A., Alonso, J. L. (2011). Mapa Geológico digital continuo E. 1:50.000, Zona Cantábrica (Zona-1000). In: J. Navas (ed.), Mapa Geológico Digital continuo de España (GEODE). [on line]. Sistema de Información Geológica Continua: SIGECO. IGME. [Consultation year: 2022]. Available in: http://info.igme.es/cartografiadigital/ geologica/ geodezona.aspx?Id=Z1100

Miall, A. D. (1985). Architectural elements analysis: A new method of facies analysis applied to fluvial deposits. Earth-Science Reviews 22, 261-308.

Miall, A. D. (1996). The Geology of Fluvial Deposits. In: Sedimentary Facies, Basin Analisis and Petroleum Geology. Springer, Berlin 582 pp.

Miall, A. D. (2014). Fluvial Depositional Systems. Springer Geology, 316 pp.

Montañez, I. P., Tabor, N. J., Niemeier, D., Di Michele, W. A., Frank, T. D., Fielding, C. R., Isbell, J. L., Birgenheier, L. P., Rygel, M. C. (2007). CO2-forced climate and vegetation instability during Late Paleozoic deglaciation. Science 315, 87–91

Mujal, E., Gretter, N., López-Gómez, J. , Falconnet, J., Díez, J. B., de la Horra, R., Bolet, A., Oms, O., Arche, A., Barrenechea, J. F., Steyer, J. S., Fortuny, J. (2016). Constraining the Permian/ Triassic transition in continental environments: Stratigraphic and paleontological record from the Catalan Pyrenees (NE Iberian Peninsula). Palaeogeography, Palaeoclimatology, Palaeoecology 445, 18-37.

Muñoz, J. A. (1992): Evolution of a continental collision belt: ECORS-Pyrenees crustal balanced section. In: K. R. McClay (ed.), Thrust Tectonics, Chapman and Hall, London, pp. 235-246.

Owen, A., Ebinghaus, A., Hartley, A. J., Santos, M. G. M., Weissmann, G. S. (2017). Multi-scale classification of fluvial architecture: An example from the Palaeocene-Eocene Bighorn Basin, Wyoming. Sedimentology 64 (6), 1572-1596.

Platt, N. H., Wright, V. P. (1992). Palustrine carbonates and the Florida Everglades: towards an exposure index for the fresh-water environment. Journal of Sedimentary Petrology 52, 1058-1071.

Pulgar, J. A., Alonso, J. L., Espina, R. G., Marín, J. A. (1999). La deformación alpina en el basamento varisco de la Zona Cantábrica. Trabajos de Geología 21, 283-295.

Pulgar, J.A., Gallart, J., Fernández-Viejo, G., Pérez Estaún, A., Álvarez-Marrón, J. and ESCIN Group (1996). Seismic image of the Cantabrian Mountains in the western extension of the Pyrenean belt from integrated reflection and refraction data. Tectonophysics 264, 1-19.

Ramos, A., Sopeña, A. (1983). Gravel bars in low sinuosity streams (Permian and Triassic, Central Spain). International Association of Sedimentologist, Special Publication 6, 301-312.

Retallack, G. J. (2001). Soils of the Past. Blackwell. Oxford, 404 pp.

Retallack, G. J. (2005). Pedogenic carbonate proxies for amount and seasonality of precipitation in paleosols. Geology 33, 333-336.

Ribeiro, A., Kullberg, M.C., Kullberg, J.C., Manuppella, G., Phipps, S. (1990). A review of alpine tectonics in Portugal-foreland detachment in basement and cover rocks. Tectonophysics 184, 357-366.

Rodríguez-Fernández, L. R., Heredia, N. (1987). Carboniferous stratigraphie and structure of the Pisuerga-Carrion unit. NW Spain. Cadernos do Laboratorio Xeoloxico de Laxe 12, 207–229.

Sánchez, V., Vindel, E., Martín-Crespo, T., Corbella, M., Cardellach, E., Banks, D. (2009). Sources and composition of fluids associated with fluorite deposits of Asturias (N Spain). Geofluids 9, 338–355.

Srivastava, S. P., Roest, W. R., Kovacs, L. C., Oakey, G., Le- Vesque, S., Verhoef J., Macnab, R. (1990). Motion of Iberia since the Late Jurassic: Results from detailed aeromagnetic measurement in the Newfoundland Basin. Tectonophysics 184, 229-260.

Suárez-Rodríguez, A. (1988). Estructura del área de Villaviciosa-Libardón (Asturias, Cordillera Cantábrica). Trabajos de Geología 17, 87-98.

Suárez-Vega, L. C.(1974). Estratigrafía del Jurásico en Asturias. Cuadernos de Geología Ibérica 3 (1-2), 369 pp.

Symons, D.T.A., Kawasaki, K., Tornos F., Velasco F., Rosales, I. (2017). Temporal constraints on genesis of the Caravia-Berbes fluorite deposits of Asturias, Spain, from paleomagnetism. Ore Geology Reviews 80, 754–766.

Talbot, M. R., Allen, P. A. (1996). Lakes. Sedimentary Environments: Processes, Facies and Stratigraphy. Blackwell Science. Oxford. pp 83-124.

Tanner, L. H., Hubbert, J. F. (1992). Depositional environments, paleogeography and palaeoclimatology of the Lower Jurassic McCoy Brook Formation, Fundy rift basin, Nova Scotia. Palaeogeography, Palaeoclimatology, Palaeoecology 96 (3-4), 261-280.

Teixell, A. (1998). Crustal structure and orogenic material budget in the west-central Pyrenees. Tectonics 17, 395-406.

Valverde-Vaquero, P. (1992). Permo-Carboniferous magmatic activity in the Cantabrian Zone (NE Iberian Massif, Asturias, NW Spain). MSc Thesis, Boston College, USA, 198 pp.

Velando, F., Castelló, R., Orviz, F., Ortuño, G., Caride, C., Gervilla, M., Fernández-Pello, J., Obis, A. (1975). Memoria explicativa de la Hoja del Mapa Geológico de España E. 1:50.000 n° 53 (Mieres), Segunda serie MAGNA-Primera edición. Instituto Geológico y Minero de España (IGME). Madrid, 36 pp.

Wagner, R.H., Álvarez, C. (2010). The Carboniferous floras of the Iberian Peninsula: A synthesis with geological connotations. Review of Palaeobotany and Palynology 162, 239–324

Wagner, R.H., Martínez-García, E. (1982). Description of an early Permian flora from Asturias and comments on similar occurrences in the Iberian Peninsula. Trabajos de Geología 12, 273-287.

Warren, J.K., Kendall, C. G. (1985). Comparison of Sequences Formed in Marine Sabkha (Subaerial) and Salina (Subaqueous) Settings--Modern and Ancient. AAPG Bulletin 69 (6), 1013-1023.

Weil, A. (2006). Kinematics of orocline tightening in the core of an arc: Paleomagnetic analysis of the Ponga Unit, Cantabrian Arc, northern Spain. Tectonics 25 (3), TC3012.

Weil, A., Gutiérrez-Alonso, G., Conan, J. (2010). New time constraints on lithospheric scale oroclinal bending of the Ibero-Armorican Arc: a palaeomagnetic study of earliest Permian rocks from Iberia. Journal of the Geological Society, 167, 127-143.

Ziegler, P. A. (1988). Post-Hercynian plate reorganization in the Tethys and Arctic-North Atlantic domains. In: Manspeizer W (ed.) Triassic-Jurassic rifting. Continental Breakup and the Origin of the Atlantic Ocean and Passive Margins. Developments in Geotectonics 22B. Elsevier, Amsterdam, pp. 711–755.

Ziegler P. A., Stampfli G. M. (2001). Late Paleozoic-Early Mesozoic plate boundary reorganization: collapse of the Variscan Orogen and opening on the Neotethys. Ann. Mus. Civ. Sc. Nat. Brescia 25, 17–34.

GEOLOGICAL DATABASES AND DOWNLOADS

To view and download geological maps of the visited areas:

https://info.igme.es/visor/

http://info.igme.es/cartografiadigital/portada/

All geological databases of the IGME at:

http://info.igme.es/catalogo/catalog.aspx?catalog=3&shfo=false&shdt=false&master=infoigme&lang=spa&intranet=false

ISBN: 978-84-09-42264-7